INFORMATION TO USERS

The most advanced technology has been used to photograph and reproduce this manuscript from the microfilm master. UMI films the text directly from the original or copy submitted. Thus, some thesis and dissertation copies are in typewriter face, while others may be from any type of computer printer.

The quality of this reproduction is dependent upon the quality of the copy submitted. Broken or indistinct print, colored or poor quality illustrations and photographs, print bleedthrough, substandard margins, and improper alignment can adversely affect reproduction.

In the unlikely event that the author did not send UMI a complete manuscript and there are missing pages, these will be noted. Also, if unauthorized copyright material had to be removed, a note will indicate the deletion.

Oversize materials (e.g., maps, drawings, charts) are reproduced by sectioning the original, beginning at the upper left-hand corner and continuing from left to right in equal sections with small overlaps. Each original is also photographed in one exposure and is included in reduced form at the back of the book. These are also available as one exposure on a standard 35mm slide or as a 17" x 23" black and white photographic print for an additional charge.

Photographs included in the original manuscript have been reproduced xerographically in this copy. Higher quality 6" x 9" black and white photographic prints are available for any photographs or illustrations appearing in this copy for an additional charge. Contact UMI directly to order.

U·M·I

University Microfilms International
A Bell & Howell Information Company
300 North Zeeb Road, Ann Arbor, MI 48106-1346 USA
313/761-4700 800/521-0600

Order Number 9009792

Development of the new functional integral formalism and its application to the periodic Anderson model

Tolpin, Anatoly Emiljevich, Ph.D.

City University of New York, 1989

U·M·I
300 N. Zeeb Rd.
Ann Arbor, MI 48106

Development of the New Functional Integral Formalism and Its Application to the Periodic Anderson Model

by

Anatoly E. Tolpin

A dissertation submitted to the Graduate Faculty in Physics in partial fulfillment of the requirements for the degree of Doctor of Philosophy, the City University of New York.

1989

This manuscript has been read and accepted for the Graduate Faculty in Physics in satisfaction of the dissertation requirement for the degree of Doctor of Philosophy.

11 Sept 1989
date

Chairman of the Examining Committee

11 Sept. 1989
date

Executive Officer

Melvin Lax

Peter M. Levy

Myriam P. Sarachik

Carl Kukkonen

Supervisory Committee

The City University of New York

Abstract

Development of the New Functional Integral Formalism and Its Application to the Periodic Anderson Model

by
Anatoly E. Tolpin

Adviser: Professor Joseph L. Birman

A new approach was developed to the problem of the propagator construction within the framework of the functional integral formalism. Central to this approach is the definition of a local operator construction, which defines the operators over some field(s) as being dependent on field(s) variables. This is in contrast to the usual creation and annihilation operators, which in the present context are defined as "global" operators. The relation to the standard functional integral formalism has been investigated, and the problem of the discontinuous paths in the standard functional integral formalism has been resolved. One simple application of the new formalism to the linear harmonic oscillator problem is also discussed.

The new functional integral formalism has been used to study the orbitally nondegenerate periodic Anderson problem. A smooth second-order like transition behavior around T_K has been obtained. Various saddle points, including the one corresponding to the Kondo resonance have been derived. However no stable state corresponding to the Heavy Fermion regime has been found.

The new functional integral formalism has been further applied to the degenerate lattice Anderson Hamiltonian in the Kondo regime. It has been recognized that in the coherent low temperature regime operators in the effective Hamiltonian belong to an $SU(2J+2)$ dynamical algebra. Subsequently a canonical transformation has been performed that decouples the quasiparticle branches, thereby setting up the so-called decoupling equation. It turns out that the

decoupling equation has a solution of the symmetry-breaking type. The thermodynamic response functions and other quantities were calculated for this symmetry-breaking state. This solution is a consequence of the degeneracy of the uncoupled f-orbitals. The solution is characterized by the interatomic hopping of f-electrons, which produces the spin delocalization regime and pins the the renormalized f-level close to the Fermi level. It is believed that this new state forms a correct description of the Heavy Fermion state at low temperatures.

Acknowledgement

It is a pleasure to thank Professor Joseph L. Birman, who suggested to me the problem and gave me the benefit of many helpful discussions.

TABLE OF CONTENTS

List of Tables

List of Figures

Figures

0. Thesis Outline

There are two main topics pursued in this thesis. The first topic is purely formal. In Section 2 I develop a new functional integral formalism, capable of representing a many-body propagator as the finite-dimensional Gaussian integral. This is in contrast with an infinite dimensional path-integral representation in the standard functional integral theory. I further show the equivalence of the new theory to the standard path-integral theory. Also as an added proof, I calculate the propagator for a system coupled to a linear harmonic oscillator.

The main part of the thesis, however, deals with the application of that formalism to the study of Heavy Fermion Systems, which are characterized as Kondo lattices. In Section 1.1 I review the experimental results, while Section 1.2 is devoted to the theoretical background underlying the modern theories used to explain various aspects of the Heavy Fermion Systems. Section 3 is devoted to the study of orbitally nondegenerate Kondo system. The calculated stationary states of the system are similar to those obtained by other people. It will be argued that none of those states is capable of adequately describing the complex behavior of Heavy Fermion Systems.

In the next Section (4), I apply the formalism to the study of orbitally degenerate Kondo lattice. I find a new saddle point that can only exist in the degenerate case. As I show in Sec. 4.5-4.7, this new saddle point does describe many properties of Heavy Fermion Systems at low temperature. I further describe the nature of the new ground state and how it is different from the single impurity type Kondo resonance. In Section 5 I extend the theory to higher temperatures by developing the self-consistent type pertubation theory. That pertubation theory is applied to the calculation of the conductivity by using the linear Kubo formalism. Those calculations are further extended to finite magnetic fields. The results obtained are in general agreement with experimental results. Finally in Section 6 I outline the additional work that needs to be done in understanding the Heavy Fermion Systems.

1. Introduction to Heavy Fermion Systems

1.1 Experimental Background

The term "Heavy Fermion Systems" (HFS) has been introduced to describe the highly correlated electronic systems in which the electronic quasiparticle states have a characteristic energy several orders of magnitude smaller than in ordinary metals. It means that the effective mass, which is inversely proportional to the energy scale is enhanced by the same order of magnitude. Importantly, all HFS are characterized as Kondo lattices in which the localized magnetic impurity electrons are strongly hybridized with the conduction electrons of a nonmagnetic host. This hybridization is responsible for the delocalization of the impurity electrons, leading to the appearance of long range correlations within such systems. All HFS are intermetallic compounds in which one of the constituents is a rare earth or actinide atom, with partially filled 4f- or 5f- electron shells. Examples of such systems are UBe_{13} , UPt_3 , and $CeCu_2Si_2$. Those metals become superconducting at low temperature. Other HFS, such as $NpBe_{13}$, U_2Zn_{17} , and UCd_{11} become magnetic (with the complicated nonferromagnetic type ordering). In addition, there exist two HFS with no ordering down to 0.050 K: $CeCu_6$, and $CeAl_3$. There are several unusual properties [1], which make HFS especially interesting:

i). At high temperature the f-electrons behave as if they were localized on their atomic sites, as in conventional rare earth and actinide compounds. However, while conventional compounds undergo some type of magnetic transition at low temperatures, HFS go into a Fermi liquid type regime, which is characterized by an extremely large effective mass. This can be seen from the measurements of static magnetic susceptibility, specific heat, and resistivity. As can be seen from Figs. 1 & 2, both the zero temperature magnetic susceptibility and the Sommerfeld specific heat constant γ are enormously enhanced over the corresponding values in normal metals. At the same time, however, the Wilson

ratio of susceptibility to the Sommerfeld constant is somewhat smaller than one.

ii). Unusual properties of HFS also extend to dynamical correlations. First among them are measurements of resistivity. At low temperature:

$$\rho \approx AT^2$$

which can be consistent with Fermi-liquid theory, as well as some other theories, such as paramagnon theory, developed by Doniach in 1968. It is important to note however that the experimentally observed range of such behavior is quite limited. In fact, the deviation from the quadratic temperature dependence shows up at about 0.1K to 0.3K. This constitutes an important temperature scale, characterizing the coherent state of the system. At a much larger characteristic temperature T_{max}, most HFS develop a resistivity peak, followed by a very broad shoulder. A very interesting exception to this behavior is observed in UPt_3 (Fig. 3), where ρ behaves much as in normal metals. This points to some intrinsic differences in this metal, and possibly some others.

Magnetoresistance also shows an increases in magnitude with decreasing temperature and increasing field. A plot of magnetoresistance for UBe_{13} (see Fig. 4) shows a large negative magnetoresistance that increases in magnitude with decreasing temperature and increasing field (-42% at 1.2 K and 11 T compared to the zero field resistance at the same temperature). Another interesting correlation is that at a given field, $|\Delta R|/R$ vs. T^2 coincides with C/T vs. T^2 at zero field. It should be noted that UPt_3 shows positive magnetoresistance (+40% at 1.2 K and 11 T), which again confirms some important differences between the members of this type of metal system.

iii). The highly correlated electron state of HFS produces its most unusual property - superconductivity. Although it occurs at very low temperature, this seems highly unusual in a metal where higher temperature properties are dominated by localized magnetic

moments. Below T_C , both the ultrasonic attenuation and the nuclear spin-lattice relaxation rate show very unusual behavior. Recent experiments on longitudinal ultrasonic attenuation ($\alpha(T)$) in HFS superconductors UPt_3 and UBe_{13} have yielded results that differ markedly from the predictions of BCS theory. The low temperature behavior of $\alpha(T)$ has either a T^2 or a T^3 dependence [2], rather than the exponential dependence of BCS theory. Furthermore, experiments have shown a pronounced peak in $\alpha(T)$ just below T_C . This, combined with the nonexponential behavior of the specific heat has led people to suggest the superconducting order parameter is anisotropic with zeros on the FS. Unfortunately, group-theoretical arguments [3-5] have so far been unsuccessful in unambiguously pinpointing the appropriate symmetry classes for any of the HFS superconductors. As for the relaxation rate ($1/T_1$), its behavior has been measured for $CeCu_2Si_2$ [6]. It decreases drastically just below T_C = 0.67 K down to 0.5 T_C without apparent enhanced behavior and is found to be almost temperature independent below 0.3 T_C. Although a triplet pairing model may explain the sudden decrease down to 0.5 T_C, the temperature independent behavior below 0.3 T_C remains unexplained.

As exciting as the question of superconductivity appears to be, it is generally felt that one needs a better understanding of the normal state properties of those systems, especially the nature of transition from nearly localized to Fermi liquid type behavior. As all of those metals are described as "Kondo lattices", I shall give particular emphasis in my research to the consideration of the Kondo lattice close to a magnetic transition, and I will attempt to show how electron correlations give HFS their most unusual properties.

1.2 Theoretical Background.

Here I will review various theories which have been advanced to explain normal state properties of HFS. Let me start by discussing the properties of a single magnetic impurity imbedded in the nonmagnetic metal, or equivalently the properties of a dilute alloy where interactions among impurities are taken to be zero. There

are several reasons to consider the single impurity model. First, there is a general agreement that the single impurity model has been successfully solved. Second, it seems that this model is able to explain some of the features of HFS, such as the large effective mass. The principal problem with that approach is its inherent inability to explain the onset of coherence at low temperature. It is fair to say, however, that all theories advanced to explain the HFS so far represent an outgrowth of the single impurity theory. It is therefore very important to examine those theories by starting with the single impurity model.

When a potentially magnetic atom is dissolved in a nonmetallic host, the electronic states are localized at the impurity site. The magnetic character of such state is determined by Hund's rule. In a metallic host, however, the situation is much more complicated. Because impurities are coupled to a Fermi sea, no matter how weak that coupling may be, it may lead to a nonmagnetic (nonlocalized) ground state. In such state the electrons are never truly localized and always have a finite probability of jumping into a conduction band. Such an almost bound state is called a resonance state.

a). Friedel's Theory

Friedel was the first to address the problem of the existence of such a resonance using scattering theory [7]. He represented the impurity by a potential. For a given total momentum quantum number l the potential consists of a deep hole at the core of the impurity and a centrifugal potential barrier $l(l+1)/r^2$, where the distance r is measured from the center of the impurity (see Fig. 5). In this potential hole a bound state or resonance can be formed. In this case we deal with the resonance which lies close to the Fermi surface, and thus is only partially occupied. The resonance has a finite width because the electrons may jump from the potential hole to the metallic host by tunnelling through the centrifugal barrier. Since the barrier increases for large l, relatively small width is expected for large l ($l = 3$ for HFS). According to Friedel's theory, the conduction electrons undergo a resonance scattering in which

the intermediate state is the resonance state. This resonant scattering is characterized by the energy dependent phase shift $\delta_{l,\sigma}(E)$ and the resonant state by the Lorentzian density of states $\rho_{l,\sigma}(E)$:

$$\rho_{l,\sigma}(E) = \frac{1}{\pi} \frac{\Delta}{(E - E_{l,\sigma})^2 + \Delta^2} \tag{1.2.1}$$

$$\tan \delta_{l,\sigma}(E) = \frac{\Delta}{E_{l,\sigma} - E} \tag{1.2.2}$$

Many physical quantities can be expressed in terms of phase shifts, which can be treated phemenologically. More importantly, such arguments served as the foundation of a microscopic model suggested by Anderson [8].

b). Anderson's Model

At the simplest level of this model the metallic host is represented by a single conduction band with energy ε_k and momentum k. The impurity state forming the resonance discussed by Friedel is considered as a flat orbital with energy E_0. The transition between the orbital and the conduction band is taken into account by introducing the mixing term with the phemenological transition amplitude V_k. The additional important feature of the Anderson model is an introduction of an intraatomic Coulomb repulsion U. In the limit of interest here $U \to \infty$ leads to many nontrivial many-body effects. The description of such effects has remained a major challenge to theorists up to this day, and is the source of many "infinite U" theories that I will discuss below. Collecting all the terms the Anderson Hamiltonian has the following form:

$$H = H_{band} + H_f + H_{mix} \tag{1.2.3}$$

$$H_{band} = \sum_{k\sigma} \varepsilon_k \, c^+_{k\sigma} c_{k\sigma}$$

$$H_f = \sum_{\sigma} E_{0\sigma} f^+_{\sigma} f_{\sigma} + U f^+_{\uparrow} f_{\uparrow} f^+_{\downarrow} f_{\downarrow}$$

$$H_{mix} = \sum_{k\sigma} \left[V(k) c^+_{k\sigma} f_{\sigma} + H.C. \right]$$

The important feature of the Anderson model is its ability to predict the formation of a resonance state which completely agrees with Friedel's qualitative picture. This was accomplished by using the Hartree-Fock approximation for the Anderson model [8]. Define:

$$\varepsilon_{f\sigma} \equiv E_{0\sigma} + U \langle f^+_{-\sigma} f_{-\sigma} \rangle f^+_{\sigma} f_{\sigma} \tag{1.2.4}$$

and rewrite:

$$H_{f\,\mathrm{MF}} = \sum_{\sigma} \varepsilon_{f\sigma} f^+_{\sigma} f_{\sigma} \tag{1.2.5}$$

Then one obtains the local density of states in the Lorentzian form:

$$\rho_{f\sigma}(\varepsilon) = \frac{1}{\pi} \frac{\Delta}{(\varepsilon - \bar{\varepsilon}_{f\sigma})^2 + \Delta^2} \tag{1.2.6}$$

where

$$\Delta = \pi \sum_k |V(k)|^2 \delta(\varepsilon - \varepsilon_k) \tag{1.2.7}$$

$$\bar{\varepsilon}_{f\sigma} = \varepsilon_{f\sigma} + P \sum_k \frac{|V(k)|^2}{\varepsilon - \varepsilon_k}$$

From the above density of states we can compute the occupation numbers of the localized state:

$$\langle n_{f\sigma} \rangle = \int_{-\infty}^{\varepsilon_F} d\varepsilon \ \rho_{f\sigma}(\varepsilon) \tag{1.2.8}$$

Since $\rho_{f\sigma}(\varepsilon)$ depends on $\langle n_{f-\sigma} \rangle$ we have a set of coupled equations. These may have a magnetic solution $\langle n_{f\sigma} \rangle = \langle n_{f-\sigma} \rangle$, or the two symmetrical nonmagnetic solutions. The condition for the appearance of the magnetic solution is found to be:

$$U\rho_{f\sigma}(\varepsilon_F) > 1$$

Therefore in the limit of large U one deals with the magnetic regime, and the density of states for this solution is sketched below (see Fig.6).

Within the HF approximation one can make further connection to Friedel's theory by expressing several quantities in terms of the phase shifts which play the central role in Friedel's theory. In terms of phase shifts the local density of states can be written as:

$$\rho_{f\sigma}(\varepsilon) = \frac{1}{\pi} \sum_l (2l+1) \frac{d\delta_l}{d\varepsilon} \tag{1.2.9}$$

In this case we are dealing with the single channel (l=3). Integrating (1.2.9) and comparing it to (1.2.6) and (1.2.8) one obtains:

$$\delta_{f\sigma}(\varepsilon_F) = \pi \langle n_{f\sigma} \rangle = \cot^{-1}\left(\frac{\bar{\varepsilon}_{f\sigma}}{\Delta}\right) \tag{1.2.10}$$

This is the special case of the Friedel sum rule which relates the phase shift to the number of electrons screening the excess charge of the impurity Z:

$$Z = \frac{1}{\pi} \sum_{l,\sigma} (2l+1)\delta_{l\sigma}(\varepsilon_F) \tag{1.2.11}$$

Therefore Friedel's sum rule is the expression of charge neutrality. The electron gas is displaced in the vicinity of the impurity charge. The displaced electronic charge exactly cancels the impurity charge.

The formulas above establish the connection between the Anderson and Friedel models. There is however a problem with the HF solution to the Anderson model that I should address at this point. The problem is that the ground state of the system at zero temperature should be a singlet. In that case all the phase shifts must be equal, which means that for a channel with one l the common phase shift is:

$$\delta_l = \delta = \frac{\pi Z}{2(2l+1)} \tag{1.2.12}$$

Using (1.2.12) one can calculate the induced density of states and the result is sketched in Fig. 6a. The density of states that follows from the assumption of the singlet ground state does not look like the HF density of states. The missing element in the HF picture is the narrow resonance at the Fermi surface. This resonance is due to the correlation effects which have been completely ignored in the HF approach. The width of the resonance sets a new low temperature energy scale $k_B T_K$, where T_K is the so-called Kondo temperature. It is related to the important Kondo effect which I will turn to right now.

c). Kondo Effect

The Kondo effect includes the anomalies observed in the resistivity, magnetic susceptibility and specific heat of "local moment" metals. Of particular importance were calculations of the resistivity which have been first carried out by Kondo [9]. Those calculations have been stimulated by the observation of the logarithmic increase in the resistivity of "local moment" metals below a certain temperature, eventually saturating at some finite value (see Fig. 6b). This increasing impurity contribution combined with the decreasing phonon contribution produces a minimum in the resistivity, which has not been understood for many years. Let me briefly discuss Kondo calculations, which will highlight the importance of magnetic impurities in producing the logarithmic behavior.

I begin this discussion by introducing the Kondo Hamiltonian:

$$H = H_{band} + H_{ex} \tag{1.2.13}$$

$$H_{band} = \sum_{k\sigma} \varepsilon_k \, c^{+}_{k\sigma} c_{k\sigma}$$

$$H_{ex} = - \sum_{k,\, k',\, i} J_{k,\, k'} S^{(i)} c^{+}_{k\beta} \sigma^{(i)}_{\beta\beta'} c_{k'\beta'}$$

where $S^{(i)}$ denotes the i-th component (i=1,2,3) of the localized spin and $\sigma^{(i)}$ are Pauli matrices corresponding to conduction electron spin. The above Hamiltonian unlike the Anderson Hamiltonian preserves the local charge. It is equivalent to the Anderson Hamiltonian in the large U limit ($U >> \Delta$). In this case the charge fluctuations are suppressed and only virtual spin fluctuations are present. Such fluctuations are well described by the Kondo Hamiltonian. On the formal side, the connection between the two models can be established by Schrieffer-Wolf canonical transformation applied to the Anderson Hamiltonian [9a], which eliminates $V(k)$ to the first order. In that case one obtains the

expression similar to (1.2.13), with the exchange parameter near the Fermi surface given by:

$$J_{k_F,\, k_F} = 2\left|V\left(k_F\right)\right|^2 \frac{U}{E_0\left(E_0 + U\right)} \qquad (1.2.14)$$

In this expression E_0 is measured with respect to the Fermi level, and therefore the exchange coefficient J is negative, corresponding to the antiferromagnetic coupling.

Using the above form of exchange coupling, Kondo set out to calculate the spin-flip scattering amplitude using pertubation theory. His intention was to show how this amplitude is responsible for the unusual behavior of the resistivity.

We start with the state of the system $c^{+}_{k\sigma}\left|\mathrm{FS}\,;M_i\right\rangle$ at the time $t = -\infty$, where FS denotes the unperturbed Fermi sea, and M_i denotes the impurity spin projection quantum number. Also the zero order Hamiltonian is H_{band} describing the uncoupled conduction band. We now adiabatically turn on the interaction H_{ex}. The calculation in the first Born approximation was carried out by Kasuya [10] and Yosida [11]. The probability of the spin conserving scattering can be obtained by using the "golden rule", which yields:

$$W\left(\uparrow M_i \rightarrow \uparrow M_i\right) = 2\pi J^2 M_i^{\,2} \rho_0 \qquad (1.2.15)$$

where ρ_0 is the conduction band density of states near the Fermi level. By averaging over the spin directions, $M_i^{\,2}$ is replaced by a factor $S\left(S+1\right)/3$. The contribution from the spin-flip term is obtained in the similar way:

$$W\left(\uparrow M_i \rightarrow \downarrow M_i + 1\right) = 2\pi J^2 \left[S\left(S+1\right) - M_i\left(M_i + 1\right)\right]\rho_0$$

$$W\left(\downarrow M_i \rightarrow \uparrow M_i - 1\right) = 2\pi J^2 \left[S\left(S+1\right) - M_i\left(M_i - 1\right)\right]\rho_0$$

Assuming that contributions to the electrical resistivity are additive, one obtains the total contribution to resistivity is proportional to the transition probability

$$W = 2\pi c J^2 S\left(S+1\right)\rho_0 \tag{1.2.16}$$

where c is the concentration of the impurities. Kondo performed this calculation in the next order of pertubation theory. The relevant diagrams are represented in Figs. 7a and 7b respectively. The scattering amplitudes for an electron with momentum $\boldsymbol{k}$ corresponding to the above processes are:

$$J^2 \sum_{\sigma'' k''} \left\langle \sigma' M'_i \left| S_\nu S_\mu s^\nu_{\sigma' \sigma''} s^\mu_{\sigma'' \sigma} \right| \sigma M_i \right\rangle \frac{1 - n_{k''}}{\varepsilon_k - \varepsilon_{k''}} \tag{1.2.17}$$

$$J^2 \sum_{\sigma'' k''} \left\langle \sigma' M'_i \left| S_\nu S_\mu s^\nu_{\sigma'' \sigma} s^\mu_{\sigma' \sigma''} \right| \sigma M_i \right\rangle \frac{n_{k''}}{\varepsilon_k - \varepsilon_{k''}} \tag{1.2.18}$$

When these terms are added together one obtains:

$$J^2 \sum_{\sigma'' k''} \left[\left(\frac{1}{4} S\left(S+1\right) - \left\langle \sigma' M'_i \left| \sigma \cdot S \right| \sigma M_i \right\rangle \right) + \right.$$

$$\left. + \frac{n_{k''}}{\varepsilon_k - \varepsilon_{k''}} \left\langle \sigma' M'_i \left| \sigma \cdot S \right| \sigma M_i \right\rangle \right] \tag{1.2.19}$$

We note that the Fermi distribution function enters the expression for the total scattering amplitude at this order of the pertubation theory. This is explicitly due to the spin dependent potential, and would not appear in the ordinary scattering potential theory. The difference is that the second term in (1.2.19) is due to the many-body effect and must therefore depend on the Fermi statistics, while the potential scattering theory is a typical one-body problem.

Assuming the rectangular density of states in the band

$$\rho_0(\varepsilon) = \begin{cases} \rho_0 & -D < \varepsilon < D \\ 0 & \text{otherwise} \end{cases}$$

the second term will produce a contribution proportional to

$$-\rho_0 \log\left(\frac{k_B T}{D}\right) + \text{const.}$$

and the inverse relaxation time up to this order in the pertubation theory is:

$$\frac{1}{\tau} \approx 2\pi c J^2 S(S+1)\rho_0\left[1 + 4J\rho_0 \log\left(\frac{k_B T}{D}\right)\right] \qquad (1.2.20)$$

Since the resistivity is proportional to the relaxation rate, it follows that for antiferromagnetic coupling ($J<0$, which is the case here) it *increases* with decreasing temperature, as has been observed experimentally. Another important feature here is that the logarithmic term is dominant at low temperature, and in fact diverges at zero temperature. That necessitated extending the calculations to higher orders. It is not possible to build a systematic theory amenable to diagramatic methods in a straightforward fashion. This is the usual difficulty with the spin-dependent potential, where spin itself is a dynamical quantity. The relevant class of diagrams are so-called "parquet" diagrams which can be calculated in the so-called pseudofermion representation , where the

impurity spin is represented in terms of fermion creation and annihilation operators [12]. Those diagrams have been calculated in the so-called logarithmic approximation [12]. In that approximation, only the highest order logarithmic terms are retained at each level of the pertubation. The resistivity proportional to the imaginary part of the scattering amplitude, has been found to be

$$R(T) \propto \frac{J^2 S(S+1)}{\left[1 - 2J\,\rho_0 \log\left(k_B T / D\right)\right]^2} \qquad (1.2.21)$$

At this point it is clear that for antiferromagnetic coupling ($J<0$) the above expression diverges as T reaches the temperature T_K, where

$$T_K = \frac{D}{k_B} \exp\left(\frac{1}{2J\,\rho_0}\right) \qquad (1.2.22)$$

For weak antiferromagnetic coupling $k_B T_K << D$ and therefore it establishes a new low energy scale. Other quantities such as specific heat and magnetic susceptibility also exhibit the singularity at T_K, reminiscent of the phase transition. However, this is the single impurity problem and no phase transition can occur. The origin of those divergencies is due to the narrow resonance first found by Abrikosov [12] and Suhl [13], which is centered at the Fermi surface. This resonance is called Abrikosov-Suhl resonance, and is connected to a resonance found necessary to satisfy the Friedel sum rule and the assumption of the singlet ground state.

Now, if only electrons within a characteristic energy $k_B T_K$ are involved, this implies a spatial extent of (take $\hbar$=1):

$$\xi_K = \frac{v_F}{k_B T_K} \qquad (1.2.23)$$

where v_F is the group velocity of electrons in the conduction band at the Fermi surface. ξ_K represents the length of the conduction electron cloud screening the magnetic impurity through the antiferromagnetic coupling J.

It has been noticed by Nozieres [14] that if the system is in the singlet state, then the Fermi liquid approach can be used. His argument is based on the Anderson statement derived using the scaling approach [15] that in the low temperature limit the Kondo model evolves toward a fixed point in which J is infinitely strong, i.e. $J = -\infty$. In this case a spin-1/2 impurity traps a conduction electron, thereby forming a rigid singlet. For the conduction electron it acts as an nonmagnetic, infinitely repulsive impurity. However, if J is large but finite the virtual spin fluctuations become possible. This would produce an indirect interaction between conduction electrons through the singlet polarization, as in the phonon-mediated interaction. Therefore we have replaced a magnetic impurity in a noninteracting electron gas by a nonmagnetic impurity together with a "localized" interaction. In other words, we treat the limit $J = -\infty$ as the initial zero order state, and then we expand in powers of $1/J$, which induces the effective interaction among the conduction electrons. This way the impurity is out of the way, and we deal with an interacting Fermi liquid. The above argument serves as a justification for a phemenological "Fermi liquid" expansion of phase shifts.

d). Fermi Liquid Theory

In the spirit of the Landau theory of Fermi liquids, it is assumed that there is a one-to-one correspondence between the interacting and zero order eigenstates. This effectively precludes inclusion of any triplet and higher spin states. Such is the case when the excitation frequencies of higher spin states are much greater than $k_B T$. Since the interaction is localized it is convenient to describe

the quasiparticle eigenstates α in terms of the phase shift δ_α. In the interacting theory the phase shift depends on the energy ε_α of the state and the distribution of other particles n_β. Therefore one can write

$$\delta_\alpha\left(\varepsilon_\alpha, n_\beta\right) \tag{1.2.24}$$

We consider the expansion of the phase shift starting from the zero order state. Define:

$$\delta n_\beta = n_\beta - n_{\beta 0} \tag{1.2.25}$$

and $\delta n_\beta = \delta n_\sigma\left(\varepsilon_\beta\right)$ depends on the spin and energy of the quasiparticle. Therefore we expand (1.2.24) as:

$$\delta_\sigma(\varepsilon) = \delta_0(\varepsilon) + \sum_{\varepsilon', \sigma'} \phi_{\sigma\sigma'}(\varepsilon, \varepsilon')\, \delta n_{\sigma'}(\varepsilon') + \tag{1.2.26}$$

$$+ \sum_{\substack{\varepsilon', \sigma' \\ \varepsilon'', \sigma''}} \chi_{\sigma\sigma'\,\sigma''}(\varepsilon, \varepsilon', \varepsilon'')\, \delta n_{\sigma'}(\varepsilon')\, \delta n_{\sigma''}(\varepsilon'') + \ldots$$

Since the relevant excited states are close to the Fermi level (which we take to be zero) and assuming analyticity near the Fermi level, we can write:

$$\delta_0(\varepsilon) = \delta_0 + \alpha\varepsilon + \beta\varepsilon^2 + \ldots \tag{1.2.27}$$

$$\phi_{\sigma\sigma'}(\varepsilon, \varepsilon') = \phi_{\sigma\sigma'} + \psi_{\sigma\sigma'}(\varepsilon + \varepsilon') + \ldots$$

The above expansion coefficients describe the low temperature behavior phenomenologically.

At low T and H we need δ up to the first order in ε, T and H. Since δn is linear in T and H, only four quantities enter: δ_0, α, and $\phi_{\sigma,\pm\sigma} \equiv \phi^s \pm \phi^a$. The total number of electrons is constant and ϕ^s never shows up. Therefore we obtain:

$$\delta_\sigma(\varepsilon) = \delta_0 + \alpha\varepsilon + \sigma\phi^a m \tag{1.2.28}$$

where $m = n_\uparrow - n_\downarrow$ is the "molecular" field not present in the standard scattering theory. It arises, of course, from the virtual spin fluctuations of the singlet.

From (1.2.28) one can now calculate the thermodynamic response functions by writing

$$\tilde{\varepsilon}_\sigma = \varepsilon - \frac{\delta_\sigma(\varepsilon)}{\pi\rho_0} \tag{1.2.29}$$

where ρ_0 is the conduction electron density of states for one spin direction in the pure system. Hence at $H=0$ the change in the specific heat

$$\frac{\delta C_v}{C_v} = \frac{\alpha}{\pi\rho_0} \tag{1.2.30}$$

is due to the change in the density of states. Similarly for finite H and zero T from (1.2.28) and (1.2.29) we obtain:

$$\tilde{\varepsilon}_\sigma = \varepsilon - g\mu_B H - \frac{\alpha\varepsilon}{\pi\rho_0} - \frac{\sigma\phi^a m}{\pi\rho_0} \tag{1.2.31}$$

In equilibrium the Fermi levels for each spin direction are fixed by the conditions

$$\varepsilon_{\uparrow} = \varepsilon_{\downarrow} = \mu = 0$$

Then the Pauli susceptibility is

$$\chi = \frac{g\mu_B m}{H} = 2\rho_0 (g\mu_B)^2 \left[1 + \frac{\alpha}{\pi \rho_0} + \frac{2\phi^a}{\pi} \right] \qquad (1.2.32)$$

From (1.2.30) and (1.2.32) one approximately obtains:

$$\frac{\delta C_v}{C_v} + \frac{\delta \chi}{\chi} = 1 + \frac{2\phi^a \rho_0}{\alpha} \qquad (1.2.33)$$

where $2\phi^a \rho_0 / \alpha$ is the dimensionless quantity containing all the many body effects. It has been noted using Wilson's numerical renormalization group approach [16] that in the low temperature regime, i.e. $T << T_K$ in the limit $k_B T_K << D$ (which is the appropriate limit in the Kondo problem), $k_B T_K$ is the only relevant energy scale, which determines the behavior of the system. Therefore in this universal regime the above dimensionless constant is independent of T_K, and Wilson finds that

$$\frac{2\phi^a \rho_0}{\alpha} \approx 1$$

Therefore in the interacting case the ratio in (1.2.33) is 2 rather than 1.

The argument made by Nozieres has been extended to calculate the conductivity, where at low temperature one finds the T^2

dependence and the coefficient scales that temperature by T_K in the universality regime. The above approach has been further elaborated by Newns and Hewson [17], where the extension to degenerate systems (e.g. RE ions) and comparison to experiments have been made.

e). Large N-expansion in $1/N$.

It is clear that the above picture represents a mean-field or O(1) approximation. The idea has been to develop the pertubation theory that would produce above result in O(1) approximation, and to produce a controlled expansion in some small parameter at higher orders. This is where the so-called large-N expansion which incorporates several different but ultimately equivalent approaches is successful. This expansion has application in many systems which contain the integer valued parameter N. One example is the spin system where N is the number of spin components [18]. In such systems, the partition function may be written in the form

$$Z = \int_\sigma e^{-NS(\sigma)} \tag{1.2.34}$$

where $\int_\sigma$ indicates functional integration over all degrees of freedom and $S(\sigma)$ is independent of N. Such a form can be obtained by rescaling some parameters in the system. In such a form $1/N$ expansion is similar to expansion in powers of $\hbar$ in quantum mechanics. By that analogy $N \to \infty$ represents a classical limit.

The possibility of large-N expansion for magnetic alloys was first put forward by Anderson [19]. In such alloys N denotes the total angular momentum degeneracy, which could in principle be lowered by the crystal field effects. I will now review the main large-N theories, following mostly the review article of N.E. Bickers [20].

I will consider a single impurity degenerate Anderson Hamiltonian, appropriate for RE ions:

$$H = H_{band} + H_f + H_{mix} \tag{1.2.35}$$

$$H_{band} = \sum_{km} \varepsilon_k \; c^+_{km} c_{km}$$

$$H_f = \sum_m E_{0m} f^+_m f_m + U \sum_{m > m'} f^+_m f_m f^+_{m'} f_{m'}$$

$$H_{mix} = \sum_{km} \left[V(k) c^+_{km} f_m + h.c. \right]$$

Here f^+_m creates an atomic state with the magnetic quantum number m which varies between $-J$ and J. In view of the strong spin-orbit coupling for f-electrons total angular momentum is the appropriate quantum number. c^+_{km} is interpreted as the projection of the conduction electron wave function onto the state with the magnetic quantum number m defined relative to the position of the impurity. The above Hamiltonian can be somewhat simplified in the physically relevant limit of large U. For most RE systems U is the largest parameter in the theory, and may be taken to be infinite. In that case only the zero and single occupancy of RE ions is allowed. The idea now is to project out the states with zero and single occupancy and neglect higher occupancy states which lie well above the Fermi level.

Then the infinite-U Anderson model has the following form:

$$H = H_{band} + H_f + H_{mix} \tag{1.2.36}$$

where

$$H_{band} = \sum_{km} \varepsilon_k \; c^+_{km} c_{km} \tag{1.2.37}$$

describes a free electron band, while the localized f-state at lattice site i is represented by:

$$H_f = \sum_m E_{0m} f_m^+ f_m \tag{1.2.38}$$

Finally, the mixing term is written as:

$$H_{mix} = \sum_{km} \left[V(k) c_{km}^+ P_0 f_m + h.c. \right] \tag{1.2.39}$$

where the operator P_0 projects out states with no f-electrons, thereby taking into account the infinite U repulsion. The great difficulty in treating H_{mix} as a pertubation arises because the Hubbard operators, $X_{0m} = P_0 f_m$ and $X_{m0} = f_m^+ P_0$ do not obey standard fermion commutation rules [21, 22]. Therefore Wick's theorem is not applicable. This precludes the application of standard diagrammatic techniques. Keiter and Kimball [22], recognizing this situation, have developed a new time-dependent pertubation theory, which I will now review.

Let me first of all explain the basic idea behind the pertubation theory. Let us consider a general Hamiltonian, decomposed into zero order and pertubation parts:

$$H = H_0 + V \tag{1.2.40}$$

We will use a contour integral representation for the partition function

$$Z = \mathrm{Tr} e^{-\beta H} = \int_\Gamma \frac{dz}{2\pi i} e^{-\beta z} \mathrm{Tr} (z - H)^{-1} \tag{1.2.41}$$

where Γ is a contour in the complex plane, oriented clockwise and surrounding all singularities of the resolvent $(z - H)^{-1}$. The resolvent may be expanded as

$$(z - H)^{-1} = (z - H_0)^{-1} \sum_{n=0}^{\infty} \left[V (z - H)^{-1} \right]^n \qquad (1.2.42)$$

and therefore

$$Z = \int_{\Gamma} \frac{dz}{2\pi i} e^{-\beta z} \mathrm{Tr} \left((z - H_0)^{-1} \sum_{n=0}^{\infty} \left[V (z - H)^{-1} \right]^n \right) \qquad (1.2.43)$$

The trace can be evaluated by inserting a complete set of states $|N\rangle$ which are eigenstates of H_0 between consecutive factors $V (z - H)^{-1}$. Write:

$$\mathrm{Tr} \left((z - H_0)^{-1} \sum_{n=0}^{\infty} \left[V (z - H)^{-1} \right]^n \right) = \qquad (1.2.44)$$

$$= \langle N | (z - H_0)^{-1} | N \rangle + \langle N | (z - H_0)^{-1} | N \rangle \times$$

$$\langle N | V | N \rangle \langle N | (z - H_0)^{-1} | N \rangle + \langle N | (z - H_0)^{-1} | N \rangle \times$$

$$\langle N | V | M \rangle \langle M | (z - H_0)^{-1} | M \rangle \langle M | V | N \rangle \times$$

$$\langle N | (z - H_0)^{-1} | N \rangle + \ldots = \langle N | (z - H_0)^{-1} | N \rangle \Big[1 +$$

$$\langle N | (z - H_0)^{-1} | N \rangle \Big(\langle N | V | N \rangle + \langle N | V | M \rangle \times$$

$$\langle M|\frac{1}{z-H_0}|M\rangle\langle M|V|N\rangle+\ldots\Big)+\ldots\Big]=\langle N|\frac{1}{z-H_0}|N\rangle\times$$

$$\Big[1+\langle N|\frac{1}{z-H_0}|N\rangle\langle N|V+\frac{V\,Q_N}{z-H_0}V+\ldots|N\rangle$$

$$+\ldots\Big]=\langle N|(z-H_0)^{-1}|N\rangle\Big[1+\langle N|(z-H_0)^{-1}|N\rangle\times$$

$$\langle N|V\left(1-(z-H_0)^{-1}Q_N V\right)^{-1}|N\rangle+\ldots\Big]$$

where $Q_N \equiv 1-|N\rangle\langle N|$ projects away $|N\rangle$ as intermediate states. Define the diagonal matrix $\hat{\Sigma}(z)$ called a self-energy operator with its diagonal elements defined as:

$$\hat{\Sigma}_N(z)\equiv\langle N|\hat{\Sigma}(z)|N\rangle=\langle N|V\left(1-(z-H_0)^{-1}Q_N V\right)^{-1}|N\rangle \tag{1.2.45}$$

Then one can rewrite (1.2.44) in the closed form:

$$Z=\int_\Gamma \frac{dz}{2\pi i}e^{-\beta z}\,\mathrm{Tr}\left(\frac{1}{z-H_0}\sum_{n=0}^{\infty}\left[\hat{\Sigma}(z)\frac{1}{z-H_0}\right]^n\right)$$

$$=\int_\Gamma \frac{dz}{2\pi i}e^{-\beta z}\,\mathrm{Tr}\left(z-H_0-\hat{\Sigma}(z)\right)^{-1} \tag{1.2.46}$$

As the next step let us separate the n=0 term in (1.2.43) and we write:

$$Z - Z_0 = \int_\Gamma \frac{dz}{2\pi i} e^{-\beta z} \mathrm{Tr} \left(\frac{V}{(z - H_0)^2} \sum_{n=1}^{\infty} \left[\frac{V}{z - H_0} \right]^{n-1} \right) \tag{1.2.47}$$

where

$$Z_0 = \mathrm{Tr}\, e^{-\beta H_0} \tag{1.2.48}$$

The expression on the RHS of (1.2.47) can be rearranged as follows:

$$Z - Z_0 = -\beta \int_0^1 \frac{dg}{g} \int_\Gamma \frac{dz}{2\pi i} e^{-\beta z} \mathrm{Tr} \sum_{n=1}^{\infty} \left[\frac{gV}{z - H_0} \right]^n \tag{1.2.49}$$

where g is a variable $0 \leq g \leq 1$. Similar to the derivation above one can introduce the diagonal self-energy operator:

$$\hat{\Sigma}_N (z, g) \equiv \langle N | \hat{\Sigma} (z, g) | N \rangle =$$

$$= \langle N | gV \left(1 - (z - H_0)^{-1} Q_N gV \right)^{-1} | N \rangle \tag{1.2.50}$$

and the result is:

$$Z - Z_0 = \int_0^1 \frac{dg}{g} \int_\Gamma \frac{dz}{2\pi i} e^{-\beta z} \mathrm{Tr} \frac{\hat{\Sigma} (z, g)}{z - H_0 - \hat{\Sigma} (z, g)} \tag{1.2.51}$$

I will now apply the above pertubation expansion to the infinite-U Anderson model. Define the zero order Hamiltonian as (see (1.2.37) and (1.2.38)):

$$H_0 = H_f + H_{band} \tag{1.2.52}$$

and denote its eigenstates $|N\rangle = |N_f\rangle \times |N_{band}\rangle$ where $|N_f\rangle$ and $|N_{band}\rangle$ are the eigenstates of H_f and H_{band} respectively. Also define

$$H_{band}|N\rangle = E_N^{band}|N\rangle \tag{1.2.53}$$

$$Z_{band} = Tr_{band}\, e^{-\beta H_{band}} \tag{1.2.54}$$

We now want to separate the trace over localized and band states. To do that, we shift the contour integration as follows:

$$z \rightarrow z + E_N^{band}$$

Then using (1.2.46) one can write:

$$\frac{Z}{Z_{band}} = \int_\Gamma \frac{dz}{2\pi i} e^{-\beta z} \mathrm{Tr}_f \left(z - H_f - \hat{\Sigma}_f(z) \right)^{-1} \tag{1.2.55}$$

where the self-energy operator diagonal in $|N_f\rangle$ is defined as:

$$\hat{\Sigma}_f(z) \equiv \sum_{N_{band}} \frac{e^{-\beta E_N^{band}}}{Z_{band}} \langle N_{band} | \hat{\Sigma}\left(z + E_N^{band} \right) | N_{band} \rangle \tag{1.2.56}$$

and $\hat{\Sigma}(z)$ is defined in (1.2.50). One can replace (1.2.56) with an analogue of (1.2.51), and the result is:

$$\frac{Z}{Z_{band}} = 1 + N e^{-\beta E_0} \tag{1.2.57}$$

$$-\beta \int_0^1 \frac{dg}{g} \int_\Gamma \frac{dz}{2\pi i} e^{-\beta z} \mathrm{Tr}_f \frac{\hat{\Sigma}_f(z,g)}{z - H_f - \hat{\Sigma}_f(z,g)}$$

with

$$\hat{\Sigma}_f(z,g) = \hat{\Sigma}_f(z)\Big|_{V \to Vg}$$

One can evaluate $\hat{\Sigma}_f$ using the conventional diagrammatic rules. To do that we define the vacuum propagator as:

$$G_0(z,g) \equiv \langle 0 | \frac{1}{z - H_f - \hat{\Sigma}_f(z,g)} | 0 \rangle \qquad (1.2.58)$$

Similarly we define $G_m(z,g)$. The self-energy diagrams in the first two orders of $1/N$ are shown below in Figs. 8 and 9. Rules for evaluating those diagrams are taken from ref. [20], p. 857.and are listed in the Appendix 1.

The work can be cut in half by the the fact that vacuum contribution to the partition function is equal to the occupied-state contribution, found by cyclically permuting vertices which merely shifts the dummy integration variable leaving the integral unchanged (see Appendix 1). Therefore it is sufficient to calculate only the empty state contributions and multiply them by two. Therefore we write:

$$\frac{Z}{Z_{band}} = 1 + N e^{-\beta E_0} - \qquad (1.2.59)$$

$$-\beta \int_0^1 \frac{dg}{g} \int_\Gamma \frac{dz}{\pi i} e^{-\beta z} \mathrm{Tr}_f \frac{\hat{\Sigma}_0(z,g)}{z - H_0 - \hat{\Sigma}_0(z,g)}$$

The contribution to $\hat{\Sigma}_0$ at O(1) is shown in Fig. 8:

$$\hat{\Sigma}_0^{(1)}(z,g) = N(gV)^2 \sum_k \frac{n_k}{z + \varepsilon_k - E_0} \tag{1.2.60}$$

The contribution to $\hat{\Sigma}_0$ at O($1/N$) is shown in Fig. 9. At this order one considers one electron-hole pair beyond O(1) ground state:

$$\hat{\Sigma}_0^{(1/N)}(z,g) = \frac{(N(gV)^2)^2}{N} \sum_{k\,k'} \left\{ \frac{n_k(1-n_{k'})}{(z + \varepsilon_k - E_0)^2} \times \right.$$

$$\left. \times \frac{1}{z + \varepsilon_k - \varepsilon_{k'} - \hat{\Sigma}_0^{(1)}(z + \varepsilon_k - \varepsilon_{k'}, g)} \right\} \tag{1.2.61}$$

Let us now calculate the leading contribution to the partition function. Using (1.2.60) in (1.2.59) and integrating over g one obtains:

$$\frac{Z^{(1)}}{Z_{band}} = 1 + N e^{-\beta E_0} + \beta \int_\Gamma \frac{dz}{2\pi i} e^{-\beta z} \ln\left[\frac{z - \hat{\Sigma}_0^{(1)}(z)}{z} \right] \tag{1.2.62}$$

Integration by parts gives:

$$\frac{Z^{(1)}}{Z_{band}} = N e^{-\beta E_0} + \int_{\Gamma} \frac{dz}{2\pi i} e^{-\beta z} \frac{1 - \partial \hat{\Sigma}_0^{(1)}(z)/\partial z}{z - \hat{\Sigma}_0^{(1)}(z)} \tag{1.2.63}$$

The first term represents a contribution of completely localized (integral occupancy) f-electrons, while the second term represents an empty state contribution. The first term is of order $O(N)$ and therefore is dominant at high temperatures. However, at low temperatures it becomes exponentially small as the system goes into the mixed valence or Kondo regime. The partition function to $O(1/N)$ may be obtained in the similar fashion (see ref. [20], p.858).

The dominant contribution to (1.2.63) arises from a pole at ε_f, which is the most negative solution of the equation

$$\omega - \hat{\Sigma}_0^{(1)}(\omega) = 0 \tag{1.2.64}$$

For a rectangular density of states band at zero temperature one obtains:

$$\omega = \frac{N\Delta}{\pi} \int_{-D}^{0} d\varepsilon \frac{n(\varepsilon, \beta)}{\omega - E_0 + \varepsilon} = \frac{N\Delta}{\pi} \ln \left| \frac{E_0 - \omega}{D} \right| \tag{1.2.65}$$

Define the Kondo temperature as:

$$T_K \equiv E_0 - \varepsilon_f \tag{1.2.66}$$

Then in the Kondo limit $|E_0| >> N\Delta$ one obtains:

$$T_K = \frac{D}{k_B} \exp\left[\frac{\pi E_0}{N\Delta} \right] \tag{1.2.67}$$

Therefore in the low temperature regime where $T << T_K$ one obtains:

$$\frac{Z^{(1)}}{Z_{band}} = N e^{-\beta E_0} + e^{-\beta \varepsilon_f} \rightarrow e^{-\beta \varepsilon_f} \tag{1.2.68}$$

One can further calculate the valence, charge and magnetic susceptibilities as well as the specific heat at zero temperature:

$$n_f^{(1)} = \frac{\partial \varepsilon_f}{\partial E_0} \qquad \chi_c^{(1)} = \frac{\partial^{(2)} \varepsilon_f}{\partial E_0^{\,2}}$$

$$\chi^{(1)} = -\left. \frac{\partial^{(2)} \varepsilon_f}{\partial H^2} \right|_{H=0} \qquad C_v^{(1)} = -\left. \frac{\partial \varepsilon_f}{\partial T} \right|_{T \rightarrow 0} = \gamma^{(1)} T$$

Differentiating (1.2.65) with respect to the appropriate variables we obtain:

$$n_f^{(1)} = \frac{\mu}{1+\mu} \tag{1.2.69}$$

where

$$\mu = \frac{N\Delta}{\pi T_K}$$

and

$$\chi_c^{(1)} = \frac{\pi}{N\Delta}\left[n_f^{(1)}\right]^2\left[1 - n_f^{(1)}\right] \tag{1.2.70}$$

$$\chi^{(1)} = \frac{(g\mu_B)^2}{3T_K} n_f^{(1)} \tag{1.2.71}$$

$$\gamma^{(1)} = \frac{\pi^2 k_B^2}{3T_K} n_f^{(1)} \tag{1.2.72}$$

The Sommerfeld ratio has the value

$$R^{(1)} = \frac{\pi^2 k_B^2 \chi^{(1)}}{(g\mu_B)^2 \gamma^{(1)}} = 1 \tag{1.2.73}$$

at the order O(1) in the large-N expansion. This is the result for the noninteracting Fermi gas of quasiparticles. These calculations can be extended to the next order $1/N$ in the pertubation theory (see [20]). Then one obtains:

$$R = \frac{\pi^2 k_B^2 \chi}{(g\mu_B)^2 \gamma} = 1 + \frac{1}{N}\left(1 - \frac{1}{(1+\mu)^2}\right) + O\left(1/N^2\right) \tag{1.2.74}$$

This relation satisfies the Fermi liquid relation [23-25]

$$R = \frac{N}{N-1}\left(1 - \frac{\pi^2 k_B^2 \chi_c}{3N\gamma}\right) \tag{1.2.75}$$

at this order of the pertubation theory. This conclusion can also be extended to $1/N^2$ [26]. The source of the Fermi-liquid-like corrections is the appearance of singlet electron-hole pairs which do not couple to the magnetic field but do change the effective density of states near the Fermi surface sampled by the specific heat. The fact that the above formula satisfies the exact Fermi-liquid relation at each order of the pertubation theory could be interpreted as an

indication that the large-N expansion is convergent. Further evidence supporting this conclusion has been obtained by Rasul and Hewson [27] where they compared the large-N expansion to the Bethe ansatz at first two orders of the pertubation theory. This still however leaves unaddressed the problem of what happens for low N. It is in fact very clear that N=2 is the appropriate regime for RE or actinide metal, where the low value of N is due to the relatively large (as compared to the level width) crystal-field splitting.

The above technique can be extended to calculate the propagator, spectral density and other dynamical quantities (see [20]). The important point here, however, is that the spectral density so obtained does satisfy the Friedel's sum rule. It also produces a δ - function singularity at $\omega = k_B T_K$ with the weight $1 - n_f^{(1)}$ in the leading order of the pertubation theory.

The above singularity indicates that the narrow resonance at $\omega = k_B T_K$ is a many particle resonance, which means that a large number of electron-hole excitations have to be included in the intermediate state in the pertubation expansion. Likewise the above expansion is a low temperature expansion, that diverges at $T = T_K$. Again, the problem is that at higher temperatures there is a large number of electron-hole excitations in the intermediate state. This in principle necessitates the summation of all the diagrams. This is of course not feasible. It is, however, possible to do the partial resummation as in RPA or similar self-consistent approximation.

f). Partial Resummation Within the Noncrossing Approximation.

To motivate this partial resummation technique, note that the diagrams contributing to the partition function at O(1) and O(1/N) (see Figs. 8 and 9) have noncrossing conduction lines. It turns out to be possible to sum *all* noncrossing diagrams, which are represented in Fig. 10. In that case one obtains:

$$\Sigma_0(z) = NV^2 \sum_k n_k G_m(z + \varepsilon_k) \tag{1.2.76}$$

$$\Sigma_m(z) = V^2 \sum_k (1 - n_k) G_0(z - \varepsilon_k) \tag{1.2.77}$$

where

$$G_0(z) = \frac{1}{z - \Sigma_0(z)} \tag{1.2.78}$$

$$G_m(z) = \frac{1}{z - E_0 - \Sigma_m(z)} \tag{1.2.79}$$

This approximation is referred to as "noncrossing approximation", or NCA (Kuramoto [28]), and the "self-consistent approximation" or SCA (Maekawa et al. [29] and Bickers [30]). The above equations are called NCA integral equations. At zero temperature they take the following form:

$$\Sigma_0(\omega + i0^+) = \frac{N\Delta}{\pi} \int_{-D}^{D} d\varepsilon \; n(\varepsilon, \beta) G_m(\varepsilon + \omega + i0^+)$$

$$= \frac{N\Delta}{\pi} \int_{-D+\omega}^{\omega} d\varepsilon \; G_m(\varepsilon + i0^+) \tag{1.2.80}$$

$$\Sigma_m(\omega + i0^+) = \frac{\Delta}{\pi} \int_{-D}^{D} d\varepsilon \; (1 - n(\varepsilon, \beta)) G_0(\omega - \varepsilon + i0^+)$$

$$= \frac{\Delta}{\pi} \int_{-D+\omega}^{\omega} d\varepsilon \; G_0(\varepsilon + i0^+) \tag{1.2.81}$$

Since $D >> N\Delta$, we ignore the ω-dependence of the lower limit of integration. Differentiating with respect to ω obtain:

$$\frac{\partial \Sigma_0}{\partial \omega} = \frac{N\Delta}{\pi} G_m(\omega) \qquad \frac{\partial \Sigma_m}{\partial \omega} = \frac{\Delta}{\pi} G_0(\omega) \tag{1.2.82}$$

We solve the above pair of coupled differential equations with the initial condition

$$\Sigma_m(-D) = \Sigma_0(-D) = 0 \tag{1.2.83}$$

which is consistent with neglecting the ω -dependence of the lower limit of integration in (1.2.80-81). Now let us introduce the notation

$$Y_0(\omega) = -G_0(\omega)^{-1} \qquad Y_m(\omega) = -G_m(\omega)^{-1} \tag{1.2.84}$$

Then one obtains the following coupled equations:

$$\frac{dY_0(\omega)}{d\omega} = -1 - \frac{N\Delta}{\pi} Y_m^{-1}(\omega) \tag{1.2.85}$$

$$\frac{dY_m(\omega)}{d\omega} = -1 - \frac{\Delta}{\pi} Y_0^{-1}(\omega) \tag{1.2.86}$$

with

$$Y_0(-D) = D \qquad Y_m(-D) = D + E_0 \tag{1.2.87}$$

Dividing the second equation by the first obtain:

$$\left(1 + \frac{N\Delta}{\pi} Y_m^{-1}\right) dY_m = \left(1 + \frac{\Delta}{\pi} Y_0^{-1}\right) dY_0 \tag{1.2.88}$$

Integrating this equation and using the initial conditions gives:

$$Y_m + \frac{N\Delta}{\pi} \ln(Y_m / D) - E_0 = Y_0 + \frac{\Delta}{\pi} \ln(Y_0 / D) \tag{1.2.89}$$

Now using (1.2.85) and (1.2.89) we will determine $\omega\left(Y_0\right)$, which would allow us to calculate the ground state energy. Integrating (1.2.85) with respect to Y_0 write:

$$\int_{-D}^{\omega} d\varepsilon = -\int_{D}^{Y_0} \frac{dx}{1+(N\Delta/\pi)Y_m^{-1}(x)} \tag{1.2.90}$$

$$= \frac{N\Delta}{\pi}\int_{D}^{Y_0} \frac{dx}{(N\Delta/\pi)+Y_m(x)} - \left(Y_0 - D\right) \tag{1.2.91}$$

and we finally obtain:

$$\omega = -Y_0 - \frac{N\Delta}{\pi}\int_{Y_0}^{D} \frac{dx}{(N\Delta/\pi)+Y_m(x)} \tag{1.2.92}$$

It has been established numerically by Kuramoto and Kojima [31] that at the ground state energy E_G^{NCA} the inverse propagators Y_0 and Y_m vanish, and below that they are pure real. However there is no rigorous proof that this ansatz is correct. Using that ansatz one obtains:

$$E_G^{NCA} = -\frac{N\Delta}{\pi}\int_{0}^{D} \frac{dx}{(N\Delta/\pi)+Y_m(x)} \tag{1.2.93}$$

From the expression for the ground state energy, one can derive the expression for valence, charge and magnetic susceptibilities, etc. The results agree with the $1/N$ expansion up to $O(1/N)$, but not at higher orders. This is because contributions in the higher order also come from crossing diagrams, which are neglected in this approximation. It then can be explicitly shown that the derived self-energy and spectral density do not satisfy zero temperature Fermi-liquid relations established to all orders of pertubation theory

for infinite-U Anderson model by Yamada [23]. Higher temperature behavior however agrees well with the Bethe ansatz (see [30]). Within the NCA approximation Bickers, Cox, and Wilkins have investigated the scaling properties of the Kondo resonance at low temperature [30]. The resonance shows the approximate universality in terms of the reduced temperature T / T_K and frequency $\omega / k_B T_K$. As the temperature increased through T_K the resonance gradually melts away in contrast to the singular behavior in the large-N expansion. In that sense the large-N expansion and NCA can be considered as complimentary theories for a single Kondo impurity.

g). Slave Boson Model

The success of the diagrammatic techniques in treating the single impurity problem was offset by the difficulty in extending those techniques to the lattice problem. Therefore another approach more amenable to such extension has been developed. It relies on Piers Coleman's "slave boson" trick [32], which I will describe now.

The basic idea is to represent the Hubbard operators $X_{0m} = P_0 f_m$ and $X_{m\,0} = f_m^+ P_0$ as follows:

$$X_{0m} \rightarrow b^+ f_m \qquad X_{m\,0} \rightarrow f_m^+ b \tag{1.2.94}$$

where b^+, b are boson creation and annihilation operators, along with the constraint:

$$Q \equiv \sum_m n_m^f + < b^+ b > = 1 \tag{1.2.95}$$

Here < > denotes an operator average over the states generated by the Hamiltonian. Eq. (1.2.95) now replaces a much more awkward inequality:

$$\sum_m n_m^f \leq 1 \tag{1.2.96}$$

appropriate for the infinite-U Anderson model. Then the Hamiltonian (1.2.36) becomes:

$$H = H_{band} + H_f + H_{mix} \tag{1.2.97}$$

where as before

$$H_{band} = \sum_{km} \varepsilon_k \, c_{km}^+ c_{km} \tag{1.2.98}$$

$$H_f = \sum_m E_{0m} f_m^+ f_m \tag{1.2.99}$$

While the mixing term is written as:

$$H_{mix} = \sum_{km} \left[V(k) c_{km}^+ b^+ f_m + h.c. \right] \tag{1.2.100}$$

At low temperatures it is adequate to introduce the constraint in the average way (see [33], [34]). Below I will show a more precise way of introducing the constraint that relies on the path integral formalism. Then we write:

$$H \rightarrow H + \lambda (Q - 1) \tag{1.2.101}$$

In the mean-field approximation [32-34], the Hubbard operators are substituted by

$$X_{0m} \rightarrow z^{1/2} f_m$$

$$X_{m0} \rightarrow f_m^+ z^{1/2} \tag{1.2.102}$$

where

$$< b > = < b^{+} > = z^{1/2}$$

This mean field approximation is exact in the infinite-N limit, and as such serves as an appropriate starting point for the large-N expansion. Then the mean-field Hamiltonian becomes:

$$H = \sum_{km} \varepsilon_k \, c_{km}^{+} c_{km} + \sum_{m} \varepsilon_f \, f_m^{+} f_m \qquad (1.2.103)$$

$$+ \sum_{km} \left[z^{1/2} V(k) c_{km}^{+} f_m + H.C. \right] + (\varepsilon_f - E_0)(z - 1)$$

where

$$\varepsilon_f \equiv E_0 + \lambda \qquad (1.2.104)$$

To estimate z, we use the Hellman-Feynman theorem

$$\frac{\partial \langle H(\lambda) \rangle}{\partial \lambda} = \left\langle \frac{\partial H}{\partial \lambda} \right\rangle$$

and we obtain:

$$z = 1 - \langle n_f \rangle \qquad (1.2.105)$$

Similarly, differentiating with respect to z, we obtain:

$$z^{-1/2} VN \sum_{k} \langle f_m^{+} c_{km} \rangle = E_0 - \varepsilon_f \qquad (1.2.106)$$

The propagator corresponding to the mean-field Hamiltonian has the following form:

$$G_f(\varepsilon) = \frac{1}{\varepsilon - \varepsilon_f - \Sigma_f(\varepsilon)} \tag{1.2.107}$$

where

$$\Sigma_f(\varepsilon) = \sum_k \frac{zV^2}{\varepsilon - \varepsilon_k + i0^+} \approx -i\pi V^2 \rho \tag{1.2.108}$$

and the obtained density of f-states is then:

$$\rho_f(\varepsilon) = \frac{\pi^{-1}\Delta}{(\varepsilon - \varepsilon_f)^2 + \Delta^2} \tag{1.2.109}$$

where Δ represents a renormalized Lorentzian half-width and is given by the "golden rule":

$$\Delta = \pi z V^2 \rho \tag{1.2.110}$$

which is to be compared to an unrenormalized half-width:

$$\Delta_0 = \pi V^2 \rho \tag{1.2.111}$$

Since $z<1$, the effect of the Coulomb repulsion is to narrow the width of the coupled f-level by essentially suppressing the possible charge fluctuations that would violate the constraint (1.2.95). It also shifts it by λ, which I will now calculate.

To do that I will use (1.2.106). The expectation value $\sum_k \langle f_m^+ c_{km} \rangle$ may be obtained from the f-conduction electron propagator G_{fc}

$$G_{fc} = VG_f G_0$$

so that

$$\sum_k \left\langle f_m^{+} c_{km} \right\rangle = \frac{-z^{1/2} V}{\pi} \mathrm{Im} \int d\varepsilon \; n(\varepsilon) G_f(\varepsilon) G_0(\varepsilon) \quad (1.2.112)$$

Here

$$G_0(\varepsilon) = \sum_k \frac{1}{\varepsilon - \varepsilon_k + i0^{+}} \quad (1.2.113)$$

is the bare conduction-electron propagator. Again, assuming a rectangular conduction band density of states we obtain at zero temperature:

$$\sum_k \left\langle f_m^{+} c_{km} \right\rangle = \frac{-z^{1/2} \Delta_0}{\pi V} \mathrm{Im} \int_{-D}^{0} d\varepsilon \; \frac{n(\varepsilon)}{\varepsilon - \varepsilon_f + i\Delta}$$

$$= \frac{z^{1/2} \Delta_0}{2\pi V} \ln\left(\frac{\sqrt{\varepsilon_f^{\,2} + \Delta^2}}{D} \right) \quad (1.2.114)$$

Now inserting (1.2.114) into (1.2.106) we obtain the energy shift

$$E_0 - \varepsilon_f = \frac{N \Delta_0}{\pi} \ln\left(\frac{\sqrt{\varepsilon_f^{\,2} + \Delta^2}}{D} \right) \quad (1.2.115)$$

The above equation has a solution in the Kondo limit, where E_0 is large negative. In that case we neglect ε_f on the LHS of (1.2.115), and finally obtain:

$$T_K \equiv \sqrt{\varepsilon_f^2 + \Delta^2} = \frac{D}{k_B} \exp\left(\frac{\pi E_0}{N \Delta_0} \right) \quad (1.2.116)$$

We see now how the low temperature scale, similar to (1.2.67) emerges in this theory. In fact the equivalence of the Keiter-Kimball diagrammatic technique and the slave boson approach has been clearly demonstrated by Bickers [20] at each level of the pertubation theory. Therefore the results for all the thermodynamic quantities obtained within the slave boson approach are similar to those obtained above. Also all of the appropriate Fermi-liquid relations are similarly satisfied.

The main advantage of the slave boson approach is that it allows us to apply the standard diagrammatic techniques for electron-boson interaction. In this particular case two bosonic fields emerge. One field can be obtained by expanding in powers $b - \langle b \rangle$, while the second field is obtained by expanding λ around its mean-field value $E_0 - \varepsilon_f$. The most natural way to do that is to use the path-integral representation which was developed by Read and Newns [33,34]. Let me now briefly sketch that theory.

h). Path Integral Approach

We again start with the Hamiltonian (1.2.97). Adding the constraint (1.2.95) and applying the path-integral formalism we obtain the partition function:

$$Z = \int \frac{i\beta\, d\lambda}{2\pi} \int Db\, Db^{+} Df\, Df^{+} Dc\, Dc^{+} \exp\left[- \int_0^\beta d\tau\, L(\tau) \right] \tag{1.2.117}$$

where

$$L(\tau) = b^{+} \frac{d}{d\tau} b + \sum_m f_m^{+} \left(\frac{d}{d\tau} + E_0 \right) f_m$$

$$+ \sum_m c_{km}^{+} \left(\frac{d}{d\tau} + \varepsilon_k \right) c_{km} + V \sum_{km} \left[c_{km}^{+} b^{+} f_m + H.C. \right]$$

$$+ i\lambda\,(Q - 1) \tag{1.2.118}$$

and Db , Db^{+}, etc. denote the path integral measure, while the fermion operators f and c are represented by Grassman variables.

The above representation of fermion and boson operators is sometimes referred to as the "cartesian gauge". We now make a transformation to polar coordinates (or to the so called "radial gauge"):

$$b\,(\tau\,) = r\,(\tau\,)\exp(i\,\theta\,(\tau\,)) \tag{1.2.119}$$

so that $db\,db^{+} = r\,dr\,d\Theta$, and other quantities transform as follows:

$$f_m\,(\tau\,) \rightarrow f_m\,(\tau\,)\exp(-\,i\,\theta\,(\tau\,)) \tag{1.2.120}$$

$$c_k\,(\tau\,) \rightarrow c_k\,(\tau\,)$$

$$\lambda \rightarrow \lambda + \frac{\partial \Theta}{\partial \tau}$$

In terms of the transformed quantities we now obtain:

$$Z = \int \frac{i\,\beta\,d\lambda}{2\pi} \int Db\;Db^{+}\,Df\;Df^{+}\,Dc\;Dc^{+} \exp\left[-\int_0^{\beta} d\tau\, L'(\tau\,)\right] \tag{1.2.121}$$

where

$$L'(\tau\,) = \sum_m f_m^{+}\left(\frac{d}{d\tau} + E_0 + i\lambda\right) f_m + \sum_m c_{km}^{+}\left(\frac{d}{d\tau} + \varepsilon_k\right) c_{km}$$

$$+ Vr \sum_{km}\left[\,c_{km}^{+} f_m + H\,.\,C\,.\right] + i\lambda\,(r^{\,2} - 1) \tag{1.2.122}$$

In this gauge $\theta(\tau)$ disappears, as well as the term $\int_0^\beta r \frac{\partial r}{\partial t} d\tau$ due to the periodicity of b^+, b between 0 and β.

The mean-field or static approximation can be obtained as the saddle point of the above propagator. The corresponding r-saddle point r_0 is identified as $z^{1/2}$ (see (1.2.102-104)), and the λ-saddle point is identified as $\varepsilon_f - E_0$. The results at the mean-field level

$$z = 1 - \langle n_f \rangle$$

$$E_0 - \varepsilon_f = \frac{N \Delta_0}{\pi} \ln\left(\frac{\sqrt{\varepsilon_f^2 + \Delta^2}}{D} \right)$$

are then completely equivalent to the results obtained above.

To go beyond the mean-field approximation, we expand r and λ around their mean-field values. The diagrams are similar to those in the "cartesian gauge" and are sketched in Fig. 11. It is not surprising then that the corrections that emerge are also similar to the ones obtained in the Keiter-Kimball diagrammatic technique, and in particular the Wilson ratio satisfies the Fermi-liquid relation (1.2.75).

The difference between the two gauges are mainly in manipulations and they clearly emerge as one goes beyond the mean-field level. The radial gauge formulation has the advantage that the constraint (1.2.95) is treated in the natural way without a need of introducing a Legendre-type transformation. There is another problem, which is a little more profound and it emerges once we extend the slave boson model to the lattice of impurities which I will consider below. But before I generalize this discussion to the lattice problem, let me close the review of the single impurity problem by discussing the variational ansatz. That approach draws upon the analogy to ^3He, and uses the Gutzwiller variational ansatz

[35-37]. Consider the nondegenerate Anderson Hamiltonian (1.2.3). Then the variational ansatz for the ground state has the following form:

$$| \psi \rangle = [1 - n^f_\uparrow n^f_\downarrow] \prod_{k\sigma} [1 + a(\mathbf{k}) f^+_{k\sigma} c_{k\sigma}] | FS \rangle \qquad (1.2.123)$$

where the projection operator P is defined as:

$$P \equiv [1 - n^f_\uparrow n^f_\downarrow] \qquad (1.2.124)$$

P is applied to exclude double occupancy, and $a(\mathbf{k})$ serves as the variational coefficient. The variational treatment gives the result equivalent to substituting for P its average value. As in a slave boson model above, such approximation would renormalize the hybridization term. Since at this level of calculations at most one electron-hole excitation is included, the determination of the ground state becomes a one body calculation. Higher order approximations result from including the additional electron-hole pairs to the zero order state. The results at zero temperature are equivalent to the slave boson model. In fact, a theoretical equivalence between two theories has recently been demonstrated [38].

The upside of this theory is its physical simplicity, as it is most clearly connected to the Fermi liquid theory. Indeed it can be shown [39] that the higher order states generated this way can be placed in one-to-one correspondence to the noninteracting Fermi sea. Also it may be possible to extend the variational approach to more realistic models than the one considered above. The down side of the variational approach is that it cannot be trivially extended to higher temperatures and the expansion itself is not well controlled.

i). Lattice Theories

Let me now turn my attention to the lattice of impurities. The localized f-electrons acquire an additional site index μ. Then the corresponding Anderson Hamiltonian becomes (compare to (1.2.3)):

$$H = H_{band} + H_f + H_{mix} \tag{1.2.125}$$

$$H_{band} = \sum_{k\sigma} \varepsilon_k \, c^+_{k\sigma} c_{k\sigma}$$

$$H_f = \sum_{\mu m} E_{0m} f^+_{\mu m} f_{\mu m} + U \sum_{\mu,\, m' > m} f^+_{\mu m} f_{\mu m} f^+_{\mu m'} f_{\mu m'}$$

$$H_{mix} = \frac{1}{\sqrt{N_L}} \sum_{\mu m k \sigma} \left[V(k) c^+_{k\sigma} f_{\mu m} + H.C. \right]$$

where N_L denotes the number of lattice sites. In the single impurity problem one could represent the conduction electron wave function as a sum of harmonics with different values of quantum numbers l, m_l. Thus the mixing term would be proportional to $c^+_{km} f_{\mu m}$, and all other harmonics with different J would become decoupled. In that form the Hamiltonian possesses a $1/N$ expansion. This, however, is not the case in the lattice, where conduction electrons propagate from site to site and J is not conserved. In two key works on the subject [40] and [41] this complication is ignored and the mixing term of the type $c^+_{km} f_{\mu m}$ is introduced. In my view that simplification misses some important physics that I will discuss in Sec. 4. In any case, by making that approximation the problem then does possess a $1/N$ expansion.

In the reference [40] the "cartesian gauge" has been used. This gauge leads to the appearance of the infrared divergencies which cancel order by order in all physical quantities. The origin of this divergence has to do with the fact (see [42]) that in the zero order

theory we fix the phase of bosonic fields at all sites. Since the phase of any quantum field and the number operator are two conjugate quantities it follows that there is an infinite uncertainty in the number operator. This then violates the condition (1.2.95). Therefore in a true ground state there can be no correlation between different sites (since (1.2.95) is a local constraint) and the mean-field ansatz does in fact break that symmetry. Therefore the fluctuations must act to restore the symmetry. This results in an infinite number of "soft" excitations which are responsible for infrared divergencies.

Such complication can be avoided if one considers this problem in the radial gauge [41]. Then no explicit phase correlation is required and no such divergencies appear. The disadvantage of the radial gauge approach is that the functional integral treatment is not as transparent and the transformed f-operators have no direct physical meaning. Therefore, following [40], I choose to represent the theory in the "cartesian" gauge.

Let me now briefly sketch the principal results of [40]. We start with an infinite-U lattice Anderson Hamiltonian

$$H = H_{band} + H_f + H_{mix} \tag{1.2.126}$$

where as before

$$H_{band} = \sum_{km} \varepsilon_k \; c_{km}^{+} c_{km} \tag{1.2.127}$$

$$H_{mix} = \frac{1}{\sqrt{N_L}} \sum_{km} \left[V(k) c_{km}^{+} b_{\mu}^{+} f_{\mu m} + H.C. \right] \tag{1.2.128}$$

Again we introduce an additional constraint

$$Q_{\mu} \equiv \sum_{m} n_{\mu m}^{f} + < b_{\mu}^{+} b_{\mu} > = 1 \tag{1.2.129}$$

Then again we introduce a Legendre-type transformation and write:

$$H \rightarrow H + \sum_{\mu} \lambda_{\mu} \left(Q_{\mu} - 1 \right)$$

Transforming the Hamiltonian to the k-representation obtain:

$$H' = \sum_{km} \left\{ \varepsilon_k \; c^{+}_{km} c_{km} + E_{0m} f^{+}_{km} f_{km} + V \sum_{q} \left[c^{+}_{km} b^{+}_{q-k} f_{qm} + HC \right] \right\} \tag{1.2.130}$$

To generate the $1/N$ expansion one redefines several physical quantities:

$$\tilde{A}_{\mu} \equiv \frac{1}{\sqrt{N}} b_{\mu} \tag{1.2.131}$$

$$V_0 \equiv \frac{V}{\sqrt{N}}$$

$$1 = Q_{\mu} \equiv q_0 N$$

where one regards q_0 as independent of N, and at the end of the expansion set $q_0 = 1/N$. This effectively substitutes large-N limit by the thermodynamic limit. Note that large-N limit is *not* a thermodynamic limit because of the local constraint (1.2.129). Going to the thermodynamic limit one effectively substitutes the local constraint by the state that satisfies the constraint only in the average way (i.e. the constraint is averaged over all sites) which might or might not be correct. Formally taking $q_0 = 1/N$ pushes us beyond the region of validity of $1/N$ expansion, and there is no general proof that the corresponding series is still convergent.

Let me at any rate proceed with the theory. As in the single impurity problem they make a broken symmetry ansatz:

$$< \tilde{A}_{\mu} > = < \tilde{A}^{+}_{\mu} > = z^{1/2} \qquad (1.2.132)$$

$$\tilde{\lambda}_{\mu} = \varepsilon_f - E_0$$

Going to the wave vector representation one obtains:

$$< \tilde{A}_k > = < \tilde{A}^{+}_k > = z^{1/2} \delta_{k0} \qquad (1.2.133)$$

$$\tilde{\lambda}_k = (\varepsilon_f - E_0) \delta_{k0}$$

and shifting the above quantities so that

$$\tilde{A}_k = A_k + z^{1/2} \delta_{k0} \qquad (1.2.134)$$

$$\tilde{\lambda}_k = \lambda_k + (\varepsilon_f - E_0) \delta_{k0}$$

Then one may rewrite (1.2.126) as:

$$H = H_0 + H_{\text{int}} + H_A \qquad (1.2.135)$$

$$H_0 = \sum_{km} \varepsilon_k \; c_{km}^{+} c_{km} + \varepsilon_f \, f_{km}^{+} f_{km} + Vz^{1/2}\left[c_{km}^{+} f_{km} + HC \right]$$

$$+ N \sum_k (\varepsilon_f - E_0) A_k^{+} A_k + Nz^{1/2} \sum_k \lambda_k \left(A_k^{+} + A_k \right)$$

$$H_{\text{int}} = V \sum_{km} \left[c_{km}^{+} A_q^{+} f_{k+qm} + H.C. \right]$$

$$+ \sum_{kq} \lambda_q \left(N A_{k+q}^{+} A_k + \sum_m f_{k+qm}^{+} f_{km} \right)$$

$$H_A = N (\varepsilon_f - E_0) z^{1/2} \left(A_0^{+} + A_0 \right) + N (z - q_0) \lambda_0$$

The zero order Hamiltonian already contains the mean-field contribution. It can be diagonalized by appropriate Bogoliubov-type transformation and the dispersion relations obtained are as follows

$$\lambda_{1(2)} = \frac{1}{2} \left(\varepsilon_k + \varepsilon_f \pm \sqrt{(\varepsilon_k - \varepsilon_f)^2 + 4zV^2} \right) \qquad (1.2.136)$$

and are plotted in Fig. 12. We can now define bare fermion Green's functions:

$$G_c^{\,m}(k, \tau) = \left\langle T_\tau \, c_{km}(\tau) c_{km}^{+} \right\rangle_0 \qquad (1.2.137)$$

$$G_f^{\,m}(k, \tau) = \left\langle T_\tau f_{km}(\tau) f_{km}^{+} \right\rangle_0$$

$$G_m^{\,m}(k, \tau) = \left\langle T_\tau f_{km}(\tau) c_{km}^{+} \right\rangle_0$$

plus the bare boson propagator

$$D_0(k,\tau)=\begin{bmatrix} \langle T_\tau A_k^{+}(\tau)A_k\rangle_0 & \langle T_\tau A_k^{+}(\tau)A_{-k}^{+}\rangle_0 \\ \langle T_\tau A_{-k}(\tau)A_k\rangle_0 & \langle T_\tau A_k(\tau)A_k^{+}\rangle_0 \end{bmatrix} \tag{1.2.138}$$

The fermion and bosons interact via H_{int}, and the appropriate graphs are sketched in Fig. 13. The terms in H_A and the last term in H_{int} lead to tadpole diagrams sketched in Fig. 14. Requiring that those diagrams vanish determines ε_f and z, and one obtains:

$$q_0 = z\left(1+\rho_0 V^2/\varepsilon_f\right) \equiv z\,\rho_0 V^2/\varepsilon_f \tag{1.2.139}$$

$$\varepsilon_f = D\exp\left(E_0/\rho_0 V^2\right)$$

where ρ_0 is the conduction electron density of states per spin, and the rectangular density of states in the band is assumed:

$$\rho_0(\varepsilon)=\begin{cases}\rho_0 & -D<\varepsilon<D\\ 0 & \text{otherwise}\end{cases}$$

The Eq. (1.2.139) and the corresponding dynamical quantities are similarto the single impurity result. The Sommerfeld ratio defined in (1.2.73) is one. Going to the next order of the theory, one obtains ε_f and z beyond their mean-field values from the higher order tadpole diagrams in Fig. 15. Then the contributions to the free energy come from the higher order loop diagrams (see Fig. 16) and also by putting the higher order corrections to ε_f and z in lower order diagrams. Then the calculated Sommerfeld ratio to the order $O(1/N)$ becomes:

$$R = \frac{1}{1 - a / N} \qquad (1.2.140)$$

where

$$a = 1 - \left(1 - n_f\right)^2$$

so that $a \approx 1$ in the Kondo limit. Therefore the criterion for the system to be stable against magnetic ordering is just

$$N > 1$$

Note that the Sommerfeld constant is slightly greater than one, whereas in the experimental results for HFS R is typically of order 0.4, so there is some discrepancy with experiments.

Let me now turn to the discussion of the differences between this picture and the single impurity problem. It has been discussed above that the mechanism for the spin compensation in the single impurity case is the formation of the conduction cloud of opposite spin around the impurity. The characteristic dimension of that cloud is $\xi_0 = v_F / k_B T_K$, where v_F is the Fermi velocity.

This picture cannot be extended to the lattice since ξ_0 is much greater than the lattice constant. Also since the characteristic low energy scale is $k_B T_K$, the number of conduction electrons within $k_B T_K$ of the Fermi surface is $\approx k_B T_K / D$ which is much less than one. Therefore the mechanism of spin compensation must be fundamentally different from the single impurity problem. To resolve this problem the authors calculated the imaginary part of the dynamical susceptibility which shows that after a time long compared to ε_f^{-1} the f-electrons get delocalized: this is not a bound orbital but a resonance since it lies within the conduction band.

Then they argue that the Pauli principle makes it unfavorable to put the f-electrons in the same spin state (i.e. there is more phase space for electrons with opposite spins). Then it is unnecessary to form a compensating cloud at each site.

While this seems like a very plausible mechanism for spin compensation I see two problems with this picture. First of all in the limit $n^f \rightarrow 1$ the f-electrons cannot very well hop from site to site since most sites are already occupied. Then it is not clear how the proposed theory can adequately account for the observed spin compensation in HFS. There is however another more fundamental problem. This theory does not explain the mechanism for the observed low temperature coherence in HFS. In fact, I will show in Sec. 4 how those the questions of spin compensation and low temperature coherence are intimately related, which leads to new physics not obtained within the slave boson or other Fermi-liquid theory.

2. A New Approach to the Functional Integral Formalism

2.1 Review of the Standard Formalism

Consider a system where there is a multitude of interactions between the individual members (subsystems) of that system. In the extreme case one would need to consider all those interactions in order to form a proper description of the dynamics of that system. One important approach to dealing with that problem is the Green's Function method [43]. One needs to calculate the single particle Green's Functions in order to obtain the one-particle spectrum, or many-particle Green's Functions in order to calculate the possible collective excitations. The difficulty is that the calculation of the single particle Green's Functions by standard equation of motion method requires the knowledge of the two particle Green's Functions, which in turn requires finding the three

particle Green's Functions, and so on. This reflects the real complexity of the many-body system where the behavior of a single particle not only depends on the pair-wise interaction of that particle with all the other particles in the system, but, indirectly, on the interaction of the rest of particles among themselves (vertex corrections). Mathematically, such a complication has to do with the fact that the two- and four-fermion operators do not close under commutation. One approach to the problem is to neglect the three particle Green's Functions, so as to create a closed system of equations for one and two particle Green's Functions. It is however clear that such an approximation is not always valid [43]. Another approach is to eliminate the two particle Green's Functions altogether by introducing the mean-field approximation. This does not really solve the problem, since one still has to estimate the fluctuation corrections which may turn out to be important.

The important idea of the Functional Integral Formalism is that it allows us to eliminate the direct interactions between particles Instead, those particles couple to the effective fields, and indirectly- to each other. Direct interactions between particles can then be recovered in a second and higher order expansion in powers of those fields. Let us see how such a transformation can be accomplished [44]. Consider a Hamiltonian H for which:

$$H = H_0 + A^2 \tag{2.1.1}$$

where A^2 represents a many-body term in the Hamiltonian, and H_0 and A in general do not commute. Then:

$$\exp\left(-t\left(H_0 + A^2\right)\right) = \lim_{N \to \infty} \left(1 - \frac{t\left(H_0 + A^2\right)}{N}\right)^N \tag{2.1.2}$$

$$= \lim_{N \to \infty} \exp\left(-\frac{t H_0}{N}\right) \exp\left(-\frac{t A^2}{N}\right)$$

The reason (2.1.2) is correct is because for any X (operator or c-number) one can write:

$$e^{X} = \lim_{N \to \infty} \left(1 + \frac{X}{N}\right)^{N} \tag{2.1.3}$$

The commutator of H_0 and A, however, has a prefactor $1/N^2$, and therefore does not contribute to the exponent as we go to the limit $N \to \infty$. A second important formula is the Hubbard-Stratanovich identity which asserts that for any operator A^2 one can write (Hubbard-Stratanovich) [45]:

$$\exp(-A^2) \equiv \int_{-\infty}^{+\infty} dy \exp(-\pi y^2 - 2\sqrt{\pi}\, i\, y\, A) \tag{2.1.4}$$

In the future, I will use $\langle f(y_1, \ldots, y_n) \rangle_G$ to indicate the Gaussian integral over all the dummy variables y. In this case the Hubbard-Stratanovich identity takes the following form:

$$\exp(-A^2) \equiv \langle \exp(-2\sqrt{\pi}\, i\, y\, A) \rangle_G \tag{2.1.5}$$

Now using (2.1.2) and (2.1.4) and remembering that any term with prefactor of order smaller than 1/N does not contribute, the RHS of (2.1.2) then becomes:

$$\lim_{N \to \infty} \left(\int_{-\infty}^{+\infty} dy \exp\left(-\left[\pi y^2 + t H_0 / N + 2i\, y \sqrt{\pi t / N}\, A\right]\right)\right)^{N} \tag{2.1.6}$$

At this point I will introduce index n (n=1,...,N) to label all N dummy variables. Then (2.1.6) takes the following form:

$$S(t) = \lim_{N \to \infty} \prod_{n=1}^{N} \int_0^{\infty} dy_n \exp\left(- \bar{\Lambda}(y_n)\right) \tag{2.1.7}$$

$$\bar{\Lambda}(y_n) \equiv \pi y_n^{\,2} + H_0 t / N + 2 i y_n A \sqrt{\pi t / N}$$

where

$$S(t) \equiv \exp\left(- t \left(H_0 + A^2\right)\right)$$

Finally, using the time-ordering operator T (index n now corresponds to time $\tau_n \equiv nt/N$), write:

$$S(t) = T \lim_{N \to \infty} \int_0^{\infty} \left\{ \prod_{n=1}^{N} dy_n \right\} \exp\left(- \sum_n \bar{\Lambda}_n(y_n) \right) \tag{2.1.8}$$

where, $\bar{\Lambda}_n$ is identical to $\bar{\Lambda}$, and subindex n is used for ordering purposes. Making a change of variable, $z_n \equiv y_n \sqrt{N/t}$, one then obtains:

$$\exp\left(- t \left(H_0 + A^2\right)\right) = \tag{2.1.9}$$

$$= \lim_{N \to \infty} T \left(\int \left\{ \prod_{n=1}^{N} D z_n \right\} \exp\left(- \sum_{n=1}^{N} \frac{t}{N} \times \right. \right.$$

$$\left. \left. \times \left[\pi z_n^{\,2} + H_{0n} + 2 i z_n \sqrt{\pi} A_n \right] \right) \right)$$

where $Dz \equiv dz \sqrt{\frac{N}{t}}$. The sum in the exponent is now converted to an integral ($\tau_n \to \tau$), and one writes:

$$S(t) = e^{-Ht} = T \int Dz \exp\left(- \int_o^t d\tau \, \Lambda'_{\tau}(z_{\tau}) \right) \tag{2.1.10}$$

$$\Lambda'_{\tau}(z_{\tau}) = \pi z_{\tau}^{\,2} + H_{0\tau} + 2 i z_{\tau} \sqrt{\pi} A_{\tau}$$

So what this does is as follows: at each infinitesimal interval of time $\delta\tau \equiv t/N$ an event occurs, namely a particle "sees" some field z_τ. From this, a chain of events up to time t (called "path") is constructed. And the infinite-dimensional integration (summation) is over all such paths.

The utility of this formalism is that it allows us to represent the many-body term in the Hamiltonian as the one particle operator coupled to stochastic fields, weighted by the Gaussian weight factor [44]. This certainly eliminates the problem described above in the Green's Functions approach, without introducing any drastic approximations. There is, however, a price to pay. The price is that one deals with an infinite, ill-defined integration and an infinite number of Gaussian variables which are coupled to various one fermion operators. Therefore in practice the perturbative approach in the Functional Integral Formalism may be even more difficult than in the conventional Green's Functions approach [46].

It is important at this point to mention two problems associated with the above construction, which will serve as a reference for the future discussion.

Problem #1: A path $z(\tau) = z_\tau$ is in general discontinuous everywhere and the limit $\Delta\tau = t/N \rightarrow 0$ is not well defined. (see Fig. 17)

Now, let us suppose we want to apply a canonical transformation to the propagator (say we want to diagonalize it, or just present it in a more convenient form). Then one obtains [47] for each value of τ::

$$\tilde{\Lambda}_\tau(z_\tau) \equiv U_\tau^{-1} \Lambda'_\tau(z_\tau) U_\tau \tag{2.1.11}$$

and then

$$S(t) = U_t \, T \int Dz \, e^{-\int_o^t d\tau \, \Lambda_\tau^{eff}(z_\tau)} \, U_0^{-1} \tag{2.1.12}$$

$$\Lambda_\tau^{eff} = \tilde{\Lambda}_\tau - P_\tau \tag{2.1.13}$$

$$P_\tau = \lim_{\Delta\tau \to 0^+} U_\tau^{-1} \frac{U_\tau - U_{\tau - \Delta\tau}}{\Delta\tau} \qquad (2.1.14)$$

Problem #2: Since there is no definite correlation between times τ and $\tau - \Delta\tau$, it follows that P_τ is in general infinite.

Now, both problems discussed in this section arise from the fact that there is no correlation between times τ and $\tau - \Delta\tau$. It is intuitively obvious that in order to give a finite contribution to physical observables the paths should not vary too rapidly in time. No one, however, has really explored the question as to the limit on how fast the curves can vary in time, except for the ad hoc assumption that z_τ, representing a time ordered path is a continuous function of τ (see for example [48]). This is an important question that I will address in Sec. 2.3 when I draw comparison between the propagator construction described above and the one based on the local operator construction, that I will describe in the next section.

2.2 Propagator Construction Using the Concept of Local Operators

It has been pointed out in the previous section that while the standard formalism allows us to "linearize" the many-body Hamiltonian which eliminates the infinite chain of equations in the Green's Functions approach, the down side of that approach is that one is forced to deal with an infinite, ill-defined integration and an infinite number of Gaussian variables which are coupled to one-particle operators. It is therefore my objective to construct the many-body propagator in the "linearized" form which would also be expressed in terms of a *finite* number of Gaussian variables. That would not only simplify the equations for Green's Functions, but also allow the application of other powerful nonpertubative techniques, such as the diagonalization of the effective Hamiltonian as well as the generalized mean-field approach.

Before I go further let me mention two conditions that must be satisfied by any propagator one may construct. I consider the propagator in the form e^{-Ht}. Then the following conditions are both sufficient and necessary to uniquely determine the propagator $L(t)$:

$$H = -\frac{d}{dt} L(t) \Big|_{t=0} \tag{2.2.1}$$

$$L(t)\, L(t') = L(t + t') \tag{2.2.2}$$

The first condition is called the initial condition, while the second condition is called the additivity condition. The validity of those two conditions can be proved by induction (see Appendix 2). As an example of how those two conditions might be used let me go back to the Hamiltonian given by (2.2.1). Now write:

$$H = -\frac{d}{dt} e^{-Ht} \Big|_{t=0} = -\frac{d}{dt} e^{-H_0 t} e^{-A^2 t} \Big|_{t=0}$$

The last equation is true since the commutator of $H_0 t$ and $A^2 t$ is proportional to t^2 and therefore two operators can be treated as numbers in the limit $t \to 0$. Now using (2.1.4) write:

$$H = -\frac{d}{dt} \left\langle e^{-H_{mf}(Y,t)} \right\rangle_G \Big|_{t=0} \tag{2.2.3}$$

where

$$H_{mf} = H_0 t + 2iY\, A \sqrt{\pi t} \tag{2.2.4}$$

It therefore follows that the initial condition is satisfied. Let us now see whether the additivity condition is satisfied as well. I will introduce a new variable $y \equiv Y/\sqrt{t}$. Then I can write:

$$H = -\frac{d}{dt}\left\{ \left\langle e^{-t\,H_{mf}(y)} \right\rangle_G \right\}_{t=0} \qquad (2.2.5)$$

$$H_{mf}(y) = H_0 + 2i\,y\sqrt{\pi}\,A$$

To verify the additivity condition write:

$$L(t)L(t') = \left\langle e^{-t\,H_{mf}(y)}\, e^{-t'H_{mf}(y')} \right\rangle_G$$

Since in general $[H_0, A] \neq 0$, it follows that $[H_{mf}(y), H_{mf}(y')] \neq 0$ so that $L(t)L(t') \neq L(t+t')$ and the additivity condition does not hold. It should be noted however that two exponents in $\langle\rangle$ are additive for $y = y'$. This simple observation is essentially behind the idea of local operators. The important thing to note in that respect is that the operators such as A are independent of y. In other words, the A that multiplies y in the first exponent is identical to the A that multiplies y' in the second exponent. Let us however change that and define a new operator equal to A (times the normalization factor which I will define below) in some small neighborhood of y and zero outside. The same can be done for the second exponent. In that case the corresponding operators become y-dependent and are called local operators, as opposed to an operator such as A which will be referred to as the global operator. It should be obvious now that the product of two local operators defined around y and y' is zero unless $y = y'$. In that case the above problem of noncommutativity disappears and the additivity condition will hold.

With this in mind let me proceed with the formal definition of local operators. Let R represent a real line over which the Gaussian variable y is defined. Take $N_\Delta(x)$ to be an open segment around point x, and let Δ be its length. Now define the localization projection operator as follows:

$$P_x f(y) = \Theta_x(y) f(y) \tag{2.2.6}$$

where

$$\Theta_x(y) = \begin{cases} 1/\Delta & y \in N_\Delta(x) \\ 0 & \text{otherwise} \end{cases} \tag{2.2.7}$$

More generally,

$$P_x f_1(y_1) \cdots f_n(y_n) = \\ = \Theta_x(y_1) \cdots \Theta_x(y_n) f_1(y_1) \cdots f_n(y_n) \tag{2.2.8}$$

Now let A(y) belong to some closed algebra, defined over R. Then the local operator $A_x(y)$ is defined as follows:

$$A_x(y) = P_x A(y) \tag{2.2.9}$$

$A_x(y)$ is a "local" operator, that corresponds to the "global" operator A(y). So, basically, local operator is equal to its global counterpart, times the normalization factor within some small interval, and is zero outside.

Consider now a discrete set of points x, such that $R = \bigcup_x N_\Delta(x) + \bar{S}$, where $\bar{S}$ is a closed complement of $\bigcup_x N_\Delta(x)$. Take $\bigcup_x N_\Delta(x)$ to be dense everywhere in R. Then $\bar{S}$ is of measure zero, and as such could be neglected in the construction of the Lebesgue integral [49] (question of boundaries will be avoided by the different and more systematic construction to be presented in the next section). We can then let $\Delta \to 0$, while keeping $\bar{S}$ of measure zero. Then from (2.2.9), one has:

$$A(y) = \sum_x A_x(y) \Delta \tag{2.2.10}$$

Similarly, define a local wave-function $\psi_x(y)$, corresponding to a global wave-function $\psi(y)$:

$$\psi_x(y) = \Theta_x(y)\psi(y) \tag{2.2.11}$$

Then similarly to (2.2.10), one has:

$$\psi(y) = \sum_x \psi_x(y)\Delta \tag{2.2.12}$$

Now let us introduce time dependence, i.e. let $A=A(t)$. Then from (2.2.6) and (2.2.9) we get:

$$A_x(y,t)A_{x'}(y',t') =$$

$$= \Theta_x(y)\Theta_{x'}(y')\Theta_x(y')A(y,t)A(y',t')$$

First Θ-function essentially localizes y around $N_\Delta(x)$, and the second Θ-function localizes y' around $N_\Delta(x')$. Third Θ-function forces $N_\Delta(x)=N_\Delta(x')$, which in the limit $\Delta \to 0$ means that $y = y'$.

It is natural in the limit $\Delta \to 0$ to substitute the summation in (2.2.10) and (2.2.12) by integration. Defining $\int dx \equiv \sum_x \Delta$, and integrating over all variables, get:

$$\int dx\,dy\,dx'dy'\,A_x(y,t)A_{x'}(y',t') = \tag{2.2.13}$$

$$= \int dx\,dy\,\Theta_x(y)A(y,t)A(y,t')$$

Let us now consider two operators A and B. Each operator can be represented as an integral over corresponding local operators. In other words, define R_1 and R_2 to be two real lines (or in general some fields). Then according to (2.2.10) write:

$$A(y_1) = \int_{R_1} dx_1 A_{x_1}(y_1) \tag{2.2.14}$$

and

$$B(y_2) = \int_{R_2} dx_2 B_{x_2}(y_2) \tag{2.2.15}$$

so that

$$A(y_1)B(y_2) = \int_{R_1}\int_{R_2} dx_1 dx_2 \; A_{x_1}(y_1) B_{x_2}(y_2) \tag{2.2.16}$$

Here $x_1, y_1 \in R_1$ and $x_2, y_2 \in R_2$. It is important to emphasize at this point that since x_1 and x_2 belong to two different fields, they do not have any correlation, and the commutation rule for the local operators is:

$$\left[A_{x_1}, B_{x_2}\right] = P_{x_1} P_{x_2} [A, B] \tag{2.2.17}$$

I will adopt a convention of using different subindices on the localization indices belonging to the different fields, as with x_1 and x_2 above. Same applies to the Gaussian variables y_1 and y_2.

Let us now go back to (2.1.1), and see how we can apply the above concept to the solution of our problem. Following the last section write:

$$\begin{aligned} H &= -\frac{d}{dt} e^{-Ht}\Big|_{t=0} = -\frac{d}{dt} e^{-H_0 t} e^{-A^2 t}\Big|_{t=0} = \\ &= -\frac{d}{dt}\left\{\left\langle \int dx_1 \int dx_2 \; O_{H_0 x_1}(Y_1) O_{A x_2}(Y_2)\right\rangle_{G}\right\}_{t=0} \end{aligned} \tag{2.2.18}$$

where

$$O_{H_0 x_1}(Y_1) \equiv e^{-t H_{0x_1}(Y_1)} \tag{2.2.19}$$

$$O_{A x_2}(Y_2) \equiv e^{-2i Y_2 \sqrt{\pi t} A_{x_2}} \tag{2.2.20}$$

and $H_{0x_1}(Y_1) = H_{0x_1}$, so that $O_{H_0 x_1}(Y_1)$ is formally Y_1-independent. It should be obvious however that the dependence of the operator $O_{H_0 x_1}$ on its localization index comes from the requirement that $Y_1 \in N_\Delta(x_1)$. However, since $O_{H_0 x_1}$ is Y_1 independent, it follows that $O_{H_0 x_1}$ does not depend on x_1, and one may just as well substitute x_1 by x_2. Therefore one can write:

$$H = -\frac{d}{dt}\left\{\left\langle \int dx \; O_{H_0 x} \; O_{A x}(Y) \right\rangle_G \right\}_{t=0} \tag{2.2.21}$$

From (2.2.21) it follows that:

$$H = -\frac{d}{dt}\left\{\left\langle \int dx \; O_{H_0 x} \; O_{A x}(Y) \right\rangle_G \right\}_{t=0} = \tag{2.2.22}$$

$$= -\frac{d}{dt}\left\{\left\langle \int dx \, e^{-H'_{mx}(Y,\,t)} \right\rangle_G \right\}_{t=o} \equiv -\frac{d}{dt} L(t)$$

where

$$H'_{mx}(Y) = t H_{0x} + 2i Y \sqrt{\pi t} A_x$$

Now let us introduce a new variable $y \equiv Y/\sqrt{t}$. I will also introduce a new measure. Define $\delta \equiv \frac{\Delta}{\sqrt{t}}$, so that:

$$\int Dx \equiv \delta \cdot \sum_x$$

With this definition write:

$$H = -\frac{d}{dt}\left\{ \left\langle \int Dx\, e^{-t H_{mx}(y)} \right\rangle_G \right\}_{t=o} \qquad (2.2.23)$$

$$H_{mx}(y) = H_{0x} + 2i\, y \sqrt{\pi}\, A_x$$

Let me also define the propagator density:

$$\tilde{A}(y,t) \equiv \exp\left(-H_m(y,t) - \pi t\, y^2\right)$$

One can now rewrite (2.2.13) in terms of new variables with the new measure, and from this it follows that:

$$L(t)\,L(t') = \int Dy\, Dy'\, Dx\, Dx'\, \tilde{A}_x(y,t)\, \tilde{A}_x(y',t') =$$

$$= \int Dy\, Dx\, \Theta_x(y)\, \tilde{A}(y,t)\, \tilde{A}(y,t')$$

Now, since the Hamiltonian in (2.1.1) and therefore in (2.2.23) does not have explicit time dependence, it follows that $\tilde{A}$ (y,t) . $\tilde{A}$ (y,t') $= \tilde{A}$ (y,t+t'), then:

$$L(t)\,L(t') = \int Dy\, Dx\, \tilde{A}_x(y, t+t') = L(t+t')$$

so (2.2.2) is satisfied. From (2.2.22) it follows that (2.2.1) is also satisfied. Therefore:

$$e^{-Ht} = L(t) \tag{2.2.24}$$

It is to be emphasized that (2.2.23)-(2.2.24) holds only if H in (2.1.1) is time independent. One can now calculate its spectral function. In this case there are no four-fermion operators (direct coupling) in the propagator just derived. Instead, one-particle Green's Functions are coupled to effective fields which should then be integrated with the Gaussian weight factor. Therefore one-particle Green's Functions will only be coupled to other one-particle Green's Functions (and not to two-particle Green's Functions) in a system of self-consistent type equations. Unlike in the standard path-integral formalism, however, one does not have to deal with an infinite-dimensional integration which should greatly simplify the calculations. Alternatively, one can diagonalize (2.2.24) (see Appendix 3) and therefore calculate its trace as well as its various logarithmic derivatives.

The above discussion can easily be generalized to include complex fields. This is a more general situation, corresponding to a general two body interaction term in the Hamiltonian. Then the real field R is generalized to the complex field C, which is now divided into open squares $N_{\Delta}^{(2)}(x)$ of area Δ^2, and the localization function is also appropriately modified:

$$\Theta_x^{(2)}(z) = \begin{cases} 1/\Delta^2 & z \in N_{\Delta}^{(2)}(x) \\ 0 & \text{otherwise} \end{cases}$$

I will also consider complex fields when discussing the harmonic oscillator problem in Sec. 2.4

Let us now discuss the physical significance of local operators. Let A be some relevant operator, describing a certain property of the system. Then, what is the meaning of A_x? It is clear that A_x can

only refer to H_x and is orthogonal to all the operators with a different localization label x'. Therefore a system described by A_x can only exist in a state of the system in an "effective field x". And the partition function (App. 3, Eq. (A3.4)) is essentially a sum over such states. The electron system, coupled to the multitude of such fields recreates a complex behavior of a real system.

In fact, in comparing these results to the Feynman integral formalism (see Sec. 2.3) I find that for the Hamiltonians, that do not have any explicit time dependence (in the Schrödinger representation) the two models are equivalent. Indeed, it would be much harder to find $L(t)$ for a time-dependent Hamiltonian, such that the additivity condition (2.2.2) is satisfied.

2.3 Equivalence of the local operator construction to the standard formalism

Let me now present the informal arguments and the motivation for the formal proof below. Let us rewrite (2.1.10) in the form:

$$S(t) = T \int \left\{ \lim_{N \to \infty} \prod_{n=1}^{N} D z_n \right\} \times \exp\left(- t F_d(z_1, \ldots, z_N, t) \right) \tag{2.3.1}$$

by defining

$$F_d(z_1, \ldots, z_N, t) = \frac{1}{t} \int_0^t d\tau \; \Lambda'_\tau(y_\tau) \tag{2.3.2}$$

This is not really an allowed step, but is appropriate for this informal argument. From (2.3.2) it follows (at least qualitatively) that all events belonging to the particular path are averaged over all time intervals, and a certain time average corresponding to that sequence of events is obtained.

It should be noted here that Λ'_τ is not an explicit function of τ. This is very important for this informal argument as well as the formal derivation below. Indeed, formula (2.3.2), as I just pointed out, represents certain time average over many events, that build up some path. Since there is no explicit time dependence, each event comes in with τ independent weight factor, i.e. as a simple arithmetic average (call it an "average" event). Therefore for a given path $(z_1,\ldots,z_N)$, the average event is $X_1 \propto \frac{1}{N}\sum_{i=1}^{N} z_i$. It should follow then that $F_d(z_1,\ldots,z_N,t)=F(X_1)$. Formula (2.1.10) represents the sum over all possible paths (with the corresponding weight factor $\exp\left(-\int_o^t d\tau\, \Lambda'_\tau(z_\tau)\right)$, which is now equivalent to summing over all "average" events (with appropriate average weight factors $\exp(-t\,F(X_1))$, and this is exactly the gist of my theory.

On a more formal side now, since there is no explicit time dependence, the order of the events is unimportant, and therefore one may drop time ordering, and τ subscripts on all operators. To show this, consider for example the second order expansion of RHS of (2.1.10). The relevant quantity is:

$$\frac{1}{2}\left(\Lambda_{\tau_1}(y_{\tau_1})\Lambda_{\tau_2}(y_{\tau_2})\Theta(\tau_1-\tau_2)+\Lambda_{\tau_2}(y_{\tau_2})\Lambda_{\tau_1}(y_{\tau_1})\Theta(\tau_2-\tau_1)\right)$$

where $\Theta(X)$ is a Heavyside step function. At this point τ index on all operators becomes irrelevant (since time ordering is assured by the Heavyside function). Now I want to integrate over y_τ. Define:

$$Y \equiv \int Dy_\tau\, \Lambda(y_\tau) \qquad (2.3.3)$$

Important point is that Y is now τ independent operator. Integrating over time variables, second order expansion takes the following form:

$$\frac{1}{2}\left(\int_0^t d\tau_1 Y \int_0^{\tau_1} d\tau_2 Y + \int_0^t d\tau_2 Y \int_0^{\tau_2} d\tau_1 Y \right) = \frac{t^2}{2} Y^2 \qquad (2.3.4)$$

It is obvious now, that because Y is time independent time ordering does not play a role, and the same result would obviously be obtained without time ordering. Therefore, we can now drop τ indices for all operators, which serves to put the operators in a time ordered fashion. But one must realize at this point, that T-ordering operator not only orders all operators with different τ indices, but also groups together all operators with the same τ index. One may therefore substitute T-ordering operator by a less stringent grouping operator Gr, which simply groups together all operators with the same index τ . The apparent problem with the grouping operator is that it does not commute with the Gaussian integral, i.e. $Gr \int D z \neq \int D z \; Gr$. What I will show below, is that one *can* in fact commute Gr with an integral sign, which would explain the apparent singularities in the standard functional integral formalism (see the discussion in the previous subsection). The same proof will also be used to establish the equivalence for the propagator obtained within the local operator construction, and the standard Feynman propagator.

The argument that I will give below resolves two questions. First of all, it resolves the problem of P_τ being infinite. In fact, I will argue that all those infinities must cancel and the result is finite (Points 1-4 below). Continuing those arguments it will then be a straightforward matter to show the equivalence of the propagator obtained within the local operator construction, and the propagator obtained in the framework of the standard formalism (Point 5 below).

Again consider:

$$H = H_0 + A^2 \tag{2.3.5}$$

In the discrete form, the corresponding propagator is:

$$S(t) = \lim_{N \to \infty} \prod_{i=1}^{N} \int_0^{\infty} dy_i \exp\left(- \bar{\Lambda}(y_i)\right) \tag{2.3.6}$$

$$\bar{\Lambda}(y_i) \equiv \pi y_i^2 + H_0 t / N + 2i y_i A\sqrt{\pi t / N} \tag{2.3.7}$$

Define the transformation in the N-dimensional space:

$$X_1 = \frac{1}{\sqrt{N}} \sum_{i=1}^{N} y_i \tag{2.3.8}$$

All other X_i are orthogonal to X_1 . Consider first [H_0, A] = 0, then one can show that:

$$S(t) = \int_0^{\infty} dX_1 \exp\left(- \Lambda(X_1)\right) \tag{2.3.9}$$

$$\Lambda(X_1) = \pi X_1^2 + H_0 t + 2i X_1 A\sqrt{t} \tag{2.3.10}$$

Indeed, in this case

$$\left[\bar{\Lambda}(y_i), \bar{\Lambda}(y_j)\right] \propto [H_0, A](y_i - y_j) = 0 \tag{2.3.11}$$

Therefore

$$S(t) = \lim_{N \to \infty} \int_0^{\infty} \left\{ \prod_{i=1}^{N} dy_i \right\} \exp\left(- \sum_i \bar{\Lambda}(y_i) \right) \tag{2.3.12}$$

Changing the variables to X_i , obtain

$$\sum_i \bar{\Lambda}(y_i) = \pi \sum_i y_i^2 + H_0 t + 2iA\sqrt{t}\left(\frac{1}{\sqrt{N}} \sum_i y_i\right) \qquad (2.3.13)$$

$$= \pi \sum_{i \neq 1} X_i^2 + \Lambda(X_1)$$

$$S(t) = \lim_{N \to \infty} \int_0^\infty \left\{ \prod_{i=1}^{N} dX_i \right\} \exp\left(- \sum_{i \neq 1} \pi X_i^2 - \Lambda(X_1) \right)$$

$$= \int_0^\infty dX_1 \exp(-\Lambda(X_1))$$

The trace of the RHS of (2.3.9) must have at least one saddle point, call it X_S with the peak width Δ_1 (see Fig. 18).

The important assumption used in the argument below is that for $[H_0, A] \neq 0$, $\Delta_1 \sim O(1) = O((1/N)^0)$, i.e. Δ_1 may be arbitrarily large but must be finite. Otherwise the propagator density would be independent of X_1. Above assumption can be proved self-consistently. Here are the central points of the argument:

1. Λ_τ is not an explicit function of τ, therefore the saddle point, corresponding to each variable y_i is independent of i. Call this saddle point y_S.

Since

$$X_1 = \frac{1}{\sqrt{N}} \sum_{i=1}^{N} y_i$$

it follows that

$$y_s = \frac{X_s}{\sqrt{N}} \qquad (2.3.14)$$

2. Let Δ_y denote the fluctuations of each y_i around y_S. Then

$$\Delta_y \approx \frac{\Delta_1}{\sqrt{N}} \tag{2.3.15}$$

Paths defined by (2.3.15) I will call important paths. Reversing the above argument one can show that only important paths have a finite contribution to physical observables (see Fig. 19)

3. Because Λ_τ is not an explicit function of τ and taking into account the above restriction on Δ_y, it will be proved that the T-ordering could be substituted by the grouping operator Gr inside the integral sign. Gr groups together all operators with the same index τ. In other words, the explicit order of operators with different indices τ is not important. What is important is that all operators with the same index τ be grouped together, so that their relative order is unchanged. Then one can rearrange the operators of different indices τ, such that any chain of events is represented by a monotonic path. To prove this, again consider the expression

$$S(t) = \lim_{N \to \infty} \prod_{i=1}^{N} \int_0^\infty dy_i \exp\left(-\bar{\Lambda}(y_i)\right)$$

$$\bar{\Lambda}(y_i) \equiv \pi y_i^{\,2} + H_0 t / N + 2iy_i A\sqrt{t/N} \tag{2.3.16}$$

This expression represents a sum over the various paths $(y_1,\ldots,y_N)$. For a particular path the propagator density is

$$\prod_{i=1}^{N} \exp\left(-\bar{\Lambda}(y_i)\right)$$

It is my intention to show now that one can multiply above exponents in any order, and the correction is at least of order 1/N, so that it vanishes in the limit $N \to \infty$. I will, however, prove even stronger result, which will have an important application later on. Write:

$$\prod_{i=1}^{N} \exp\left(-\bar{\Lambda}(y_i)\right) = \tag{2.3.17}$$
$$= \exp\left(-\sum_i \bar{\Lambda}(y_i)\right) + \text{CORRECTIONS}$$

It is my contention now that the corrections are at most of order 1/N. To prove that let us consider what kind of corrections are involved. First of all, let us observe that all corrections must be proportional to the powers of $y_i - y_j$, i,j = 1,...,N. Second of all, first order correction proportional to the first power of $y_i - y_j$ will vanish upon integration. Therefore the first nonzero correction comes in the second order of $y_i - y_j$ and is proportional to

$$\sum_{i,j} (y_i - y_j)^2 [[H_0, A], A] \left(\frac{t}{N}\right)^2 \tag{2.3.18}$$

Now, without any restriction on $y_i - y_j$, above corrections are of order O(1). Indeed, the factor proportional to $1/N^2$ is summed $N \times N$ times, so that the final contribution is finite. But y_i , y_j outside the region $y_s \pm \Delta y$ have zero contribution to the propagator density, and therefore the first nonzero correction is of order 1/N, which vanishes upon taking the limit $N \to \infty$. Next order contributions come from a triple summation, and have three kinds of contributions. The first two are of the form:

$$\sum_{i,j,k} (y_i - y_j)^2 [H_0, [[H_0, A], A]] \left(\frac{t}{N}\right)^3 \tag{2.3.19}$$

$$\sum_{i,j,k} (y_i - y_j)^2 [H_0, A]^2 \left(\frac{t}{N}\right)^3 \tag{2.3.20}$$

while the third one is:

$$\sum_{i,\,j,\,k} (y_i - y_j)^2\, y_k{}^2 \left(\frac{t}{N}\right)^3 \times \text{BRACKETS} \tag{2.3.21}$$

where the brackets involve all nonzero brackets of the array {H_0, A, A, A, A}. All corrections are also of the order 1/N. Before going to even higher order corrections, let us pause and carefully re-examine the formulas (2.3.18)-(2.3.21). First correction, expressed in the (2.3.18) contains double summation and array of three operators { $H_0 t/N$, $y_i A\sqrt{t/N}$, $y_j A\sqrt{t/N}$ }. Next order correction comes from adding index k to the sum and adding another operator to the array. In this case the operator may be $H_0 t/N$ or $(y_k A\sqrt{t/N})^2$, because adding $y_k A\sqrt{t/N}$ would make the contribution odd, which would vanish upon integration. The corresponding arrays now are: { $H_0 t/N$, $H_0 t/N$, $y_i A\sqrt{t/N}$, $y_j A\sqrt{t/N}$ } or { $H_0 t/N$, $y_k A\sqrt{t/N}$, $y_k A\sqrt{t/N}$, $y_i A\sqrt{t/N}$, $y_j A\sqrt{t/N}$}. It therefore follows that the higher order corrections come from adding another index to the sum (which increases the order of the contribution by the factor N) and adding either $H_0 t/N$ or $(y_k A\sqrt{t/N})^2$ to the array, which gives the additional factor 1/N, thereby leaving the order of the next contribution (in powers of 1/N) unchanged. The quadruple sum, for example, contains all the possible brackets of two arrays - { $H_0 t/N$, $H_0 t/N$, $H_0 t/N$, y_i A\R(t/N), y_j A\R(t/N) }, and { $H_0 t/N$, y_i A\R(t/N), $y_j A\sqrt{t/N}$, $y_k A\sqrt{t/N}$, $y_k A\sqrt{t/N}$), $y_l A\sqrt{t/N}$, $y_l A\sqrt{t/N}$) }. It is obvious that all contributions coming from the first array are of the order 1/N, while the contributions from the second array are of the form

$$\sum_{i,\,j,\,k,\,l} (y_i - y_j)^2\, y_k{}^2\, y_l{}^2 \left(\frac{t}{N}\right)^4 \times \text{BRACKETS} \tag{2.3.22}$$

which is also of the order 1/N. It follows by the induction then that the total correction is of order 1/N, which vanishes upon taking the limit $N \to \infty$. Q.E.D.

4. Go back to (2.1.11-2.1.14):

$$\Lambda_\tau^{eff} = \tilde{\Lambda}_\tau - P_\tau$$

$$P_\tau = \lim_{\Delta\tau \to 0^+} U_\tau^{-1} \frac{U_\tau - U_{\tau - \Delta\tau}}{\Delta\tau}$$

It is now convenient to make a change of variables. Define:

$$z \equiv \frac{y}{\sqrt{\Delta\tau}}$$

Then

$$\Lambda'(z) = \pi z^2 + H_0 + 2i z\sqrt{\pi} A$$

Take $U = e^{i\alpha R} \qquad R \in G$

In this case $P_\tau \sim \frac{d\alpha}{d\tau} = \frac{d\alpha}{dz} \cdot \frac{dz}{d\tau}$. The reason for changing the variables is that $\frac{d\alpha}{dz} \sim O(1)$, i.e. α is a good function of z. Now for the monotonic path:

$$\Delta y \approx \frac{\Delta_y}{N} = \frac{\Delta_1}{\sqrt{N^3}} \Rightarrow \Delta z \propto O\left(\frac{1}{N}\right) \qquad (2.3.23)$$

Also, since

$$\Delta\tau = \frac{t}{N}$$

it follows

$$\frac{\Delta z}{\Delta\tau} \propto O(1) \qquad (2.3.24)$$

and therefore $\frac{d\alpha}{d\tau} \sim O(1)$, so that P_τ is finite. Therefore, even if time ordered path is discontinuous ($\Delta_y \propto O\left(\frac{1}{\sqrt{N}}\right) \Leftrightarrow \Delta_z \propto O(1)$), it is shown here that it has the same contribution as the continuous path, but with no T-ordering. Therefore all infinities must cancel out, and the final contribution is finite.

5. Finally, let me show the equivalence of the propagator $S(t)$ to the propagator $L(t)$, obtained from the local operator construction. Since it is true that

$$\prod_{i=1}^{N} \exp\left(-\bar{\Lambda}(y_i)\right) = \exp\left(-\sum_i \bar{\Lambda}(y_i)\right) + O\left(\frac{1}{N}\right) \tag{2.3.25}$$

it follows that

$$S(t) = \lim_{N\to\infty} \int_0^\infty \left\{\prod_{i=1}^{N} dy_i\right\} \exp\left(-\sum_i \bar{\Lambda}(y_i)\right) \tag{2.3.26}$$

and again, changing the variables to X_i, obtain

$$S(t) = \lim_{N\to\infty} \int_0^\infty \left\{\prod_{i=1}^{N} dX_i\right\} \times \tag{2.3.27}$$

$$\times \exp\left(-\sum_{i\neq 1} \pi X_i^2 - \Lambda(X_1)\right) =$$

$$= \int_0^\infty dX_1 \exp\left(-\Lambda(X_1)\right)$$

Now it is easy to show that $S(t)$ can be diagonalized, and the final form is:

$$S(t) = \int dX_1 \exp\left(-F(X_1, t)\right) \tag{2.3.28}$$

$F(X_1, t)$ is the diagonal operator, linear in the elements of G, and

$$X_1 = \frac{1}{\sqrt{N}} \sum_{i=1}^{N} y_i$$

The assumption that $\Delta_1 \sim O(1)$ can now be verified for various explicit forms of the Hamiltonian. The above result shows that $S(t)$ evaluated over the important paths is identical to $L(t)$.

2.4 System Coupled to an Harmonic Oscillator.

As one explicit illustration of the equivalence of the local operator construction to the standard formalism, let me consider the problem of a system of particles coupled linearly to an harmonic oscillator. This problem has been extensively studied by Feynman [47]. To better illustrate the equivalence, I will follow the notation as well as the spirit of his third paper [47]. The Hamiltonian of the combined system is:

$$H = H_p + H_{osc} - \Gamma q \tag{2.4.1}$$

where

$$H_{osc} = \frac{1}{2m}\left(p^2 + \omega^2 q^2\right) \tag{2.4.2}$$

and p is the momentum conjugate to q, the coordinate of the oscillator. Also H_p refers to an uncoupled system of particles, and Γ contains operators pertaining to particles. In contrast to [47], Γ is taken to be time independent. Now before proceeding with calculations, let me state an important relation, that will be used below (proof is in the Appendix 4). Namely, define

$$S_1(t) = a_-(t)b^+ + a_+(t)b \tag{2.4.3}$$

where b^+, b are boson operators, that obey the standard commutation rule:

$$\left[b, b^+\right] = 1$$

while $a_\pm(t)$ is a c-number. Then the following formula is correct:

$$T\ \exp\left(\int_{t'}^{t''} dt\ S_1(t)\right) = \exp\left(\int_{t'}^{t''} dt\ S_1(t) + \right.$$
$$\left. + \frac{1}{2}\left\{\int_{t'}^{t''} dt \int_{t'}^{t} ds\ a_+(t)a_-(s) - a_-(t)a_+(s)\right\}\right) \tag{2.4.4}$$

Following the procedure described in Sec. 2.2, write ($\tilde{z} \equiv z/\sqrt{t}$):

$$H = -\frac{d}{dt}\left\langle \int Dx\ e^{-H_{mx}(\tilde{z}, \tilde{z}^*, t)} \right\rangle_G \Big|_{t=o} \tag{2.4.5}$$
$$\equiv -\frac{d}{dt} L(t)$$

where

$$H_m = t\left(H_p + H_{osc} + \sqrt{\pi}\left(\Gamma \xi + q \xi^* \right) \right) \tag{2.4.6}$$

Then following the last section define:

$$\tilde{A}\left(\xi, \xi^*, t \right) \equiv \exp\left(- H_m\left(\xi, \xi^*, t \right) - \pi\, t\, |\xi|^2 \right) \tag{2.4.7}$$

Also define:

$$L(t) \equiv \int dx\, D\xi\, D\xi^*\, \tilde{A}_x\left(\xi, \xi^*, t \right) \tag{2.4.8}$$

where $\tilde{A}_x$ is the local counterpart of $\tilde{A}$. It is easy now to verify the additivity requirement (2.2.2). Requirement (2.2.1) is verified by combining (2.2.9), (2.4.5), (2.4.7), and (2.4.8). So now one obtains:

$$e^{-Ht} = L(t) \tag{2.4.9}$$

Since there are now no cross-terms with different x, combining (2.4.6)-(2.4.9) finally obtain:

$$e^{-Ht} = \left\langle \exp\left(-t \left\{ H_p + H_{osc} + \sqrt{\pi}\left(\Gamma \xi + q \xi^* \right) \right\} \right) \right\rangle_G$$

It is convenient for the discussion below to go back to the variable $z = \xi \sqrt{t}$, so that one obtains:

$$e^{-Ht} = \left\langle \exp\left(-t \left\{ H_p + H_{osc} + \sqrt{\frac{\pi}{t}}\left(\Gamma z + q z^* \right) \right\} \right) \right\rangle_G \tag{2.4.10}$$

It is my intention now to show that this form of the propagator is identical to the one obtained by Feynman in his third paper [47]. Now write

$$q = \frac{1}{\sqrt{2\omega}}\left(Q + Q^+ \right)$$

where Q^+, Q are boson operators, that obey the standard commutation rule.

Following the Feynman's rules, write ($t \equiv t'' - t'$):

$$e^{-Ht} = \Big\langle \exp\Big(-\Big\{ t H_p + t H_{osc} + \sqrt{\pi t} \times\Big(\Gamma z + \frac{z^*}{\sqrt{2\omega}}(Q + Q^+)\Big)\Big\}\Big)\Big\rangle_G = e^{-\int_{t'}^{t''} d\tau\, H_{p\tau}} e^{-t'' H_{osc}} \times \Big\langle e^{-\sqrt{\frac{\pi}{t}}\int_{t'}^{t''} d\tau \left(\Gamma_\tau z + \frac{z^*}{\sqrt{2\omega}}(Q(\tau) + Q^+(\tau))\right)}\Big\rangle_G e^{t' H_{osc}} \tag{2.4.11}$$

Here subindex τ indicates that the operators are to be time ordered in accordance to the usual rules. Also:

$$Q(\tau) \equiv e^{H_{osc}\tau} Q_\tau e^{-H_{osc}\tau} = Q_\tau e^{-\omega t} \tag{2.4.12}$$

$$Q^+(\tau) \equiv e^{H_{osc}\tau} Q_\tau^+ e^{-H_{osc}\tau} = Q_\tau^+ e^{\omega t} \tag{2.4.13}$$

as can be verified using the commutation rules. Following [47], I will calculate the matrix element

$$\langle \chi_{t''} \phi_m | e^{-Ht} | \phi_n \chi_{t'} \rangle$$

where χ_t refers to the particle state at time t, while ϕ_m refers to the m-th oscillator state. As discussed in [47], the above matrix element can be re-written as the matrix element between the states $\chi_{t''}$ and $\chi_{t'}$ of the matrix

$$M = \exp\Big(-\int_{t'}^{t''} d\tau\ H_{p\tau}\Big) G_{mn}$$

where in this formalism G_{mn} is the reduced matrix element defined as follows:

$$G_{mn} = \langle \phi_m(t'') | \Big\langle \exp\Big(-\sqrt{\frac{\pi}{t}} \int_{t'}^{t''} d\tau \Big(\Gamma_\tau z + \frac{z^*}{\sqrt{2\omega}}(Q(\tau) + Q^+(\tau))\Big)\Big) \Big\rangle_G | \phi_n(t') \rangle \tag{2.4.14}$$

and

$$|\phi_n(t')\rangle \equiv e^{t' H_{osc}} |\phi_n\rangle$$

Using (2.4.4), (2.4.12) and (2.4.13) re-write (2.4.14) as (notice no τ subindices on Q- operators):

$$G_{mn} = \langle \phi_m(t'') | \Big\langle \exp\Big\{ -\sqrt{\frac{\pi}{t}} \int_{t'}^{t''} d\tau \Big(\Gamma_\tau z + \tag{2.4.15}$$

$$+ \frac{z^*}{\sqrt{2\omega}} (Q e^{-\omega t} + Q^+ e^{\omega t}) \Big) \Big\} \times \exp\Big\{ \frac{1}{2} \Big(\int_{t'}^{t''} d\tau$$

$$\times e^{-\omega\tau} \int_{t'}^{t} d\rho\, e^{\omega\rho} - \int_{t'}^{t''} d\tau\, e^{\omega\tau} \int_{t'}^{t} d\rho\, e^{-\omega\rho} \Big) \times$$

$$\times \frac{\pi z^{*2}}{2\omega t} \Big\} \Big\rangle_G |\phi_n(t')\rangle$$

which using the Baker-Hausdorff formula can be re-written as:

$$G_{mn} = \langle \phi_m(t'') | \Big\langle \exp\Big(-\sqrt{\frac{\pi}{t}} \int_{t'}^{t''} d\tau\, \Gamma_\tau z \Big) \times \tag{2.4.16}$$

$$\times \exp\Big(-\sqrt{\frac{\pi}{t}} \int_{t'}^{t''} d\tau\, \frac{z^*}{\sqrt{2\omega}} Q^+ e^{\omega t} \Big) \times$$

$$\times \exp\Big(-\sqrt{\frac{\pi}{t}} \int_{t'}^{t''} d\tau\, \frac{z^*}{\sqrt{2\omega}} Q\, e^{-\omega t} \Big) \times$$

$$\times \exp\Big(\frac{1}{2} \Big(\int_{t'}^{t''} d\tau \int_{t'}^{t''} d\rho\, e^{-\omega(\tau-\rho)} \Big) \frac{\pi z^{*2}}{2\omega t} \Big) \times$$

$$\times \exp\Big(-\int_{t'}^{t''} d\tau \int_{t'}^{t} d\rho\, \sinh(\omega(\tau-\rho)) \frac{\pi z^{*2}}{2\omega t} \Big) \Big\rangle_G |\phi_n(t')\rangle$$

This integral can be evaluated by the saddle-point method, which corresponds to taking

$$z^* = -\sqrt{\frac{t}{\pi}}\, \Gamma_\tau$$

as follows from varying the exponent in (2.4.10) with respect to z and setting the derivative equal to zero. The subindex τ comes from the application of the time-ordering operator T to Γ as in (2.4.11). Therefore evaluating (2.4.16) now get:

$$\langle \phi_m(t'') | \Big\langle\ e^{\frac{Q^+}{2\omega} \int_{t'}^{t''} d\tau\, e^{\omega\tau} \Gamma_\tau}\ e^{\frac{Q}{2\omega} \int_{t'}^{t''} d\tau\, e^{-\omega\tau} \Gamma_\tau} \tag{2.4.17}$$

$$\times\, e^{\frac{1}{4\omega}\left(\int_{t'}^{t''} d\tau \int_{t'}^{t''} d\rho\, e^{-\omega(\tau-\rho)}\, \Gamma_\tau\, \Gamma_\rho\right)} \times$$
$$e^{-\frac{1}{2\omega}\int_{t'}^{t''} d\tau \int_{t'}^{t} d\rho\, \Gamma_\tau\, \Gamma_\rho \sinh(\omega(\tau-\rho))} \Big\rangle_G \left|\phi_n(t')\right\rangle$$

Now one can write:

$$\int_{t'}^{t''} d\tau \int_{t'}^{t''} d\rho\, e^{-\omega(\tau-\rho)} - 2\int_{t'}^{t''} d\tau \int_{t'}^{t} d\rho \sinh(\omega(\tau-\rho)) =$$

$$= \int_{t'}^{t''} d\tau \int_{t'}^{t''} d\rho\, e^{-\omega(\tau-\rho)} + 2\int_{t'}^{t''} d\tau \int_{t}^{t''} d\rho \sinh(\omega(\tau-\rho)) =$$
$$= \int_{t'}^{t''} d\tau \int_{t'}^{t} d\rho\, e^{-\omega(\tau-\rho)} + \int_{t'}^{t''} d\tau \int_{t}^{t''} d\rho\, e^{\omega(\tau-\rho)} =$$
$$= \int_{t'}^{t''} d\tau \int_{t'}^{t''} d\rho\, e^{-\omega|\tau-\rho|} \qquad (2.4.18)$$

Combining (2.4.17) and (2.4.18), write:

$$\left\langle \phi_m(t'')\right| \Big\langle\ e^{\frac{Q^+}{2\omega}\int_{t'}^{t''} d\tau\, e^{\omega\tau}\Gamma_\tau}\, e^{\frac{Q}{2\omega}\int_{t'}^{t''} d\tau\, e^{-\omega\tau}\Gamma_\tau} \times$$
$$e^{\frac{1}{4\omega}\left(\int_{t'}^{t''} d\tau \int_{t'}^{t''} d\rho\, e^{-\omega|\tau\cdot\rho|}\Gamma_\tau\Gamma_\rho\right)} \left|\phi_n(t')\right\rangle \qquad (2.4.19)$$

And performing the Wick rotation $t \to it$, we finally obtain:

$$\left\langle \phi_m(t'')\right| \Big\langle\ \exp\left(\frac{Q^+}{2\omega}\int_{t'}^{t''} d\tau\, e^{i\omega\tau}\Gamma_\tau\right) \times$$
$$\times \exp\left(\frac{Q}{2\omega}\int_{t'}^{t''} d\tau\, e^{-i\omega\tau}\Gamma_\tau\right) \exp\left(-\frac{1}{4\omega} \times\right. \qquad (2.4.20)$$
$$\left. \times \left(\int_{t'}^{t''} d\tau \int_{t'}^{t''} d\rho\, e^{-i\omega|\tau-\rho|}\Gamma_\tau\Gamma_\rho\right)\right) \left|\phi_n(t')\right\rangle$$

which is the result identical to the one obtained in [47].

2.5 Summary of Section 2

The alternative way of propagator construction for time-independent Hamiltonians using the local operator approach has been developed. It allows us to represent the propagator as a single or double integral, as opposed to an infinite dimensional path integral in the standard path integral theory. This may greatly simplify the calculation of the relevant propagators.

This approach has been compared to the standard functional integral formalism. The principal problem of the standard formalism has to do with the fact that most paths are highly discontinuous. The criterion as to how fast those paths can vary in time in order to give a finite contribution to the physical observables has been developed. The Feynman integral evaluated over the corresponding important paths gives the result identical to the one obtained within the local operator construction.

I have solved the harmonic oscillator problem, and the result obtained is equivalent to the obtained in [47], *provided* the Hamiltonian is not time-dependent.

3. Application of the Local Operator Construction to the Orbitally Nondegenerate Anderson Model

3.1 Introduction

In this section I will apply the local operator formalism to the study of thermodynamic properties of the orbitally nondegenerate lattice Anderson Hamiltonian. This model can be used to study mixed valence phenomena [50, 51] as well as the question of the low temperature coherent behavior in the Heavy Fermion Systems (HFS) [1, 52]. The new approach allows one to go beyond the mean field approximation [53, 54], and to actually include all relevant fluctuations. In particular, the fluctuations between two states with different symmetries are responsible for a tremendous enhancement of thermodynamic response functions in the spirit of the fluctuation-dissipation theorem.

I have numerically evaluated the Gaussian integrals derived for the partition function and its various derivatives. In particular I did numerical calculations in the region close to a transition regime between magnetic and nonmagnetic states of the Anderson model. The expected increase in response functions corresponding to smoothed-out second order phase transition between two regimes has been obtained. The behavior of the system above the transition regime is a typical local moment behavior as can be observed from numerical evaluations. However below the transition regime the situation can be much more complicated.

To better understand the situation I have used the "many-saddle" point approximation. Of particular interest was the study of a lattice in the Kondo regime close to a magnetic transition. That study was motivated by the desire to better understand the Heavy Fermion Systems (HFS) where f-electrons are in the Kondo regime. It means that in the absence of hybridization between the odd number of f-electrons and the conduction band of the host, the f-ions would act as localized magnetic moments, interacting via the effective spin-spin coupling, thus forming some type of magnetic order at low temperatures. With the hybridization turned on, however, the system at low temperature becomes nonmagnetic with tremendously enhanced values of the specific heat coefficient γ and zero temperature magnetic susceptibility χ. Therefore my next goal after calculating the partition function was to find the appropriate saddle points of the free energy density, which not only preserves the spin rotation symmetry at low temperatures, but also explains other unusual properties of HFS, most notably the low temperature coherence.

It has been very instructive to go through the derivation of the above described Kondo regime. In particular it shows some of the pitfalls associated with the saddle point approximation. In fact I will discuss how to avoid some of the problems associated with the saddle point approximation. The results derived through that approach are similar to the results found by other theories. In particular the low temperature scale similar to Kondo temperature

has been derived. It has been noted however that the above saddle point does not provide a mechanism for the low temperature coherence. In fact in the orbitally degenerate case with small crystal field splitting discussed in the next section the above saddle point becomes unstable in the low temperature Kondo limit.

This Section is organized as follows. In the next subsection (3.2) I will represent the lattice Anderson Hamiltonian in a modified kq-representation, which is described in Appendix 5. This representation is derived from the kq-representation [55] by integrating the localized delta-functions over the quasicoordinate variable, thus forming a localized wave packet around each site, translated over the whole lattice. This representation is useful for the lattice Anderson Hamiltonian. where the localized atomic orbitals are coupled to the delocalized conduction band. The next step is to calculate the propagator using the local operator approach to the functional integral formalism. I simplify the propagator by dropping the incoherent contributions to the scattering term. As I will discuss below, that should be a good approximation at low temperatures, and at higher temperatures the effect of the incoherent scattering can qualitatively be taken into account by integrating over the peak widths (which can be taken as phemenological constants) of the dominant saddle points. Next I recognize that the simplified propagator is generated by a dynamical SU(2) algebra. Therefore one can apply the Bogoliubov type transformation to diagonalize and decouple the effective bands, thus enabling us to calculate the partition function and its various derivatives.

In subsection 3.3 I describe the procedure and results of the numerical evaluation of relevant formulas in Section 3.2 for several representative regimes. The results of those calculations are summarized in the Figs. 20-25. In the next subsection (3.4) I evaluate the relevant Gaussian integrals using the many-saddle point approximation. I discuss the possible saddle points of the system. In particular I discuss how the functional integral procedure ought to be modified in order to obtain all the possible saddle points with different dynamical symmetries. I also write

down the formulas for the thermodynamic functions, which are simplified using the many-saddle point approximation. I further discuss the significance of various terms contributing to the response functions, especially the contributions of symmetry-breaking fluctuations when the system is close to a phase transition.

3.2 Application to the orbitally nondegenerate lattice Anderson Hamiltonian.

The starting Hamiltonian in this problem is the Anderson Hamiltonian:

$$H = H_{band} + H_f + H_{mix} \tag{3.2.1}$$

$$H_{band} = \sum_{k\sigma} \varepsilon_k \, c^{+}_{k\sigma} c_{k\sigma}$$

$$H_f = \sum_{\mu\sigma} E_{0\sigma} f^{+}_{\mu\sigma} f_{\mu\sigma} + U \sum_{\mu} f^{+}_{\mu\uparrow} f_{\mu\uparrow} f^{+}_{\mu\downarrow} f_{\mu\downarrow}$$

$$H_{mix} = \frac{1}{\sqrt{N}} \sum_{\mu k\sigma} \left[V_m(k) \, c^{+}_{k\sigma} f_{\mu\sigma} + H.C. \right]$$

Here μ represents the lattice site index and σ is the spin index. Also f^{+}, f represent localized electron operators, and c^{+}, c represent itinerant electron operators. Let us now rewrite. (3.2.1) as:

$$H = H_0 + \frac{U}{2} \sum_{\mu} \left(n_{\mu\uparrow} - n_{\mu\downarrow} \right)^2 \tag{3.2.2}$$

where

$$H_0 = \sum_{\mu\sigma} (E_0 + \frac{U}{2}) \, n_{\mu\sigma} + \sum_{k\sigma} \varepsilon_k \, c^{+}_{k\sigma} c_{k\sigma} +$$

$$+\frac{1}{\sqrt{N}} \sum_{\mu\sigma k} V_k \left(f_{\mu\sigma}^{+} c_{k\sigma} + h.c. \right)$$

and

$$n_{\mu\sigma} \equiv f_{\mu\sigma}^{+} f_{\mu\sigma}$$

Following the functional integral formalism developed in Section 2.2 write:

$$H = -\frac{d}{dt} \left\langle e^{-H_{MF}} \right\rangle_G \Big|_{t=0}$$

where

$$H_{MF}(Y, t) = H_0 t + \sum_{\mu} Y_{\mu} \left(n_{\mu\uparrow} - n_{\mu\downarrow} \right) \sqrt{\pi U t}$$

Define $y_\mu \equiv Y_\mu/\sqrt{t}$. Then

$$H_{MF}(y, t) = t \left(H_0 + \sum_{\mu} y_{\mu} \left(n_{\mu\uparrow} - n_{\mu\downarrow} \right) \sqrt{\pi U} \right) \tag{3.2.3}$$

I now wish to express H in the kq-representation (see Appendix 5 for further discussion). Referring to the formulas (A5.7a-d), we rewrite $H_m(y,t)$ in the following form:

$$H_{MF}(y, t) = t \left(\sum_{\sigma k} h_{0\sigma k} + \sqrt{\frac{2\pi U}{N}} \sum_{kQ} y_Q \times \right.$$

$$\left. \times \left(f_{k+Q\uparrow}^{+} f_{k\uparrow} - f_{k+Q\downarrow}^{+} f_{k\downarrow} \right) \right) \tag{3.2.4}$$

where

$$h_{0\sigma k} = \Sigma\left(E_0 + \frac{U}{2}\right) f^{+}_{k\sigma} f_{k\sigma} + \varepsilon_k \, c^{+}_{k\sigma} \, c_{k\sigma} +$$

$$+V_k \left(f^{+}_{k\sigma} \, c_{k\sigma} + h.\, c.\right)$$

$$y_Q \equiv \frac{1}{\sqrt{N}} \sum_{\mu} y_\mu \, e^{-iR_\mu Q}$$

where Q is the vector in the first Brillouin zone. Assume now that the system is in a coherent periodic state. Then one can show that the free energy, corresponding to (3.2.1) may have several saddle points, corresponding to several states of the system. One may have a saddle point with all y_μ having the same sign, and equal to $\pm\sqrt{\frac{U}{2\pi N}}$. This corresponds to the ferromagnetic state, since from (3.2.3) it is clear that the positive y_μ corresponds to spin-down moment at the site μ, and the spin-up moment for the negative y_μ. Another possible state is when all y_μ have the same absolute value as in the ferromagnetic state, but with opposite signs, forming a periodic system (antiferromagnetic state). One may also have all $y_\mu = 0$, which corresponds to nonmagnetic state.

In the coherent case (for Heavy Fermion Systems) or ferromagnetic case $y_{Q,\,i} = 0$ for Q nonzero. For the antiferromagnetic case only $y_{K/2,\,i} \neq 0$ where K is the reciprocal lattice vector. Other more complicated orderings can be considered as well. My intention here however is twofold. First of all I want to find a saddle point capable of describing the Heavy Fermion Systems. Secondly I want to illustrate how one can obtain very narrow but smooth transitions within the framework of this theory. Consequently, to simplify I will write the Coulomb term in the dispersionless form with $Q=0$. Therefore within this approximation, as the actual system goes into the magnetic regime, it is not clear what kind of magnetic order will actually be established. It is not

important however for the purposes of this discussion. I will again return to this question in Sec. 3.4.

With this in mind, the Hamiltonian takes the following form:

$$H_{MF}(y) = \sum_{\sigma k} h_{\sigma k} \tag{3.2.5}$$

where

$$h_{\sigma k} = h_{0\sigma k} + \sqrt{2\pi U}\,\sigma\, y \sum_{k} n_{\sigma k}$$

and

$$y \equiv y_0 = \frac{1}{\sqrt{N}} \sum_{\mu} y_{\mu}$$

$$h_{0\sigma k} = \left(E_0 + \frac{U}{2}\right) f^{+}_{k\sigma} f_{k\sigma} + \varepsilon_k\, c^{+}_{k\sigma} c_{k\sigma} +$$

$$+ V_k \left(f^{+}_{k\sigma} c_{k\sigma} + h.c.\right)$$

Then again following the formalism define:

$$\hat{l}(y, t) \equiv \exp\left(-t\, H_{MF}(y) - \pi t\, y^2\right) \tag{3.2.6}$$

Also:

$$\hat{L}(t) \equiv \int Dx\, Dy\ \hat{l}_x(y, t) \tag{3.2.7}$$

Using the properties of local operators, one can verify the additivity requirement

$$\hat{L}(t)\,\hat{L}(t') = \hat{L}(t + t')$$

The initial condition

$$H = -\frac{d}{dt}\hat{L}(t)\Big|_{t=0}$$

is verified by combining (3.2.1), (3.2.6) and (3.2.7). So finally one obtains:

$$e^{-Ht} = \hat{L}(t) \tag{3.2.8}$$

Writing the propagator density explicitly:

$$\hat{l}(y, t) = \int Dx\, e^{-tH_{MFx}(y) - \pi t y^2} \tag{3.2.9}$$

where

$$H_{MFx}(y) = \sum_{\sigma k} h_{\sigma k x} \tag{3.2.10}$$

$$h_{\sigma k x} = h_{0\sigma k x} + \sqrt{2\pi U}\,\sigma\, y \sum_{k} n_{\sigma k x}$$

Now we diagonalize $\hat{L}(t)$. Define R, such that R_x diagonalizes H_{MFx}, and $R = \int dx\, R_x$. R_x is defined by the Bogoliubov transformation (drop the common subindex k for a moment):

$$\alpha_{\sigma x} = u_\sigma f_{\sigma x} + v_\sigma c_{\sigma x} \tag{3.2.11}$$

$$\beta_{\sigma x} = u_\sigma c_{\sigma x} - v_\sigma f_{\sigma x}$$

From the commutation relations, plus the requirement that all nondiagonal terms in H_{MFx} vanish, we obtain:

$$u_\sigma = \frac{1}{2}\left(1 + \frac{\Delta_\sigma}{\sqrt{1+\Delta_\sigma{}^2}}\right) \tag{3.2.12}$$

$$v_\sigma = \frac{1}{2}\left(1 - \frac{\Delta_\sigma}{\sqrt{1+\Delta_\sigma{}^2}}\right)$$

where

$$\Delta_\uparrow \equiv \frac{\left(\varepsilon_c - E_0 - U/2 - x\sqrt{2\pi U}\right)}{2V} \tag{3.2.13}$$

$$\Delta_\downarrow \equiv \frac{\left(\varepsilon_c - E_0 - U/2 + x\sqrt{2\pi U}\right)}{2V}$$

The diagonalized form of $h_{dx\sigma}$ now becomes:

$$h_{dx\sigma} = \lambda_{a\sigma}\,\alpha_{x\sigma}{}^{+}\alpha_{x\sigma} + \lambda_{b\sigma}\,\beta_{x\sigma}{}^{+}\beta_{x\sigma} \tag{3.2.14}$$

where

$$\lambda_{a(b)\sigma} = \frac{1}{2}\left(E_{U\sigma}(y) + \varepsilon_c \pm \sqrt{\left(E_{U\sigma}(y) - \varepsilon_c\right)^2 + 4V^2}\right) \tag{3.2.15}$$

where:

$$E_{U\sigma}(y) = E_0 + \frac{U}{2} + \sigma y\sqrt{2U\pi} \tag{3.2.16}$$

Again, following the described procedure one can transform back to global operators, and obtain:

$$e^{-Ht} = \int Dy\ \hat{I}_d(y, t) \tag{3.2.17}$$

where

$$\hat{I}_d(y,t) = \exp\left(-t\,H_d(y,t) - t\,y^2\right) \tag{3.2.18}$$

$$H_d = \sum_{\sigma k} h_{d\sigma k}$$

$$h_{d\sigma k} = \lambda_{a\sigma k}\,\alpha^{+}_{\sigma k}\,\alpha_{\sigma k} + \lambda_{b\sigma k}\,\beta^{+}_{\sigma k}\,\beta_{\sigma k}$$

I now want to calculate the trace of the RHS of (3.2.17). First define p to be an effective band index. Namely, p=-1 refers to the lower band and p=1 refers to the higher band. Then from (3.2.17)-(3.2.18) obtain ($t \to \beta \equiv 1/k_B T$):

$$Tr\ e^{-H\beta} = \sqrt{\beta}\int dy\ \exp\left(-\pi\,\beta\,y^2\right)\times$$

$$Tr\ \exp\left(-\beta\sum\log\left(1+\exp\left(-\beta\,\lambda_{p\sigma k}(y)\right)\right)\right) \tag{3.2.19}$$

and from (3.2.15)

$$\lambda_{p\sigma k} = \frac{1}{2}\left(E_{U\sigma}(y) + \varepsilon_c(k) + p\times\right.$$

$$\left.\times\sqrt{\left(E_{U\sigma}(y) - \varepsilon_c(k)\right)^2 + 4V^2}\ \right)$$

Going to the continuum limit of wave vector $\boldsymbol{k}$, i.e.:

$$\sum_k \to \frac{\Omega}{(2\pi)^3}\int d^3k$$

where $\Omega / (2\pi)^3$ is the reciprocal of the volume of first Brillouin Zone.

Now define the "mean-field" free energy (call it free energy density):

$$f(y, \beta) = -\pi \beta y^2 - \frac{\Omega}{(2\pi)^3} \sum_{p\sigma} \int_{BZ} d^3k \times$$

$$\log\left(1 + \exp\left(-\beta \lambda_{p\sigma k}(y)\right)\right) + \frac{1}{2} \log \beta \qquad (3.2.20)$$

Then combining (3.2.19) and (3.2.20) obtain:

$$Z \equiv Tr\ e^{-H\beta} = \int dy\ e^{f(y, \beta)} \qquad (3.2.21)$$

which is the final expression for the partition function of the periodic Anderson Hamiltonian. Then one obtains an integral expression for thermal energy and specific heat:

$$E = -\frac{d}{d\beta} \log Z = -\int dy\ \frac{e^{f(y, \beta)}}{Z} \frac{d}{d\beta}(f(y, \beta)) \equiv$$

$$\equiv -\left\langle \left[\frac{df(y, \beta)}{d\beta} \right] \right\rangle \qquad (3.2.22)$$

$$C = R\beta^2 \left\{ \left\langle \Delta^{(2)} \left[\frac{df(y, \beta)}{d\beta} \right] \right\rangle + \left\langle \left[\frac{d^2 f(y, \beta)}{d\beta^2} \right] \right\rangle \right\} \qquad (3.2.23)$$

where

$$< \Delta^{(2)} O > \equiv \sqrt{< O^2 > - < O >^2}$$

If we introduce the magnetic field along the spin axis of quantization, and couple it to the spins of bare electrons, i.e.

$$\varepsilon_{p\sigma}(H) = \varepsilon_{p\sigma}(0) + \mu_B\, g\, H\, (\sigma/2)$$

one obtains the magnetization:

$$M = -\frac{1}{\beta}\frac{d}{dH}\log Z = -\frac{1}{\beta}\left\langle\left[\frac{df}{dH}\right]\right\rangle \qquad (3.2.24)$$

where now

$$f(y, \beta, H) = -\pi\beta y^2 - \frac{\Omega}{(2\pi)^3}\sum_{p\sigma}\int_{BZ} d^3k \;\times$$

$$\times \log\left(1 + \exp\left(-\beta\lambda_{p\sigma k}(y, H)\right)\right) + \frac{1}{2}\log\beta$$

$$\lambda_{p\sigma}(H) = \lambda_{p\sigma}(0) + \mu_B\, g\, H\, (\sigma/2)$$

$$\frac{df}{dH} = -\frac{\mu_B\,\beta\, g}{2}\,\frac{\Omega}{(2\pi)^3}\sum_{p}\int_{BZ} d^3k\;\left(n_{pk\uparrow} - n_{pk\downarrow}\right)$$

$$n_{pk\sigma}(y, \beta, H) = \frac{1}{1 + \exp\left(\beta\lambda_{p\sigma k}(y, H)\right)}$$

and static magnetic susceptibility is:

$$\chi = \frac{1}{\beta}\left\{\left\langle \Delta^{(2)}\left[\frac{df}{dH}\right]\right\rangle^2 + \left\langle\left[\frac{d^2 f}{dH^2}\right]\right\rangle\right\}_{H=0} \qquad (3.2.25)$$

Now, looking at (3.2.23) and (3.2.25), we see that both response functions are represented as thermal fluctuations of the free energy density. Therefore (3.2.25) represents the well known fluctuation-dissipation theorem.

It is apparent now that e^f is the most rapidly varying part of the integrands in (3.2.23) and (3.2.25). Therefore, contributions from the regions around one or more possible extrema or maxima of f would be most dominant, and these parts of the integral are the only ones that have to be taken into account. Let us say now, that there is one saddle-point. Then all of the above integrands have a sharp peak around this point, as can be verified numerically. In the language of generalized mean-field theory, this peak corresponds to the mean-field value. Any contribution to the thermodynamic response functions comes from fluctuations around that value, which are relatively small [56], and response functions are relatively unenhanced. This smallness validates the pertubative expansion around that peak.

But what if there are, say, two saddle points ? Then there are two possibilities. If contribution from one peak is much larger than from another one, then one can still do mean-field + perturbation theory around the larger peak, and neglect a second one altogether (this second peak would correspond to the metastable state). But if the two peaks are about equal, then one must take into account not only the fluctuations around each peak, which are again relatively small, but also the fluctuations *between* the two peaks, which are usually much larger. From the physical point of view, two peaks represent two thermodynamic phases, and at the transition, fluctuations are greatly enhanced. Therefore all thermodynamic response functions would be enhanced likewise. At this point mean field + pertubation theory fails completely, and one is usually forced to resort to phemenological theories. The usefulness of the present theory is that it displays a smooth transition between various phases, and as such, may provide quantitative information about various systems at transition regimes.

3.3 Numerical Results.

This section is devoted to numerical studies of systems close to the magnetic transition. I have numerically evaluated various thermodynamic functions for characteristic input parameters,

contained in the Table 1, based on formulas derived in Sec. 3.2. The routine, written in Fortran identifies all of the peaks in the free energy density, whether or not they are numerically significant. This is important in order to identify the possible metastable states. For further calculation only numerically significant peaks are considered. Next step in the procedure is to identiry each peak's width. Actual integration is performed within the width of each peak. The error is controlled by doubling the number of intervals and comparing the results. It turns out that the specific heat is the hardest quantity to calculate with good precision, because Gaussian fluctuations of the specific heat are represented as the difference of two large integrals that are almost equal, times the the square of the inverse temperature (3.2.23). Hence, any error in calculations is magnified many orders of magnitude. Therefore it required a tremendous amount of computer time to evaluate the specific heat with the degree of precision typically 0.1%. Figures 20-25 show graphs of various thermodynamic quantities for three different regimes, denoted **a**, **b**, and **c**. With all other input parameters fixed (see Supplement, table 1), E_0 was used as a variational parameter. Other quantities could also be used as variational parameters, but results would be qualitatively the same. Accordingly, regime **c** has the highest value of E_0, while regime **a** has the lowest.

With this in mind, let us now consider those graphs. Figure 20 shows low temperature static magnetic susceptibility for three regimes. It can be seen that graph **a** is closest to a magnetic regime, and in fact, closely follows the Curie power law, while two other graphs **b** and **c** have a peak at two different characteristic temperatures $T_{\max}$, which correspond to an approximate location of the renormalized f-level (ε_f). The difference between bare electron energy values for three graphs is of the order of this characteristic energy, which is small compared to energy scale of E_0, or other input parameters. This means that one will not be able to obtain this kind of behavior through ordinary pertubation expansion, but only through numerical, or some other nonpertubative approach.

The high temperature inverse magnetic susceptibility for all three regimes is shown in Fig. 22. All three graphs are virtually indistinguishable, therefore I did not use letters to denote each graph. It is clear from that figure that all three regimes follow the Curie law at temperatures high compared to T_{max}, and the demagnetizing effect begins to set in only at $T \approx T_{max}$. It is interesting now to compare Fig. 20 to Fig. 21, 23, and 25. Starting with the specific heat, one may observe that in the regime **a** the specific heat shows no enhancement, while both graphs **b** and **c** show large peaks at the temperatures, where corresponding susceptibilities have their peak also. This tremendous enhancement is due to large thermal fluctuations associated with the phase transition, while regime **a** shows no such transition.

Further insight into the problem is obtained by considering the thermal energy for three regimes. I have chosen a convenient energy scale, so as to better show the details of their behavior. Again, one can see that graph **a** is almost horizontal, which is mirrored by a small value of the specific heat. But, as one goes away from the Curie behavior (graph **b** and then graph **c**), one observes an increasingly large drop in thermal energy at corresponding characteristic temperatures. At this point it should become apparent, that what we are dealing with here is a smooth second-order-like phase transition. In a typical second order phase transition, the thermal energy has a step-like jump, and specific heat is therefore infinite. Here, however, such transition is perfectly smooth, and specific heat has a large, but finite peak. This demonstrates the advantage of this theory, namely, its ability to properly take into account the symmetry-breaking fluctuations.

More insight into the behavior of magnetic susceptibility is provided by Fig. 24a-c. Here three figures (corresponding to three regimes **a**, **b**, and **c**) show occupation numbers of three different quasiparticle bands. Fourth band (p=1, spin up) lies well above the Fermi level and its occupation number is zero. Again, only regimes **b** and **c** shows the onset of the spin compensation, which explains a peak and subsequent drop in corresponding susceptibilities below

T_{max}. All of the above results are in qualitative agreement with the single impurity results [57, 58].

Finally, Fig. 25a-c show relative weight factors $W(x)$ for three regimes. Here W is defined as:

$$W(x) \equiv \frac{\exp(f(x))}{\exp(f_{max})} \qquad i = 0, 1 \tag{3.3.1}$$

where

$$f_{max} \equiv \max(f_0, f_1) \tag{3.3.2}$$

Figure 25a shows that in regime a two peaks are roughly equal, so that κ is fairly constant, and Curie behavior is therefore observed. It is to be contrasted with two others, where magnetic peak shows a rapid decay as the system goes into a nonmagnetic regime. Also, one can see that both peaks become narrower as temperature decreases, which is a general feature of all three graphs. This narrowness of the peaks serves as the justification for the many-saddle point approximation described in the next section.

3.4 Many saddle-point approximation and its applications.

This approximation can be improved by expanding the free energy density around each saddle point. The domain of that expansion should be limited by the half-width of each peak. Such pertubation theory will not produce any infrared divergences, associated with soft Goldstone modes. This is because the pertubation around each saddle point preserves the symmetry associated with that saddle point. The strength of this formalism is that it isolates the symmetry-breaking fluctuations, which are responsible for such divergences. Let me note in this respect that the above expansion can qualitatively take into account the contribution of the incoherent scattering term in the Anderson Hamiltonian. This can be achieved by treating the half-width of

each peak as the phemenological parameter. Indeed, the incoherent scattering would serve to increase the width of each peak, while lowering its height. This would not, however, significantly affect the dominance of those peaks at low temperatures and consequently affect the calculated thermodynamic quantities.

Let us now go back to (3.2.20). The goal now is to find all possible maxima of $f(y, \beta)$. Write:

$$0 = \frac{df(y,\beta)}{dy} \tag{3.4.1}$$

From (3.4.1) and (3.2.20) get:

$$y = \sqrt{\frac{U}{2\pi}} \sum_{p\sigma} \int_{BZ} d^3k \;\; \sigma \, n_{pk\sigma}(y,\beta) u^2_{p\sigma}(k,y) \tag{3.4.2}$$

where

$$u^2_{p\sigma}(k,y) = \frac{1}{2}\left[1 + p \frac{E_{f\sigma}(y) - \varepsilon_c(k)}{\sqrt{\left(E_{f\sigma}(y) - \varepsilon_c(k)\right)^2 + 4V^2}}\right] \tag{3.4.3}$$

Equation (3.4.2) is essentially a "mean-field type" self-consistency equation. One simple solution of it is $y = 0$, in which case $n_{\uparrow} = n_{\downarrow}$ (I will call this a nonmagnetic solution). Other solutions are somewhat less trivial. First of all, note that $f(y)$ is an even function of x, which is a consequence of time-reversal symmetry. Let us therefore restrict all integrals to $y > 0$. Then going back to (3.2.15), (3.2.16), and (3.4.3), it is clear that, as y increases:

$$\sum_{p\sigma} \sigma \, n_{pk\sigma}(y,\beta) u^2_{p\sigma}(k,y) \to 1$$

Then the RHS of (3.4.2) would asymptotically approach $\sqrt{U/2\pi}$. Intersection of two functions, represented by each side of (3.4.2) would yield us solutions of that equation. This is sketched schematically in Fig. 26 below.

As can be verified from that sketch, there are three solutions of (3.4.2). First, $y=0$ is a trivial solution, mentioned above. Then there are two other solutions: $y \approx \frac{1}{2}\sqrt{U/2\pi}$ which is a local minimum of free action; and $y \approx \sqrt{U/2\pi}$ - another maximum. This maximum represents a magnetic solution.

Numerical results (see Sec. 3.3) graphically show how magnetic susceptibility, specific heat and other thermodynamic quantities vary, as one goes from magnetic regime ($y \approx \sqrt{U/2\pi}$ peak is dominant) to nonmagnetic regime ($y = 0$ peak is dominant). Specifically, they show a tremendous enhancement of response functions at the point of transition, where two peaks are roughly equal. This intermediate regime, therefore, presents a great deal of interest, and must be further explored. To this end, I will introduce the double-saddle point approximation, in which only two saddle points are taken into account. It will turn out to be an analytically useful approximation. The numerical validity of this approximation has been discussed in Sec. 3.3.

In this section, therefore, I will introduce the double saddle-point approximation, and then use it to calculate the susceptibility and the specific heat in this approximation. Now, let me use index i to denote two peaks: $i=0$ corresponds to $x=0$ peak, while $i=1$ corresponds to ferromagnetic peak. In a two saddle-point approximation, the partition function becomes:

$$Z = e^{f_0} + 2e^{f_1} \tag{3.4.4a}$$

$$f_i = -\pi\beta y_i^2 - \frac{\Omega}{(2\pi)^3}\sum_{p\sigma}\int_{BZ} d^3k \times$$

$$\times \log\left(1+\exp\left(-\beta\,\lambda_{p\sigma k}(y_i)\right)\right)+\frac{1}{2}\log\beta \qquad (3.4.4b)$$

Let us make a change of variables:

$$\frac{\Omega}{(2\pi)^3}\sum_{p\sigma}\int_{BZ} d^{\,3}k \;\rightarrow\; \sum_{p\sigma}\int d\lambda\, N_{ip\sigma}(\lambda)$$

where

$$N_{ip\sigma}(\lambda)=\left(\frac{d\lambda_{ip\sigma}}{d\varepsilon_c}\right)^{-1}\left(\frac{\Omega\, m\, k}{2\pi^2}\right) \qquad (3.4.5a)$$

$$\frac{d\lambda_{ip\sigma}}{d\varepsilon_c}=u_{-\,p\sigma}^{2}(k,x_i)= \qquad (3.4.5b)$$

$$=\frac{1}{2}\left[1-p\,\frac{E_{f\sigma}(x)-\varepsilon_c(k)}{\sqrt{\left(E_{f\sigma}(x)-\varepsilon_c(k)\right)^2+4V^2}}\right]$$

Then (3.4.4b) takes the following form:

$$f_i=-\pi\beta\, y_i^{\,2}-\sum_{p\sigma}\int d\lambda\, N_{ip\sigma}(\lambda)\times$$

$$\times \log\left(1+\exp\left(-\beta\,\lambda_{p\sigma k}(y_i)\right)\right)+\frac{1}{2}\log\beta \qquad (3.4.6)$$

Now, following this approximation, let me rewrite (3.2.25). First let me consider the contribution of the Gaussian fluctuation of df/dH. Write:

$$\chi_{Gauss} = \kappa \cdot \chi_{C.W.} \tag{3.4.7}$$

where

$$\chi_{C.W.} = \beta \frac{(\mu_B g)^2}{4} \left\{ \sum_{p\sigma} \int d\lambda \, N_{ip\sigma}(\lambda) \frac{\sigma}{1+\exp(\beta\lambda)} \right\} \tag{3.4.8}$$

$$\kappa \equiv \frac{1}{1+\frac{1}{2}\exp(f_0 - f_1)} \tag{3.4.9}$$

κ turns out to be a very important factor in this theory. It represents a correction to the Curie power law, which is due to fluctuations between two phases. A second contribution to the magnetic susceptibility will have a Pauli-like character and come from the region around the Fermi level. From (3.2.25) and (3.4.5a) write:

$$\chi_{Pauli} = \beta \frac{(\mu_B g)^2}{4} \left\{ \sum_{p\sigma} \int d\lambda \, N_{ip\sigma}(\lambda) \frac{\exp(\beta\lambda)}{(1+\exp(\beta\lambda))^2} \times \right.$$

$$\left. \times \left(\delta_{i0}(1-\kappa) + \delta_{i1}\kappa \right) \right\} \tag{3.4.10}$$

Two contributions (3.4.7) and (3.4.10) together can be used to describe different regimes of the lattice Anderson Hamiltonian.

First of all, it is clear that when the f_1 peak dominates, $\kappa \approx 1$, so that χ_{Gauss} follows the Curie power law. At the same time from (86) it is clear that the localized portions of $\lambda_{p\sigma k}$ must lie well below the Fermi surface. Consequently the contribution to χ_{Pauli} can only come from the delocalized portions of $\lambda_{p\sigma k}$, which means that χ_{Pauli} is essentially unenhanced over the uncoupled

conduction band value. Therefore the Curie power law should dominate at all temperatures.

A second possibility is when the f_0 peak is dominant. In this case $\kappa \approx 0$ and $\chi_{Gauss} \approx 0$. The localized portions of λ_{pole} may either lie above the Fermi level (for $U >> 2|E_0|$) which corresponds to a complete delocalization of atomic orbitals, or lie below the Fermi level (for $U \leq 2|E_0|$) which corresponds to a double occupancy state. Such a double occupancy would not be energetically favorable (for $U > 0$) if it were not for the hybridization interaction. The portions of c-band interact with the lower lying atomic orbitals, thus lowering the energy of the c-electrons. Doubling the number of lower lying atomic orbitals further lowers the energy of c-electrons, which may compensate the Coulomb repulsion. In either case the contribution of the localized portions of λ_{pole} to χ_{Pauli} is zero, and the only contribution to χ_{Pauli} comes from the delocalized portions of λ_{pole}.

To summarize, the f_0 peak may give zero or double occupancy states, and the combined contribution to χ is always small. Of course the single occupancy state derived from the f_1 peak lies between those two states. The corresponding phase diagrams depend on four parameters in this theory: the energy of the uncoupled orbital E_0, the width of the conduction band W, the hybridization strength V and the Coulomb repulsion U. I did not take into account the indirect exchange J, which would add yet another parameter to the phase diagrams. Obviously the analytical calculation of the phase boundaries from (3.4.6) would be very difficult. What I have done in the next section is to perform numerical evaluation of the various thermodynamic quantities as one goes from one side of the phase boundary to another. It is shown how all of the relevant quantities display a smooth phase transition, which in the discontinuous limit of the mean-field theory would become a second order phase transition.

Let me now calculate the specific heat in the double saddle point approximation. From (3.2.23) we obtain two contributions to the specific heat. First of all, the contribution coming from the Gaussian fluctuation of $df/d\beta$ can now be written as:

$$C_{Gauss} = \beta \left\{ \sum_i \frac{e^{f_i}}{Z} \left(\frac{df_i}{d\beta} \right)^2 - \left(\sum_i \frac{e^{f_i}}{Z} \frac{df_i}{d\beta} \right)^2 \right\} =$$

$$= \beta^2 R \kappa (1-\kappa) \left[\frac{d(f_0 - f_1)}{d\beta} \right]^2 \qquad (3.4.12)$$

It is clear now that the dominant contribution to C_{Gauss} comes near the phase boundaries, i.e. when $0 < \kappa < 1$. It is due to the fluctuations between two different phases. This contribution gives a large peak in the specific heat at the transition regime. Far from the phase boundaries, however, C_{Gauss} is always exponentially small.

A second contribution to the specific heat is analogous to the Pauli susceptibility and is due to low energy thermal excitations just above the Fermi level. By analogy with the susceptibility I will label this contribution C_{Pauli}. Then one can write:

$$C_{Pauli} = \beta^2 \left\{ \sum_{p\sigma} \int d\lambda \, N_{ip\sigma}(\lambda) \frac{\lambda^2 \exp(\beta\lambda)}{(1+\exp(\beta\lambda))^2} \times \right.$$

$$\left. (\delta_{i0}(1-\kappa) + \delta_{i1}\kappa) \right\} \qquad (3.4.13)$$

As was the case with the Pauli susceptibility, the contributions to C_{Pauli} are essentially unenhanced, although such contributions will dominate the Gaussian contribution away from the transition regime.

a). Remark on the Many Saddle-Point Approximation.

Let me now turn to a different aspect of the many-saddle point approximation. It is clear that the many-body term in (3.2.3) proportional to $n_{\mu\uparrow} - n_{\mu\downarrow}$ vanishes in the spin-symmetric state. It is also clear that the relevant interaction many-body term must be proportional to $n_{\mu\uparrow} + n_{\mu\downarrow}$. The problem is that while $n_{\mu\uparrow} - n_{\mu\downarrow}$ belongs to the SU(2) algebra described above, $n_{\mu\uparrow} + n_{\mu\downarrow}$ belongs to an enlarged algebra, namely U(1). It then follows that a symmetric many-body term cannot be generated from an antisymmetric term. Therefore it cannot possibly produce the saddle points describing the spin-symmetric state, except for the trivial point $y=0$. This points us to a very important problem. The many body term in (3.2.1) can in general be represented as:

$$n_{\mu\uparrow} n_{\mu\downarrow} = \frac{1}{4}\left[\left(n_{\mu\uparrow} + n_{\mu\downarrow}\right)^2 - \left(n_{\mu\uparrow} - n_{\mu\downarrow}\right)^2\right] \qquad (3.4.14)$$

One would then obtain an effective Hamiltonian represented as the linear combination of the symmetric and antisymmetric terms, each coupled to its own Gaussian field after the Hubbard-Stratonovich transformation. What I did above was to use the specific property of the fermion algebra $n_\sigma^2 = n_\sigma$ to reexpress the interaction term as:

$$n_{\mu\uparrow} n_{\mu\downarrow} = \frac{1}{2}\left[\left(n_{\mu\uparrow} + n_{\mu\downarrow}\right) - \left(n_{\mu\uparrow} - n_{\mu\downarrow}\right)^2\right] \qquad (3.4.15)$$

In this case the first term is essentially a one-body term and it was incorporated into one-body zero order Hamiltonian. The second term, however, is the effective many-body operator, which becomes

antisymmetric after the linearizing H.-S. transformation. The advantage of the above method is that it lowers the dimensionality of a Gaussian integral, without which the numerical computations will become impossibly long. It does not, however, work well in the many-saddle point approximation, as it fails to produce points with a different dynamical symmetry.

b). Improved Many Saddle-Point Approximation.

Let me now discuss the representation of the many-body operator given by (3.4.14) in more detail. In analogy to (3.2.2) represent (3.2.1) as:

$$H = H_0 + \frac{U}{4} \sum_{\mu} \left[\left(n_{\mu\uparrow} + n_{\mu\downarrow} \right)^2 - \left(n_{\mu\uparrow} - n_{\mu\downarrow} \right)^2 \right] \qquad (3.4.16)$$

where

$$H_0 = \sum_{\mu\sigma} E_0 \, n_{\mu\sigma} + \sum_{k\sigma} \varepsilon_k \, c^{+}_{k\sigma} c_{k\sigma} + \sum_{\mu\sigma k} \frac{V_k}{\sqrt{N}} \left(f_{\mu\sigma}{}^{+} c_{k\sigma} + h.c. \right) \qquad (3.4.17)$$

Following through the same calculations as in Sec. 3.2 we obtain:

$$Z \equiv Tr \; e^{-H\beta} = \int dy \, dz \; e^{f(y,z,\beta)} \qquad (3.4.18)$$

$$f(y,z,\beta) = -\pi \beta \left(y^2 + z^2 \right) - \frac{\Omega}{(2\pi)^3} \sum_{p\sigma} \int_{BZ} d^3k \; \times$$

$$\log\left(1 + \exp\left(-\beta \lambda_{p\sigma k}(y,z)\right)\right) + \frac{1}{2} \log \beta$$

where

$$\lambda_{p\sigma k} = \frac{1}{2}\left(\varepsilon_f(y,z) + \varepsilon_c(k) + p \times \right. \tag{3.4.19}$$

$$\left. \times \sqrt{\left(\varepsilon_f(y,z) - \varepsilon_c(k)\right)^2 + 4V^2} \right)$$

$$\varepsilon_f(y,z) = E_0 + \sqrt{U\pi}\,(\sigma y + i z)$$

To deal with the complex factor iz we follow the standard procedure [33,34] and extend z to a complex plane, namely define:

$$z = z' - i z''$$

Then we look for maxima of the free energy density. Following the same derivation as the one leading to (3.4.2) we obtain:

$$y = \sqrt{\frac{U}{4\pi}} \sum_{p\sigma} \int_{BZ} d^3k \;\; \sigma\, n_{pk\sigma}(y,z,\beta)\, u^2_{p\sigma}(k,y,z) \tag{3.4.20}$$

$$z'' = \sqrt{\frac{U}{4\pi}} \sum_{p\sigma} \int_{BZ} d^3k \;\; n_{pk\sigma}(y,z,\beta)\, u^2_{p\sigma}(k,y,z) \tag{3.4.21}$$

$$z' = 0$$

In this case there are two many-body terms in (3.4.16). The first term becomes symmetric after the H.-S. transformation, and is coupled to a field z. The second term becomes antisymmetric after the H.-S. transformation, and is coupled to a field y. It is clear then that the antisymmetric field y may have two saddle points: a trivial solution $y = 0$, and the magnetic solution $y \approx \sqrt{U/4\pi}$. The situation with the symmetric field z is a little bit more complicated. Let us first of all consider the possible solutions to (3.4.21) for $y = 0$. Since we are in the spin-symmetric state we can drop the spin index. Now it is clear that $\varepsilon_f(0,z)$ $z>0$ lies within the

conduction band. In that case it is important to consider the contributions of the conduction band above and below $\varepsilon_f(0,z)$. To facilitate the discussion I give the table below which is valid in the large U limit.

Conduction- and Localized-like Regions for Upper and Lower Bands.

$\varepsilon_f(0,z) < \varepsilon_{ck}$		$\varepsilon_f(0,z) > \varepsilon_{ck}$	
lower band	upper band	lower band	upper band
$p = -1$	$p = -1$	$p = -1$	$p = -1$
dispersion relation	dispersion relation	dispersion relation	dispersion relation
$\lambda_{pk} \approx \varepsilon_f(0,z)$	$\lambda_{pk} \approx \varepsilon_f(0,z)$	$\lambda_{pk} \approx \varepsilon_f(0,z)$	$\lambda_{pk} \approx \varepsilon_f(0,z)$
Bogoliubov coefficients	Bogoliubov coefficients	Bogoliubov coefficients	Bogoliubov coefficients
$u_p^2(k,0,z) \approx 1$	$u_p^2(k,0,z) \approx 0$	$u_p^2(k,0,z) \approx 0$	$u_p^2(k,0,z) \approx 1$

Table 2

It is clear now that for $z=0$ ε_f is below the Fermi level, but it increases as we increase z. From the table it then follows that as long as ε_f is below the Fermi level, the RHS of (3.4.21) is approximately $\sqrt{U/\pi}$. Indeed the dominant contribution to the RHS of (3.4.21) for $\varepsilon_f < \varepsilon_{ck}$ comes from $p = -1$ branch, while for

$\varepsilon_f > \varepsilon_{ck}$ the dominant contribution comes from $p = 1$ branch. Also the factor two comes from the spin sum. Now as ε_f goes just above the Fermi level, it follows that the contribution from the above branches would fall off very rapidly, so that the contributions from delocalized conduction-like branches which are much smaller would become dominant. The resultant plot of both sides of (3.4.21) is sketched in Fig. 27. The width of the region in which the RHS of (3.4.21) rapidly falls off is proportional to the critical temperature at which the saddle point represented by the intersection of two graphs in Fig. 27 becomes stable. That temperature will be identified below as the Kondo temperature, and will represent the low energy scale in the problem.

But before I do that let me consider the possible saddle points for z in the magnetic regime $y \approx \sqrt{U/4\pi}$. Assuming very large U the dominant contribution to the RHS of (3.4.21) will come from the first column of the table above ($p = -1$) for spin down branch. In that case the RHS of (3.4.21) is approximately equal to $\sqrt{U/4\pi}$ (see Fig. 28) Substituting this value of z into (3.4.19) and remembering that $y \approx \sqrt{U/4\pi}$, we obtain the standard dispersion relations for the magnetic regime, namely

$$\lambda_{-1\downarrow} \approx E_0 \qquad \lambda_{1\uparrow} \approx E_0 + U \tag{3.4.22}$$

while two other branches are conduction-like.

Now, comparing these results to the ones obtained using the "antisymmetric representation" (3.4.15) for the many-body term it is clear that the description of the magnetic saddle point is essentially equivalent. A major difference however arises in the description of the nonmagnetic saddle point. In the first instance the antisymmetric many-body operator can only give a trivial zero solution. In that sense the antisymmetric field y can be understood as an antisymmetric order parameter. Therefore the trivial solution tells us that the y parameter vanishes, which means that the system

goes into the state of different symmetry. It does not however tells us explicitly what that symmetry is, or what are other physical properties of the new state.

It therefore follows that in order to correctly account for all the possible saddle points of the system one needs to break a many-body Hamiltonian into all the possible operators with different gauge symmetries coupled to the corresponding Gaussian fields. In that case the corresponding saddle point will represent the state with that gauge symmetry.

To close this section let me go back to the discussion of the symmetric state of the Anderson Hamiltonian. I want to calculate the critical temperature at which the symmetric state becomes stable. Using the dispersion relations (3.4.19) and (3.4.22) and assuming that the critical temperature is low, we obtain:

$$E_0 = \frac{\Omega}{(2\pi)^3} \int_{BZ} d^3k \ \lambda_{pk}(0, z_c)\ n_{pk}(\beta) \tag{3.4.23}$$

where $p = -1$ for $\varepsilon_f(0, z_c) < \varepsilon_{ck}$ and $p = 1$ for $\varepsilon_f(0, z_c) > \varepsilon_{ck}$. Let us again assume a simple rectangular density of states in the band:

$$\rho_0(\varepsilon) = \begin{cases} \rho_0 & -D < \varepsilon < D \\ 0 & \text{otherwise} \end{cases}$$

Using (3.4.19) and expanding (3.4.23) in powers of V^2 we obtain:

$$E_0 - \varepsilon_f = \rho_0 \int d\varepsilon \ \frac{V^2}{\varepsilon - \varepsilon_f} n(\beta_c) \tag{3.4.24}$$

Since $\varepsilon_f(0, z_c) \approx 0$, integrating (3.4.24) we finally obtain:

$$E_0 = \rho_0 V^2 \ln \frac{k_B T_c}{D}$$

or

$$k_B T_c = D \exp\left(\frac{E_0}{\rho_0 V^2} \right) \tag{3.4.25}$$

which is exactly the expression for the Kondo temperature. One can further calculate the renormalized peak width. To calculate the peak width one needs to calculate the f-electron self-energy. The leading order diagram is shown in Fig. 29. For the unrenormalized state one then simply obtains:

$$\Sigma_f(\varepsilon) = \frac{\Omega}{(2\pi)^3} \int_{BZ} d^3k \; V^2 G_c(\varepsilon, k) =$$

$$= \frac{\Omega}{(2\pi)^3} \int_{BZ} d^3k \; \frac{V^2}{\varepsilon - \varepsilon_k + i0^+} \tag{3.4.26}$$

Again assuming the rectangular band we obtain:

$$\Delta_0 = \mathrm{Im}\, \Sigma_f(0) = \pi \rho_0 V^2 \tag{3.4.27}$$

and the derived density of states

$$\rho_f^{(0)}(\varepsilon) = \frac{\Delta_0}{(\varepsilon - E_0)^2 + \Delta_0^2} \tag{3.4.28}$$

Now in the symmetric state the renormalized conduction electron Green's function acquires the weight factor $u_p^2(k, 0, z_c)$. As can be seen from the table 2 that weight factor is very small for conduction-like branches. Indeed this weight factor represents the probability for f-electrons to become delocalized, i.e. one may

identify $u_p^2(k,0,z_c) \approx 1 - n_f$ which becomes small in the Kondo limit $n_f \to 1$. Therefore one obtains:

$$\rho_f(\varepsilon) = \frac{\Delta}{(\varepsilon - \varepsilon_f)^2 + \Delta^2} \tag{3.4.29}$$

where

$$\Delta = u_p^2(k,0,z_c)\Delta_0 \tag{3.4.30}$$

Therefore in the magnetic regime one obtains a relatively broad resonance centered around E_0, while in the symmetric Kondo regime one obtains a much narrower resonance centered around ε_f. The narrowing of that resonance is essentially due to large Coulomb repulsion which essentially suppresses the charge fluctuations, so that $u_p^2(k,0,z_c) \approx 1 - n_f$ is small. Using the density of states obtained, one can calculate the occupation numbers which are found to satisfy the Friedel sum rule (see Sec. 1.2). All of these results are completely equivalent to the results found previously and are essentially similar to the single impurity results. However when one applies these results to the lattice, the problems that I discussed at the end of Sec. 1.2 still apply. In particular this state does not provide a mechanism for the long range coherence in the lattice. Moreover, as I will show in the next section the above saddle point may become unstable in the orbitally degenerate case with small crystal-field splitting.

3.5 Summary of Section 3

In Section 3 the local operator formalism has been applied to the study of thermodynamic properties of the orbitally nondegenerate

lattice Anderson Hamiltonian. It allows one to go beyond the mean field approximation to include the relevant fluctuations. As the first important point, two types of fluctuations have been differentiated. In the study of possible states of the system, which are represented as a saddle point of the free energy density, we have found a nonmagnetic state, and two magnetic states, related by time inversion symmetry. One kind of fluctuation involves those around each of the corresponding saddle points, i.e. the fluctuations arising from the finite peak width around each saddle point. As I have shown in this Section the corresponding peak width is very small in the low temperature regime, although it does become wider as temperature increases. Therefore the main effect of those fluctuations is to renormalize the relevant physical parameters without fundamentally altering the ground state of the system. Such renormalization can be calculated by straightforward expansion of the free energy density around each saddle point with the domain of expansion limited by the half-width of each peak.

Another kind of fluctuation (so called symmetry-breaking type) involves those between the magnetic and nonmagnetic saddle points. The importance of that type of fluctuation depends on the relative weights of two saddle points. When the relative weight of one of those two saddle points is much greater than the second one (which corresponds to a stable state far from the transition regime) the symmetry breaking fluctuations are exponentially small. The situation becomes drastically different, however, when two saddle points have a comparable weight. That situation corresponds to the transition regime and in that case the symmetry-breaking fluctuations become very important, especially in the calculation of the various response functions, represented by second derivative of the free energy. In that case the symmetry-breaking fluctuations are represented by quadratic (Gaussian) fluctuations of the first derivatives of the free energy density, which have a sharp *but finite* peak around the transition point. Therefore the main advantage of the functional integral treatment of this problem is that it allows one to describe a smooth transition between the magnetic and nonmagnetic regimes. This is in contrast to the typical mean-field

approach, where such transitions are infinite in second order derivatives of the free energy. Numerical evaluation of the relevant response functions essentially confirms above observations. The behavior of the system above the transition regime is a typical local moment behavior as can be observed from numerical evaluations. However below the transition regime the situation can be much more complicated.

As an analytical tool in understanding the behavior of a lattice in the Kondo regime close to a magnetic transition I have used the "many-saddle" point approximation. It was my intention to find the saddle points of the free energy density which preserve the spin rotation symmetry at low temperatures, and may possibly explain the unusual properties of HFS, such as the enhanced specific heat and the low temperature coherence.

One point that the saddle point calculation has shown is the importance of expressing the many body term as the quadrature of generators with all possible symmetries relevant to the system. After applying the H.-S. transformation, the many-body term becomes a linear combination of those generators coupled to the corresponding Gaussian fields. Nonzero saddle points of each Gaussian field represents the state of the system with the symmetry of the corresponding generator. In that sense those Gaussian fields represent the order parameter for the corresponding symmetry state of the system. In particular, in the system under consideration we deal with the symmetric and antisymmetric spin states. It has been shown in Sec. 3.4 that by using the most general representation of the many-body operator (Eq. (3.4.14)) one can obtain the Kondo saddle point, similar to the one found by other theories. On the other hand, by using a representation (3.4.15), which involves the quadrature of the antisymmetric term, only the antisymmetric Gaussian field can then be obtained. *All* symmetric saddle points are then represented by zero Gaussian field, which only tells us that the system is not in the antisymmetric state. Therefore in using the saddle point approximation, one should use the most general representation of the many body operator. Representation (3.4.15), however, is very useful for numerical

evaluations, which are essentially exact. Using the representation (3.4.14) would square the number of operations needed to do the numerical evaluations.

Finally it has been shown that calculated saddle points do not provide a mechanism for the low temperature coherence, which characterizes HF systems.

4. Application of the Local Operator Construction to the Orbitally Degenerate Anderson Model

4.1 Introduction

In this section I study the low temperature properties of the nearly degenerate lattice Anderson Hamiltonian in the Kondo regime. This means that I explicitly include the effect of the small crystal field splitting. This splitting is taken to be greater than the width of the uncoupled f-band, which I take to be zero. For a review of the previous work see refs. [20] and [52]. The important technique developed here involves the application of canonical transformation, generated by an $SU(2J+2)$ algebra (J is the total angular momentum of a localized electron). That transformation decouples the effective f-band and c-band. The application of canonical transformation, generated by Lie algebras provides a powerful tool for obtaining the low temperature nonpertubative results, as in the case of superfluid ^{3}He [59]. This is exactly the situation here. In fact, it turns out that after decoupling the effective f- and c-bands, one obtains the nonpertubative ground state. This means that the interacting ground state cannot be obtained from the noninteracting states by pertubation theory.

The state derived has many unusual properties. It involves the almost localized f-electrons hopping between the lattice sites in a coherent fashion with the correlation length being much larger than a lattice constant. The hopping pins those quasiparticles close to the Fermi surface, thereby producing the large enhancement in the specific heat coefficient γ, and the static magnetic susceptibility χ. The stability of such a state at low temperature is due to the fact that the orbital degeneracy of localized electrons is higher than the degeneracy of conduction electrons. In this respect it is important in my opinion not to make the simplification of making the degeneracy of the conduction band equal to the degeneracy of the localized electrons [40,41]. In addition, I have calculated the Wilson ratio, and it is in approximate agreement with the experimental results [1].

The Section is organized as follows. In Section 4.2 various forms of the propagator representation for the near degenerate lattice Anderson

Hamiltonian, utilizing the local operator construction are given. Next I discuss an equivalent form of the propagator which are particularly useful for the degenerate lattice Anderson Hamiltonian. This new form of the propagator has the advantage of enabling us to calculate additional stationary states that preserve the spin rotational symmetry. Next section (4.3) discusses the algebraic structure of the effective Hamiltonian. I write down the appropriate SU($2J$+2) generators and the useful commutation relations. Further, I write down the canonical transformation in terms of SU($2J$+2) generators. Actual calculations of appropriate parameters of the canonical transformation are referred to Appendix 6, where I set up the appropriate closed system of recursion relations and actually calculate the brackets of the generator of the canonical transformation with the effective Hamiltonian to all orders. This allows me to explicitly write down the equation that decouples the effective f- and c-bands, which specifies the corresponding parameters of the canonical transformation. Also in Appendix 6 I solve the decoupling equation. It turns out that the small lattice-induced splitting in the f-band produces a qualitatively new solution of the "symmetry-breaking" type. In Section 4.4 I study the possible saddle points of the system. In particular, I find a new saddle point which corresponds to the symmetry-breaking solution. In Sections 4.5 and 4.6 I study the physical properties of the new saddle point. The important properties of the corresponding ground state are characterized by the spin delocalization regime, which along with the short range Coulomb repulsion is responsible for the long range phase correlation of the quasiparticle excitations. I compare my results with the results obtained by the slave boson model and its extensions to a lattice [40,41]. In my view the extension of the slave boson model to a lattice suffers from several fundamental questions concerning its assumptions. Discussion of those and other questions is given at the end of Sec. 4.6. Section 4.7 addresses a question of the empty state contribution to the partition function.

4.2 Propagator Representations for the Nearly Degenerate Anderson Hamiltonian.

Consider the almost degenerate Anderson Hamiltonian:

$$H = H_{band} + H_f + H_{mix} \tag{4.2.1}$$

$$H_{band} = \sum_{k\sigma} \varepsilon_k \, c^+_{k\sigma} c_{k\sigma}$$

$$H_f = \sum_{\mu m} E_{0m} \, f^+_{\mu m} f_{\mu m} + U \sum_{\mu,\, m > m'} f^+_{\mu m} f_{\mu m} f^+_{\mu m'} f_{\mu m'}$$

$$H_{mix} = \frac{1}{\sqrt{N_L}} \sum_{\mu k m \sigma} \left[V_m(k) \, c^+_{k\sigma} f_{\mu m} + H.C. \right]$$

$$E_{0m} = E_0 + \delta(T) |m| + \mu_B \, g \, H \, m$$

Here f^+, f represent localized electron operators, and c^+, c represent itinerant electron operators. Notation: k represents the conduction electron wave-vector, $\sigma = \pm 1/2$ indicates the conduction electron spin along the axis of quantization, $m = -J, \ldots, J$ is the projection of the total angular momentum of the localized electrons, and $\mu = 1, \ldots, N_L$ numbers the cells in which those electrons are localized. Also, it is assumed that at very low temperatures the thermal fluctuations in the lattice are sufficiently small so that a small splitting δ in $2J+1$ levels arises. This splitting should preserve the time inversion symmetry, and is therefore coupled to the absolute value of the total angular momentum quantum number. Therefore $\delta(T)$ is given by:

$$\delta(T) = \begin{cases} \delta & T < T_L \\ 0 & T > T_L \end{cases} \tag{4.2.2}$$

Here T_L represents the characteristic lattice temperature at which such a splitting occurs.

Now as in Sec. 3.4 we rewrite the many-body operator in (2.1) in the representation using the square of the antisymmetric combination (in indices m, m') of $n_{\mu m}$ and $n_{\mu m'}$:

$$H = H_0 - \frac{U}{2} \sum_{m > m'} \sum_{\mu} \left(n_{\mu m} - n_{\mu m'} \right)^2 \tag{4.2.3}$$

$$H_0 = \sum_{\mu m} \left(E_{0m} + UJ \right) n_{\mu m} + \sum_{k\sigma} \varepsilon_k \, c^+_{k\sigma} c_{k\sigma} +$$

$$+ \frac{1}{\sqrt{N_L}} \sum_{\mu k m \sigma} \left[V_m(k) c^+_{k\sigma} f_{\mu m} e^{-ikR_\mu} + H.C. \right]$$

where

$$n_{\mu m} \equiv f^+_{\mu m} f_{\mu m}$$

Following the functional integral formalism procedure as in Sec. 3.2 and using the coherent Q=0 approximation we obtain:

$$H = -\frac{d}{dt} \left\langle e^{-t H_{MF}(y)} \right\rangle_G \Big|_{t=0} \tag{4.2.4}$$

where:

$$H_{MF}(y) = \sum_{mk} \varepsilon_{fm}(y) f^+_{km} f_{km} + \sum_{\sigma k} \varepsilon_k \, c^+_{k\sigma} c_{k\sigma} + \tag{4.2.5}$$

$$+ \sum_{m\sigma k} \left[V_m(k) c^+_{k\sigma} f_{km} + H.C. \right]$$

$$\varepsilon_{fm}(y) \equiv E_{0m} + UJ - \sqrt{2\pi U}\, s_{0m} \tag{4.2.6}$$

and

$$s_{0m} \equiv \sum_{m'<m} y_{0m\,m'} - \sum_{m''>m} y_{0m''m} \tag{4.2.7}$$

is the Q=0 Fourier component of the local Gaussian fields:

$$y_{0m\,m'} = \frac{1}{\sqrt{N_L}} \sum_{\mu} y_{\mu m\, m'}$$

The problem with this representation has been discussed in Sec. 3.4, where it has been shown that in the large U limit it produces only the antisymmetric (magnetic) saddle points as well as the trivial zero magnetic point. Since we are interested in describing all the possible symmetric saddle points, the above representation is not appropriate. In Sec. 3.4 we therefore argued that one needs to use the most general representation for the many-body operator. In this case that representation takes the following form:

$$H = H_0 + \frac{U}{4} \sum_{m>m'} \sum_{\mu} \left[\left(n_{\mu m} + n_{\mu m'} \right)^2 - \left(n_{\mu m} - n_{\mu m'} \right)^2 \right] \tag{4.2.8}$$

$$H_0 = \sum_{\mu m} E_{0m}\, n_{\mu m} + \sum_{k\sigma} \varepsilon_k\, c^+_{k\sigma}\, c_{k\sigma} +$$

$$+\frac{1}{\sqrt{N_L}}\sum_{\mu k m\sigma}\left[V_m(k)c^{+}_{k\sigma}f_{\mu m}e^{-ikR_\mu}+H.C.\right]$$

Again following a similar procedure we obtain:

$$H=-\frac{d}{dt}\left\langle e^{-tH_{MF}(y)}\right\rangle_G\Big|_{t=0} \tag{4.2.9}$$

where:

$$H_{MF}(y)=\sum_{mk}\varepsilon_{fm}(y)f^{+}_{km}f_{km}+\sum_{\sigma k}\varepsilon_k\, c^{+}_{k\sigma}c_{k\sigma}+ \tag{4.2.10}$$

$$+\sum_{m\sigma k}\left[V_m(k)c^{+}_{k\sigma}f_{km}+H.C.\right]$$

$$\varepsilon_{fm}(y)\equiv E_{0m}-\sqrt{\pi U}\;s_{0m} \tag{4.2.11}$$

and

$$s_{0m}\equiv\sum_{m'<m}\left\{y_{0m\,m'}-z_{0m\,m'}\right\}-\sum_{m''>m}\left\{y_{0m\,''m}+z_{0m''m}\right\} \tag{4.2.12}$$

denotes the Q=0 Fourier component of the local Gaussian fields. In Sec. 3.4 the above representation led to two coupled integral equations (3.4.20-21). In the present case however the number of equations is $2J(2J+1)$ which makes this approach impractical.

Let me rewrite $\hat{L}(t)$ in a different but equivalent form, appropriate for the on-site Coulomb repulsion U being the largest parameter in the theory. The new form is particularly appropriate for finding the symmetric saddle points which have the same

contribution to all quantum channels. In the previous approach this would require us to look for a maximum of free energy density with respect to some symmetrized combination of $2J(2J+1)$ Gaussian variables. However the approach I offer now produces the symmetric form of the partition function and the integration is one-dimensional rather than $2J(2J+1)$-dimensional, thereby eliminating any calculational difficulties. To be explicit, let me write:

$$Z(\beta) = Tr \int_{-\infty}^{+\infty} d\xi \sum_{N=0}^{2J+1} e^{-\beta H_{MF}^{(N)}(\xi, \beta)} \tag{4.2.13}$$

where

$$H_{MF}^{(N)}(\xi, \beta) = \sum_{k} \hat{h}_k^{(N)} \tag{4.2.14}$$

$$\hat{h}_k^{(N)} = \sum_{m} \left(E_{0m}^{(N)} + \xi \right) f_{km}^{+} f_{km} + \sum_{\sigma} \varepsilon_k c_{k\sigma}^{+} c_{k\sigma} + \tag{4.2.15}$$

$$+ \sum_{m\sigma} \left[V_m(k) c_{k\sigma}^{+} f_{km} + H.C. \right] - N\xi$$

Here N represents the filling number for the $2J+1$-degenerate energy band. $E_{0m}^{(N)}$ is given in the last column of the table 1. It basically represents the thermal energy of the system (given in the column 3) divided by the filling number N. The auxiliary complex field ξ has been introduced (see [59]) to enforce the constraint

$$\sum_{m} n_m(\beta, k) = N \tag{4.2.16}$$

where $n_m(\beta, k)$ denotes the thermal average of the number operator for f-electrons in the m -th state. Note that this constraint commutes with the uncoupled Hamiltonian (no f-c mixing). In that case the number operator in (4.2.15) can be substituted by its thermal average, and the integration over the complex ξ will produce a simple constraint-conserving delta function. I will discuss in Sec. 4.7 below how the presence of the mixing term affects the constraint (4.2.16). In fact I will show that in the coupled case the average number of electrons may be slightly less than one. This approach therefore is slightly different from the standard approach [59] (see further discussion in Sec. 4.7), but it does intuitively correspond to one's understanding of what the number of electron's should be in both coupled and uncoupled regimes.

The propagator written in this form has the advantage of preserving the rotational invariance. In fact, each term in the new propagator corresponding to some particular value of N represents the sum of the old propagator densities evaluated over all the saddle points satisfying (4.2.16). Such summation restores the rotational symmetry, which is reflected in the symmetry of each term in the new propagator.

In the large U limit only the N=0, 1 terms are relevant. Also in the Kondo regime, where E_0 is large negative it is clear that N= 1 term should dominate, which means that other terms become exponentially small at low temperatures. Below, therefore, I will only consider the terms that satisfy (4.2.16) for N=1. Since N is now fixed I will drop this subscript for now.

Below I want to explore all the possible stationary states of (4.2.13) in the Kondo limit. To do that I will try to partially diagonalize (4.2.14), so that I will now be concerned with the algebraic structure of the effective Hamiltonian.

4.3 The Algebraic Structure of the Effective Hamiltonian, and the Solutions of the Decoupling Equation.

Next I want to decouple the f and c quasiparticles in $H_{MF}^{(1)}$ by appropriate canonical transformation. It is important to note in that respect that:

$$\hat{h}_k \equiv \hat{h}_k^{(1)} \in SU\ (2J+2) \tag{4.3.1}$$

Indeed, define SU $(2J+2)$ generators (drop the common wave-vector subindex k):

$$T_{\mu\nu}^{+} = \frac{1}{\sqrt{2}}\left[a_\mu^{+}a_\nu + a_\nu^{+}a_\mu\right] \qquad \mu \neq \nu \tag{4.3.2}$$

$$T_{\mu\nu}^{-} = \frac{i}{\sqrt{2}}\left[a_\mu^{+}a_\nu - a_\nu^{+}a_\mu\right] \qquad \mu \neq \nu \tag{4.3.3}$$

$$T_\mu = a_\mu^{+}a_\mu \tag{4.3.4}$$

where

$$a_\mu = \begin{cases} \frac{1}{\sqrt{2}}\sum_\sigma c_\sigma & \mu = 0 \\ f_m & \mu = m = -J,\ldots, J \end{cases} \tag{4.3.5}$$

Here I will use the convention that the Greek subindices μ,ν, etc. (except σ which indicates the spin of conduction electrons) refer to

all the half-integral values of angular momentum between $-J$ and J (denoted by Latin subscripts) as well as to zero subscript, which refers to the antisymmetric c-channel. In terms of these generators rewrite (4.2.15) as:

$$\hat{h} = \sum_m a_m^{(0)} T_m + a_0^{(0)} T_0 + \sum_m a_{0m}^{(0)} T_{0m}^{+} + \sum_{m>n} a_{mn}^{(0)} T_{mn}^{+} \tag{4.3.6}$$

where

$$a_m^{(0)} = E_{Um} \quad a_0^{(0)} = \varepsilon_k \quad a_{0m}^{(0)} = 2V_m \quad a_{mn}^{(0)} = 0 \tag{4.3.7}$$

The goal now is to perform a canonical transformation on $\hat{h}$ such that the effective f-band is decoupled from the effective c-band. Define:

$$U = e^{R} \qquad R = i \sum_n \Theta_n T_{0n}^{-} \tag{4.3.8}$$

The transformed Hamiltonian will then have the following form (see Eqs. (A6.55) and (A6.66)):

$$H_D = \sum_k \hat{h}_k$$

where (drop the common subscript k):

$$\hat{h} = \sum_m A_m T_m + A_0 T_0 + \sum_m A_{0m} T_{0m}^{+} + \sum_{m>n} A_{mn} T_{mn}^{+}$$

and the corresponding coefficients are given by Eqs. (A6.32), and (A6.52)-(A6.54). Note that in Appendix 6 the following definitions

are used:

$$x \equiv \cos\left(\sqrt{\frac{1}{2}|\Theta|^2}\right) \qquad |\Theta|^2 \equiv \sum_n \Theta_n^2$$

$$\bar{a}_{0f}^2 \equiv \sum_m a_{0m}^{(0)2}$$

$$\Delta \equiv \varepsilon_k - E_0 - \xi$$

$$h(m) \equiv \delta |m| + \mu_B g H m$$

$$\bar{h}^{(n)} \equiv \frac{\sum_m h(m)^n \Theta_m^2}{|\Theta|^2}$$

$$\bar{h} \equiv \bar{h}^{(1)}$$

and

$$\bar{a}_{0f}(h) \equiv \sqrt{\bar{a}_{0f}^2 - 2\left(\frac{1-x^2}{x^2}\right)\left(\bar{h}^{(2)} - \bar{h}^2\right)}$$

is the renormalized f-c mixing parameter.

Our goal is to find a canonical transformation such that the effective f-band is decoupled from the effective c-band, i.e.

$$A_{0m} = 0$$

From this condition one obtains the so-called decoupling equation (see Appendix 6):

$$2\frac{x^2(1-x^2)}{(1-2x^2)^2}=\frac{\bar{a}_{0f}^2(h)}{(\Delta-\bar{h})^2} \tag{4.3.9}$$

Let me consider two types of solutions to this equation. First take h=0 (this would correspond to $T > T_L$). Define:

$$\tilde{R} \equiv \frac{\sqrt{2}(\Delta-\bar{h})}{\bar{a}_{0f}(h)} \tag{4.3.10}$$

Then (4.3.9) has four solutions:

$$x^2=\frac{1}{2}\left(1\pm\frac{\tilde{R}}{\sqrt{\tilde{R}^2+4}}\right) \tag{4.3.11}$$

As the next step consider h small (so that $T < T_L$). Then the above solutions are perturbed slightly, and there is nothing fundamentally different in those channels. As we shall see below this solution corresponds to f-electrons being completely localized ($\xi \rightarrow -\infty$), which corresponds to the saddle points of the free energy density previously obtained. However, there is another possible solution for small h. Take $x \propto h$, so that x is small. Then (4.3.9) could approximately be written as:

$$2x^4\Delta^2-\bar{a}_{0f}^2x^2+2\left(\bar{h}^{(2)}-\bar{h}^2\right)=0 \tag{4.3.12}$$

and the solutions are:

$$x^2 = \frac{\bar{a}_{0f}^2 \pm \sqrt{\bar{a}_{0f}^4 - 16\Delta^2\left(\bar{h}^{(2)} - \bar{h}^2\right)}}{4\Delta^2} \approx \begin{cases} \dfrac{\bar{a}_{0f}^2}{\Delta^2} \\ \dfrac{2\left(\bar{h}^{(2)} - \bar{h}^2\right)}{\bar{a}_{0f}^2} \end{cases} \qquad (4.3.13)$$

The first solution has to be rejected because of our assumption that x is small. Second solution, however, satisfies our assumption and is the fundamentally new "symmetry breaking" type solution. In the next section I will discuss the physical properties of this new solution. In fact, I will show that many properties of HFS can be understood within the framework of this new solution.

4.4 ∴ New Saddle Point for the Symmetry Breaking Solution of the Decoupling Equation.

Let us explore the symmetry-breaking solution in more detail. The corrections to the corresponding zero order coefficients $a_{mn}^{(0)}$, $a_m^{(0)}$, and $a_0^{(0)}$ are (see Appendix 6, Eqs. (A6.52)-(A6.54)):

$$A_{mn} \equiv \sum_{p=1}^{\infty} \frac{a_{mn}^{(p)}}{p!} = \frac{\Theta_m \Theta_n}{|\Theta|^2}\left[\mp \bar{a}_{0f}(h)\frac{\sqrt{1-x^2}}{x} - \right.$$

$$\left. - \sqrt{2}\frac{1-x}{x}\left(2\bar{h} - h(m) - h(n)\right) \right] \qquad (4.4.1)$$

$$A_m \equiv \sum_{p=1}^{\infty} \frac{a_m^{(p)}}{p!} = \frac{1}{\sqrt{2}} \frac{\Theta_m^{\,2}}{|\Theta|^2}\Big[\mp \bar{a}_{0f}(h) \frac{\sqrt{1-x^2}}{x} -$$

$$- 2\frac{1-x}{x}(\bar{h} - h(m)) \Big] \qquad (4.4.2)$$

$$A_0 \equiv \sum_{p=1}^{\infty} \frac{a_0^{(p)}}{p!} = \pm \frac{1}{\sqrt{2}} \bar{a}_{0f}(h) \frac{\sqrt{1-x^2}}{x} \qquad (4.4.3)$$

or using the symmetry-breaking solution to (4.3.9) write:

$$A_{mn} = \frac{1}{\sqrt{2}} \frac{\Theta_m \Theta_n}{|\Theta|^2}\Big[\Big(\Delta \mp \sqrt{\Delta^2 + 2\bar{a}_{0f}^2(h)} \Big) +$$

$$+ 2(2\bar{h} - h(m) - h(n)) \pm \sqrt{2}(2\bar{h} - h(m) - h(n)) \times$$

$$\times \frac{\bar{a}_{0f}}{\left(\bar{h}^{(2)} - \bar{h}^2\right)} \Big] \qquad (4.4.4)$$

$$A_m = \frac{\Theta_m^{\,2}}{|\Theta|^2}\Big[\frac{1}{2}\Big(\Delta \mp \sqrt{\Delta^2 + 2\bar{a}_{0f}^2(h)} \Big) +$$

$$+ 2(\bar{h} - h(m)) - \sqrt{2}(\bar{h} - h(m)) \frac{\bar{a}_{0f}}{\left(\bar{h}^{(2)} - \bar{h}^2\right)} \Big] \qquad (4.4.5)$$

$$A_0 = -\frac{1}{2}\left(\Delta \mp \sqrt{\Delta^2 + 2\bar{a}_{0f}^2(h)}\right) \tag{4.4.6}$$

Here A_m is understood as the localized portion of minus and plus channels, corresponding to $\mp$ signs in (4.4.5). Then the renormalized $2J+2$ energy bands are:

$$\lambda_0 = \frac{1}{2}\left(E_{0m} + \xi + \varepsilon_k \pm \sqrt{\Delta^2 + 4\bar{a}_{0f}^2(h)}\right) \tag{4.4.7}$$

$$\lambda_m = (E_{0m} + \xi) + h(m)\left(1 - \frac{2\Theta_m^2}{|\Theta|^2}\right) + \frac{1}{2}\frac{\Theta_m^2}{|\Theta|^2}(\Delta \mp \tag{4.4.8}$$

$$\sqrt{\Delta^2 + 2\bar{a}_{0f}^2(h)}\Big) - \frac{2\Theta_m^2}{|\Theta|^2}(\bar{h} - h(m))\frac{\bar{a}_{0f}}{\left(\bar{h}^{(2)} - \bar{h}^2\right)^{1/2}}$$

Here the term $2\Theta_m^2 \bar{h}/|\Theta|^2$ is absorbed by E_{0m}. Let me examine each term in (4.4.8). First of all ξ represents the energy shift with respect to the uncoupled f-level, which is the result of the constraint (4.2.16) for $N=1$, which has been introduced to account for the effect of the strong Coulomb repulsion between the localized f-electrons. The second term represents the effective field h coupled to the effective moment reduced by the factor $\left(1 - \frac{2\Theta_m^2}{|\Theta|^2}\right)$. This reduction is due to electron-hole excitations which excite an f-electron into the conduction band, which is

assumed to couple very weakly to the magnetic field, and leaves behind the hole of opposite spin.

The next term contains the dispersion relation, which results from the hybridization between the localized and the conduction bands. Here the upper sign is used when $\Delta>0$ so that the dispersion term vanishes in the limit $\bar{a}_{0f} \rightarrow 0$. Similarly, the lower sign is used when $\Delta<0$. For $\bar{a}_{0f}(h)$ small the wave-vector dependence of the dispersion term is very weak. Also, as will be shown below, the dispersion term is responsible for pinning the saddle point of the free energy density just above the Fermi level. This combined with the large density of states produces the quasiparticle-like behavior with effective mass that could be renormalized by several orders of magnitude. I will further discuss the importance of the dispersion term later on in this Section. Finally, the last term represents the correction to the third term. It accounts for the fact that at low temperatures the localized band has a splitting proportional to δ, so that there is a difference in hybridization strength of each subband, which enhances the above splitting, while preserving the total energy of all the subbands (indeed, the sum of the last term over m is equal to zero).

Let me discuss this last term in more detail. I will now argue that in a highly hybridized system the indirect hopping between the f-sites will eliminate the above splitting altogether. To illustrate the problem, let me consider a simple case of an electron localized around some atomic site. Then the total angular momentum and its quantum number are defined with respect to that site. Similarly, one can consider the localized electron in kq-representation. This corresponds to the wave-packet localized around a lattice site μ, which however is undefined. In this case one can still define the total angular momentum and its quantum number with respect to that site μ. This is because those quantities do not depend on the

exact position of the site around which the particle is localized. In the hybridization case, however, the localized electrons acquire the dispersion relation, and the Hamiltonian contains an indirect hopping term. This means that while the electrons are mostly localized around the atomic sites, they are however able to hop between those sites. This in turn creates the problem of defining the total angular momentum. In fact, if a given electron is no longer localized around a certain site μ, any splitting proportional to the quantum number m in (4.4.4) and (4.4.8) will be proportional to $1/N_L$, where N_L denotes the number of lattice sites, and is therefore negligible. In other words, if for that electron one defines certain reference point, the probability that the electron is within a small distance of that reference point is proportional to $1/N_L$. Defining the reference point does not change the total energy of the system, so the splitting must vanish in such manner as to preserve the total energy of the system. Looking at (4.4.4) and (4.4.8), this corresponds to the last term in each of those formulas being equal to zero, so that the degeneracy of $2J+1$ energy bands has been restored. It is important to keep in mind that the subindex corresponding to the angular momentum is kept in order to differentiate the corresponding quasiparticles, as well as to indicate how the particles couple to the magnetic field. It does not however have a direct relationship to the angular momentum quantum number as far as the electron-lattice coupling is concerned. Therefore equation (4.4.8) now takes the following form:

$$\lambda_m = \left(E_{0m} + \xi \right) + \mu_B \, g \, H \, m \left(1 - \frac{2\Theta_m^{\,2}}{|\Theta|^2} \right) +$$

$$+ \frac{1}{2} \frac{\Theta_m^{\,2}}{|\Theta|^2} \left(\Delta \mp \sqrt{\Delta^2 + 2\bar{a}_{0f}^2 \, (h)} \right)$$

(4.4.9)

Also defining $\varepsilon_f \equiv E_0 + \xi$, one can rewrite (4.4.9) as:

$$\lambda_m = \varepsilon_f + \mu_B\, g\, H\, m \left(1 - \frac{2\Theta_m^{\,2}}{|\Theta|^2}\right) + \frac{1}{2}\frac{\Theta_m^{\,2}}{|\Theta|^2} \times$$

$$\times \left(\Delta \mp \sqrt{\Delta^2 + 2\bar{a}_{0f}^{\,2}(h)}\right) \tag{4.4.10}$$

These are the new eigenvalues of the system.

Let me now calculate the partition function. Write:

$$Z_k = \int d\xi \prod_{m=-J}^{J} \left(1 + e^{-\beta\lambda_m}\right)\left(1 + e^{-\beta\lambda_0}\right) e^{\xi\beta} =$$

$$= \int d\xi \; e^{\sum_m \log\left(1 + e^{-\beta\lambda_m}\right) + \log\left(1 + e^{-\beta\lambda_0}\right) + \xi\beta} \equiv$$

$$\equiv \int d\xi \; e^{f_k(\xi,\,\beta)} \tag{4.4.11}$$

$$Z = \int d\xi \; e^{f(\xi,\,\beta)} \tag{4.4.12}$$

where restoring the subindex k, we write:

$$f(\xi,\beta) \equiv \frac{\Omega}{(2\pi)^3} \int d^3k \; f_k(\xi,\beta) \tag{4.4.13}$$

$$f_k(\xi,\beta) = \sum_m \log\left(1 + e^{-\beta\lambda_{mk}}\right) + \log\left(1 + e^{-\beta\lambda_{0k}}\right) + \xi\beta$$

In the spirit of the discussion, let me evaluate the partition function using the saddle point approximation [60] . Write:

$$-\frac{1}{\beta}\frac{df_k(\xi,\beta)}{d\xi} \cong \sum_m \left[n_m(\beta,k)\left(1-\frac{1}{2}\frac{\Theta_m^2}{|\Theta|^2}\times\right.\right.$$

$$\left.\left.\times\left(1-\frac{|\Delta|}{\sqrt{\Delta^2+2\bar{a}_{0f}^2(h)}}\right)\right)\right]-1 \qquad (4.4.14)$$

where

$$n_m(\beta,k) \equiv \frac{1}{1+\exp(\beta\lambda_m(k))}$$

We want:

$$\frac{df(\xi,\beta)}{d\xi} = \frac{\Omega}{(2\pi)^3}\int d^3k \ \frac{df_k(\xi,\beta)}{d\xi} = 0 \qquad (4.4.15)$$

There are two solutions to the above equation. For the minus channel ($\Delta > 0$) one can write:

$$\frac{\Omega}{2(2\pi)^3}\int d^3k \quad \left\{\frac{1}{|\Theta|^2}\left[1-\frac{\Delta}{\sqrt{\Delta^2+2\bar{a}_{0f}^2(h)}}\right]\times\right.$$

$$\left.\times\sum_m \Theta_m^2 n_m(\beta,k)\right\} \approx \frac{\Omega}{(2\pi)^3}\left\{\int d^3k \ \sum_m n_m(\beta,k)\right\}-1 \qquad (4.4.16)$$

Then ξ must be a large negative number. In the limit $U \rightarrow \infty$, which corresponds to:

$$\frac{\Omega}{(2\pi)^3} \int d^3k \sum_m n_m(\beta, k) \rightarrow 1 \tag{4.4.17}$$

then $\xi \rightarrow -\infty$. There are $2J+1$ solutions to (4.4.16) for each quantum level being occupied. Those solutions correspond to the class of saddle points in table 1 for $N=1$, and they also correspond to the transformation parameters given by (4.3.11). The symmetry-breaking solution becomes complex, i.e. it is nonexistent. In such a case the electrons are completely localized around their atomic sites. The dispersion term is then very small, and will in fact vanish in the above limit. To put it another way, the effective mixing parameter is reduced by the strong Coulomb repulsion. This is due to the fact that delocalized f-electrons have a finite probability of hopping onto another atomic site. In the Kondo regime that site is occupied by a nearly integral number fo electrons, and therefore such hopping will bring the strong Coulomb repulsion into play. That means that the dispersion term is effectively suppressed, which is reflected in the above formulae.

Another interesting solution however emerges for the plus channel. In this case write:

$$\frac{\Omega}{2(2\pi)^3} \int d^3k \left\{ \frac{1}{|\Theta|^2} \left[1 + \frac{\Delta}{\sqrt{\Delta^2 + 2\bar{a}_{0f}^2(h)}} \right] \times \right.$$

$$\left. \times \sum_m \Theta_m^2 n_m(\beta, k) \right\} \approx 1 - \frac{\Omega}{(2\pi)^3} \left\{ \int d^3k \sum_m n_m(\beta, k) \right\} \tag{4.4.18}$$

From this it follows that $\Delta \leq 0$. However, the conduction band extends all the way to the Fermi level. Therefore $E_0 + \xi \approx 0$, i.e. the renormalized quasiparticle band lies close to the Fermi level.

This is the source of the instability resulting in the tremendous enhancement of the various response functions which will be calculated below.

Let me now consider the off-diagonal terms. From the above discussion, I will rewrite (4.4.4) as:

$$A_{mn} = \frac{1}{\sqrt{2}} \frac{\Theta_m \Theta_n}{|\Theta|^2} \left(\Delta \mp \sqrt{\Delta^2 + 2\bar{a}_{0f}^2 (h)} \right)$$

For both types of saddle points A_{mn} is very small. Clearly it is zero in the limit $\xi \rightarrow -\infty$. For a symmetry-breaking type saddle point one may expand the square root using the fact that $a_{0f}(h) / \Delta \approx \sqrt{2}\, x$ (see (4.3.9)), so that one obtains $A_{mn} \propto \delta^2$. This term produces a small mixing between different quantum numbers, which is due to indirect hopping. Beyond that it will slightly renormalize the energy bands around the Fermi level, without changing the energy parameters in any significant manner. In fact the second order contribution to the n-th quasiparticle energy level is proportional to

$$\sum_{m>n} \frac{|A_{mn}|^2}{\lambda_m - \lambda_n} \propto \frac{J \Delta^2}{a_{0f}} x^3$$

which is of order x^3, and is therefore very small.

One can rewrite Z as a sum of exponentials of free energy density, evaluated over $2J+2$ saddle points. From (4.4.12) write:

$$Z(\beta) \approx (2J+1) e^{f_1(\beta)} + e^{f_0(\beta)} \tag{4.4.19}$$

where [61]:

$$f_i(\beta) = f(\xi_i, \beta) \qquad i = 0, 1$$

Here the subindex 0 is used to indicate the saddle point, corresponding to the spin delocalization state, while subindex 1 is used to indicate the other $2J+1$ saddle points corresponding to the class of saddle points in table 1. The first term in (4.4.19) is proportional to $2J+1$, so it is dominant at finite temperature. This is the result similar to the one obtained by Brandt, Keiter and Liu [59]. It is also interesting to note that the above saddle point disappears for $T > T_L$. Therefore for $T > T_L$ the f-electrons will behave as localized magnetic moments resulting in Curie-type behavior at higher temperatures.

Let me make a short detour, and briefly discuss the question of the transition between the two regimes. Obviously as the peak around ξ_0 disappears around $T \approx T_L$, the fluctuations around that saddle point will become important. Further increase in the peak width, as well as its possible displacement could be caused by contributions from the incoherent scattering. Both effects can therefore be taken into account (at least qualitatively) by evaluating (4.4.12) over peak width around ξ_0, which could be considered a parameter. The results obtained here are similar to those obtained in the first Section, and they do qualitatively describe the transition between two states. In the next section I will discuss the thermodynamic properties of the low temperature regime, dominated by the new saddle point.

4.5 Low Temperature Properties of the Symmetry Breaking State.

Returning to the low temperature regime, let me now calculate several thermodynamic properties of the system. The integrals

below will be evaluated as the sum of the saddle points discussed above. From (4.4.11-13) one can calculate the thermal energy and the specific heat as follows:

$$E = -\frac{1}{Z}\frac{dZ}{d\beta} = -\frac{1}{Z}\int Dy\ \frac{df}{d\beta}\ e^{f} \tag{4.5.1}$$

$$C = \beta^{2}\left(\left[\left\langle\left\langle\left(\frac{df}{d\beta}\right)^{2}\right\rangle\right\rangle - \left\langle\left\langle\left(\frac{df}{d\beta}\right)\right\rangle\right\rangle^{2}\right] + \right.$$

$$\left. + \left\langle\left\langle\left(\frac{d^{2}f}{d\beta^{2}}\right)\right\rangle\right\rangle\right) \tag{4.5.2}$$

where [62]

$$\frac{df}{d\beta} = -\frac{\Omega}{(2\pi)^{3}}\int d^{3}k\ \sum_{m}\lambda_{m}(k)\,n_{m}(\beta, k) \tag{4.5.3}$$

$$\frac{d^{2}f}{d\beta^{2}} = \frac{\Omega}{(2\pi)^{3}}\int d^{3}k\ \sum_{m}\lambda_{m}(k)^{2}n_{m}(\beta, k)\times$$

$$\times\left(1 - n_{m}(\beta, k)\right) \tag{4.5.4}$$

Similarly, the magnetization and the specific heat are given by:

$$M = -\frac{1}{Z\beta}\frac{dZ}{dH} = -\frac{1}{Z\beta}\int Dy\ \frac{df}{dH}\ e^{f} \tag{4.5.5}$$

$$\chi = \frac{1}{\beta}\left(\left[\left\langle\left\langle\left(\frac{df}{dH}\right)^{2}\right\rangle\right\rangle - \left\langle\left\langle\left(\frac{df}{dH}\right)\right\rangle\right\rangle^{2}\right] + \right.$$

$$+\left\langle\left\langle\left(\frac{d^2 f}{dH^2}\right)\right\rangle\right\rangle\Bigg) \tag{4.5.6}$$

where:

$$-\frac{1}{\beta}\frac{df}{dH}=\frac{\Omega}{(2\pi)^3}\int d^3k\ \sum_m \frac{d\lambda_m(k)}{dH}\, n_m(\beta, k) \tag{4.5.7}$$

$$\frac{1}{\beta}\frac{d^2 f}{dH^2}=\frac{\Omega}{(2\pi)^3}\int d^3k\ \sum_m\Bigg\{\beta\left(\frac{d\lambda_m(k)}{dH}\right)^2 n_m(\beta, k)$$

$$\left(1-n_m(\beta, k)\right)-\frac{d^2\lambda_m(k)}{dH^2}\, n_m(\beta, k)\Bigg\} \tag{4.5.8}$$

Let me now evaluate (4.5.2) and (4.5.6). First let me start with the specific heat. The term in the square brackets in (4.5.2) represents the Gaussian fluctuation of the energy density. This fluctuation can be very large near the phase transition, where there are two saddle points with approximately equal weight [63]. Indeed let me evaluate that term in the saddle point approximation. From (4.4.19) write:

$$\beta^2\left[\left\langle\left\langle\left(\frac{df}{d\beta}\right)^2\right\rangle\right\rangle-\left\langle\left\langle\left(\frac{df}{d\beta}\right)\right\rangle\right\rangle^2\right]=\kappa(1-\kappa)\times$$

$$\times\left(\frac{\Omega\beta}{(2\pi)^3}\right)^2\left[\sum_m\left(\int d^3k\ \lambda_{m1}(k)\,n_{m1}(\beta,k)\right)+\right.$$

$$\left.+\left(\int d^3k\ \sum_m \lambda_{m0}(k)\,n_{m0}(\beta,k)\right)^2\right] \tag{4.5.9}$$

where:

$$\kappa \equiv \frac{1}{1+(2J+1)^{-1}e^{f_0-f_1}} \tag{4.5.10}$$

serves as a very important quantity in this theory, which tells us which phase is more dominant. In particular, the quantity $\kappa(1-\kappa)$ has its maximum when two phases have approximately the same weight. At temperatures much lower than the transition temperature one or the other phase will dominate and therefore the above quantity will vanish. It is therefore very important to calculate κ explicitly. From (4.4.7) and (4.4.9) write:

$$f_0-f_1=\left(1-\frac{1}{2J+1}\right)\frac{\Omega\beta}{2(2\pi)^3}\times$$

$$\times\int d^3k\ \left(\Delta(k)+\sqrt{\Delta(k)^2+2\bar{a}_{0f}^2(h)}\ \right) \tag{4.5.11}$$

where

$$\Delta(k)=\Delta\left(\xi_0,k\right)$$

The coefficient of β in (4.5.11) is positive, which means that at low temperatures the delocalized phase will dominate.

The above formula has an interesting physical interpretation. Indeed:

$$\Delta(k)+\sqrt{\Delta(k)^2+2\bar{a}_{0f}^2(h)} \tag{4.5.12}$$

is proportional to the change in the kinetic energy of the electrons due to hybridization. To be more explicit the kinetic energy of the localized electron increases by

$$\frac{1}{2(2J+1)}\left(\Delta(k)+\sqrt{\Delta(k)^2+2\bar{a}_{0f}^2(h)}\right) \tag{4.5.13}$$

as it hops from site to site, producing the delocalized spin. The factor $1/(2J+1)$ is just the combinatorial probability that a given localized subband has been occupied by the electron before it jumps into the conduction band. On the other hand the kinetic energy of the conduction electrons is decreased by

$$\frac{1}{2}\left(\Delta(k)+\sqrt{\Delta(k)^2+2\bar{a}_{0f}^2(h)}\right) \tag{4.5.14}$$

This is due to the fact that while the localized electron is hopping from site to site via the conduction band, there is one less electron in that band, due to the Pauli exclusion principle. Therefore it is clear that the spin delocalization lowers the energy of the system, and that at sufficiently low temperatures the corresponding saddle point is more dominant than other $2J+1$ saddle points.

The above derivation demonstrates that in order for the delocalized spin state to be energetically favorable, one has to have a system where higher degeneracy localized electrons are coupled to the lower degeneracy conduction electrons. Therefore it is not appropriate to assume that the conduction band has the same degeneracy number as the localized band, which is the common assumption in slave boson theories and other $1/N_d$ expansions [40] (here N_d will denote the degeneracy of f-level). This dominance increases as $T \rightarrow 0$ (for $T \ll \delta$, $\kappa \rightarrow 1$). Therefore at very low

temperatures the above fluctuations would become negligible compared to the next contribution to the specific heat which I will now calculate. Write:

$$\beta^2 \left\langle \left\langle \left(\frac{d^2 f}{d\beta^2} \right) \right\rangle \right\rangle = \frac{\Omega \beta^2 \kappa}{(2\pi)^3} \int d^3k \sum_m \lambda_{m0}(k)^2 \times$$

$$\times n_{m0}(\beta, k)\left(1 - n_{m0}(\beta, k)\right) \tag{4.5.15}$$

Here the contribution from f_1 is neglected as it has no appreciable density of states near the Fermi level. To evaluate this integral I will
follow the standard procedure and change that integral to the one over energy variable λ. The density of states for the plus channel is given by:

$$\frac{N^*(\lambda)}{2J+1} \equiv N(\lambda) \frac{2}{1 + \frac{\Delta}{\sqrt{\Delta^2 + 2\bar{a}_{0f}^2(h)}}} \approx$$

$$\approx N(\lambda) \frac{\sqrt{2}\Delta^2}{\bar{a}_{0f}^2(h)} \tag{4.5.16}$$

Then one can rewrite (4.5.15) as:

$$C = -\frac{\Omega \beta N^*(0)}{2J+1} \sum_m \int_0^{\lambda_m^u} d\lambda \ \lambda^2 \frac{d n(\beta, k)}{d\lambda} \approx$$

$$\approx \frac{\pi^2 \Omega N^*(0) T}{3} \approx \frac{\sqrt{2}(2J+1)\Delta(k_F)^2}{\bar{a}_{0f}^2(h)} \frac{\pi^2 \Omega N(0) T}{3} \tag{4.5.17}$$

where λ_m^u indicates the upper bound of the resonance localized around the Fermi level. From (4.5.17) the Sommerfeld constant is just:

$$\gamma \approx \frac{\sqrt{2}\,(2J+1)\,\Delta\,(k_F)^2}{\bar{a}_{0f}^2(h)}\,\frac{\pi^2\Omega\,N(0)}{3} \tag{4.5.18}$$

Similarly one can calculate zero field magnetic susceptibility at low temperature. First of all let me discuss the Gaussian fluctuations. Write:

$$\left[\left\langle\left\langle\left(\frac{df}{dH}\right)^2\right\rangle\right\rangle-\left\langle\left\langle\left(\frac{df}{dH}\right)\right\rangle\right\rangle^2\right]=\left(\frac{\Omega}{(2\pi)^3}\right)^2\times$$

$$\times\left[\kappa\sum_m\left(\int d^3k\,\frac{d\lambda_{m1}(k)}{dH}n_{m1}(\beta,k)\right)^2+\right.$$

$$\left.+(1-\kappa)\left(\int d^3k\sum_m\frac{d\lambda_{m0}(k)}{dH}n_{m0}(\beta,k)\right)^2\right] \tag{4.5.19}$$

The term proportional to $1-\kappa$ vanishes upon the summation, so that one obtains:

$$\left[\left\langle\left\langle\left(\frac{df}{dH}\right)^2\right\rangle\right\rangle-\left\langle\left\langle\left(\frac{df}{dH}\right)\right\rangle\right\rangle^2\right]=\left(\frac{\Omega}{(2\pi)^3}\right)^2\times$$

$$\times\left[\kappa\sum_m\left(\int d^3k\,\frac{d\lambda_{m1}(k)}{dH}n_{m1}(\beta,k)\right)^2+\right. \tag{4.5.20}$$

This last contribution is proportional to β at higher temperatures. However at very low temperatures ($T<<\delta$) $\kappa \rightarrow 0$, so that the above contribution will vanish. This is of course due to the spin hopping beginning to play the dominant role. The second contribution to the magnetic susceptibility can also be evaluated by converting it to the energy integral and the result is:

$$\chi = (\mu_B g)^2 \Omega N^*(0) \frac{J(J+1)}{3}\left(1-\frac{2}{2J+1}\right)^2 \approx$$

$$\approx \frac{\sqrt{2}(2J+1)\Delta^2}{\bar{a}_{0f}^2(h)} \frac{(\mu_{\text{eff}} g)^2 \Omega N(0)}{3} \tag{4.5.21}$$

where

$$\mu_{\text{eff}} \equiv \mu_B \left(1-\frac{2}{2J+1}\right)\sqrt{J(J+1)} \tag{4.5.22}$$

Finally, the Wilson ratio:

$$R \equiv \frac{\pi^2 \chi(T=0)}{(\mu_B g)^2 \gamma J(J+1)} \approx \left(1-\frac{2}{2J+1}\right)^2 \tag{4.5.23}$$

is smaller than one. This is essentially in agreement with the experimental results [1]. The decrease in Wilson ratio is due to the decrease in the effective magnetic moment, which results from the f-c hybridization, and not from the increased γ as in the slave boson approach (see [40,41]).

There are two reasons for the discrepancy. First of all as I will show below the interacting ground state of the system is characterized by collective excitations with the phase coherence

length much larger than the lattice constant. Therefore the intermediate state contains a large number of electron-hole pairs over the phase correlation length. This is to be contrasted with a result of the slave boson approach, where there is one electron-hole pair in the intermediate state. The slave boson theory predicts an increased density of states sampled by the specific heat, and not the static magnetic susceptibility. This in turn results in the increase of γ over χ, which results in the decrease of the Wilson ratio. The second reason is a bit more technical, but also has some profound consequences. In this work I have assumed that the orbitally nondegenerate conduction band is weakly coupled to the magnetic field, while the localized moments do strongly couple to the magnetic field. This produces a decrease in the effective magnetic moment by the factor $\left(1-\frac{2\Theta_m^2}{|\Theta|^2}\right)$ (see discussion in Sec. 4.4). By contrast the assumption of the slave boson model is that the conduction band not only possesses the same degeneracy as the localized band, but it also couples to the magnetic field in at equal strength.

The above results have several important implications. In the next section, not only will I be able to account for the onset of long range coherence and demagnetization effects at low temperature, I will also show the connection between these two phenomena. Indeed, I will show that the onset of coherence is necessary for the demagnetization effect to occur. Such a long range correlation does not exist in the slave boson model. Therefore the demagnetized state in the slave boson model is energetically unfavorable, as I will explain below.

4.6 Nature of the New Ground State in the Symmetry Breaking Regime.

In this section I will try to better understand the nature of the ground state associated with the new saddle point. To do that let me calculate the phase-phase correlation function for that ground

state at zero temperature. At the end of this section I will discuss the obtained results, and I will also return to the discussion presented at the end of Sec. 4.5.

Since we are in the state where spin symmetry is nearly preserved, I will simplify the calculations and consider the conduction band coupled to the symmetrized quasi one-particle state generated by:

$$f_\mu = \frac{1}{\sqrt{N}} \sum_{m=-J}^{J} f_{\mu m} \tag{4.6.1}$$

or in k-space:

$$f_k = \frac{1}{\sqrt{N}} \sum_{m=-J}^{J} f_{km} \tag{4.6.2}$$

This means that I will ignore whatever small spin splitting remains after the spin delocalization or due to the magnetic field. Now consider the static phase correlation between the charge excitations at two different sites μ and μ':

$$\left\langle \left(c_\mu^+ f_\mu - f_\mu^+ c_\mu \right) \left(c_{\mu'}^+ f_{\mu'} - f_{\mu'}^+ c_{\mu'} \right) \right\rangle \tag{4.6.3}$$

This correlation function is useful in understanding the nature of the ground state In particular it will explain how the delocalization of the near-integral moments produces a long range coherence in the ground state.

Going over to the Fourier transform in k-space, one obtains:

$$\left\langle \left(c_{k_1}^+ f_{k_2} e^{\,i\left(\vec{k}_1 - \vec{k}_2\right)\vec{R}_\mu} - f_{k_2}^+ c_{k_1} e^{\,-i\left(\vec{k}_1 - \vec{k}_2\right)\vec{R}_\mu} \right) \times \right. \tag{4.6.4}$$

$$\left. \times \left(c_{k_3}^+ f_{k_4} e^{\,i\left(\vec{k}_3 - \vec{k}_4\right)\vec{R}_{\mu'}} - f_{k_4}^+ c_{k_3} e^{\,-i\left(\vec{k}_3 - \vec{k}_4\right)\vec{R}_{\mu'}} \right) \right\rangle$$

In the spirit of the above approximation, I will assume that after the decoupling transformation the above operators transform as:

$$c_k \rightarrow u_k c_k + v_k f_k \tag{4.6.5a}$$

$$f_k \rightarrow u_k f_k - v_k c_k \tag{4.6.5b}$$

where

$$u_k = x_k$$

$$v_k = \sqrt{1 - x_k^2} \tag{4.6.6}$$

and x_k is given by (see eqns. (4.3.10) and (4.3.11)):

$$x_k^2 = \frac{1}{2}\left(1 - \frac{\tilde{R}_k}{\sqrt{\tilde{R}_k^2 + 4}}\right) \tag{4.6.7}$$

Transforming the operators according to (4.6.5) and evaluating the thermal average in the new basis one obtains:

$$\left\langle \left(c_\mu^+ f_\mu - f_\mu^+ c_\mu\right)\left(c_{\mu'}^+ f_{\mu'} - f_{\mu'}^+ c_{\mu'}\right)\right\rangle = \frac{\Omega^2}{(2\pi)^6}\int d^3k$$

$$\times \int d^3k' \Big[\{ n_f(k, \beta)(1 - n_c(k', \beta)) + n_c(k, \beta)$$

$$\times (1 - n_f(k', \beta))\}(u_k u_{k'} + v_k v_{k'})^2 + \{ n_f(k, \beta)$$

$$\times\left(1-n_f\left(k',\beta\right)\right)+n_c\left(k,\beta\right)\left(1-n_c\left(k',\beta\right)\right)\Big\}$$

$$\times\left(u_k v_{k'}-u_k v_{k'}\right)^2\Big]\exp\Big\{\ i\left(\vec{k}-\vec{k}'\right)\cdot\left(\vec{R}_\mu-\vec{R}_{\mu'}\right)\Big\} \qquad (4.6.8)$$

where

$$n_c\left(k,\beta\right)=\frac{1}{1+\exp\left(\beta\,\lambda_0(k)\right)} \qquad (4.6.9a)$$

$$n_f\left(k,\beta\right)=\frac{1}{1+\exp\left(\beta\,\lambda_f(k)\right)} \qquad (4.6.9b)$$

$$\lambda_f(k)\equiv\frac{1}{2J+1}\sum_{m=-J}^{J}\lambda_m(k) \qquad (4.6.9c)$$

and λ_m is given by (4.4.9), while λ_0 is given by (4.4.7). From (4.6.8) the dominant contribution to the correlation function is given by:

$$\frac{\Omega^2}{(2\pi)^6}\int d^3k\int d^3k'\Big[\Big\{n_f\left(k,\beta\right)\left(1-n_c\left(k',\beta\right)\right)+ \qquad (4.6.10)$$

$$+\,n_c\left(k,\beta\right)\left(1-n_f\left(k',\beta\right)\right)\Big\}\left(u_k u_{k'}+v_k v_{k'}\right)^2\times$$

$$\times\, e^{\,i\left(\vec{k}-\vec{k}'\right)\vec{r}}\Big]$$

where

$$\vec{r}\equiv\vec{R}_\mu-\vec{R}_{\mu'}$$

Considering the dispersion relation (4.6.10), it should be obvious that the dominant contribution to the integral comes from the

shaded region in Fig. 12 around k_g (similar arguments and integration techniques can also be found in [40]). At zero temperature one can rewrite (4.6.10) as:

$$\frac{\Omega^2}{(2\pi)^6}\int d^3k \int d^3k' (u_k u_{k'} + v_k v_{k'})^2 e^{i(\vec{k}-\vec{k}')\cdot\vec{r}} \qquad (4.6.11)$$

where the integral is evaluated over the shaded region in Fig. 12 below.

Now define:

$$\bar{r}_k \equiv \frac{\bar{R}_k}{\sqrt{\bar{R}_k^2 + 4}} \qquad (4.6.12)$$

Then one can rewrite (4.6.11) as:

$$\left|\frac{\Omega}{(2\pi)^3}\int d^3k \;\; \bar{r}_k \; e^{i\vec{k}\cdot\vec{r}}\right|^2 + \left|\frac{\Omega}{(2\pi)^3}\int d^3k \;\; \sqrt{1-\bar{r}_k^2} \; e^{i\vec{k}\cdot\vec{r}}\right|^2$$

$$= \frac{1}{2}\left|\frac{\Omega}{(2\pi)^3}\int d^3k \;\; \frac{\varepsilon_k - \varepsilon_F}{\sqrt{(\varepsilon_k - \varepsilon_F)^2 + 2\bar{a}_{0f}^2(h)}} \; e^{i\vec{k}\cdot\vec{r}}\right|^2 +$$

$$+ \frac{1}{2}\left|\frac{\Omega}{(2\pi)^3}\int d^3k \;\; \frac{\sqrt{2}\,\bar{a}_{0f}(h)}{\sqrt{(\varepsilon_k - \varepsilon_F)^2 + 2\bar{a}_{0f}^2(h)}} \; e^{i\vec{k}\cdot\vec{r}}\right|^2 \qquad (4.6.13)$$

Let me evaluate the integral

$$\frac{\Omega}{(2\pi)^3}\int d^3k \; \frac{\sqrt{2}\,\bar{a}_{0f}(h)}{\sqrt{(\varepsilon_k - \varepsilon_F)^2 + 2\bar{a}_{0f}^2(h)}}\, e^{i\vec{k}\cdot\vec{r}} \tag{4.6.14}$$

In the region of integration one can write:

$$k = k_g - \frac{\varepsilon_k}{v_g} \tag{4.6.15}$$

and let us also change the variable of integration as follows:

$$x \equiv (k - k_g)r + \frac{r}{l_c} \tag{4.6.16}$$

where

$$l_c \equiv \frac{v_g}{\Delta_g} \tag{4.6.17a}$$

and

$$\Delta_g \approx \sqrt{2}\,\bar{a}_{0f}(h) \tag{4.6.17b}$$

is the minimum gap in Fig. 12. Then one can approximately rewrite the above integral as:

$$\frac{\Omega\,\rho_g\,\Delta_g}{2\pi^2 r\,k_g}\int_{r/l_c}^{\infty} dx \left\{ \frac{\sin x \cos\left(k_g r - l_c^{-1} r\right)}{\sqrt{x^2 + \Delta_g^2 r^2 / v_g^2}} + \right.$$

$$+\frac{\cos x \sin\left(k_g r - l_c^{-1} r \right)}{\sqrt{x^2 + \Delta_g^2 r^2 / v_g^2}} \Bigg\} \tag{4.6.18}$$

where

$$\rho_g \equiv m_e k_g$$

and m_e denotes the bare electron mass.

Let me examine the behavior of the correlation function in the limit $r \to \infty$. In this case one can rewrite (4.6.18) as:

$$\frac{\Omega \rho_g \Delta_g}{\sqrt{2}\pi^2 r k_g} \int_0^\infty dx \ \frac{\cos x \sin\left(k_g r - l_c^{-1} r - \frac{\pi}{4} \right)}{\sqrt{x^2 + r^2 / l_c^2}} \tag{4.6.19}$$

where I take:

$$\int_{x < r/\xi_0} dx \ \frac{\cos x}{\sqrt{x^2 + r^2 / \xi_0^2}} \approx 0$$

Finally (4.6.19) is just the integral representation for the modified Bessel function K_0, and in the above limit one writes:

$$\frac{\Omega \rho_g \Delta_g}{\sqrt{2}\pi^2 r k_g} \int_0^\infty dx \ \frac{\cos x \sin\left(k_g r - l_c^{-1} r - \frac{\pi}{4} \right)}{\sqrt{x^2 + r^2 / l_c^2}} \approx \tag{4.6.20}$$

$$\approx \frac{\Omega \rho_g \Delta_g}{2\pi^{3/2} r k_g} \left(\frac{l_c}{r}\right)^{1/2} e^{-r/l_c} \sin\left(k_g r - l_c^{-1} r - \frac{\pi}{4}\right)$$

Similarly one can evaluate the first integral in (4.6.13), and the result is:

$$\frac{\Omega}{(2\pi)^3} \int d^3k \; \frac{\varepsilon_k - \varepsilon_F}{\sqrt{(\varepsilon_k - \varepsilon_F)^2 + \Delta_g^2}} e^{i\vec{k}\cdot\vec{r}} \approx \tag{4.6.21}$$

$$\approx \frac{\Omega \rho_g \Delta_g}{2\pi^{3/2} r k_g} \left(\frac{l_c}{r}\right)^{1/2} e^{-r/l_c} \cos\left(k_g r - l_c^{-1} r - \frac{\pi}{4}\right)$$

Now combining (4.6.20), (4.4.21) and (4.6.13) one can rewrite (4.6.8) as:

$$\left\langle \left(c_\mu^+ f_\mu - f_\mu^+ c_\mu\right)\left(c_{\mu'}^+ f_{\mu'} - f_{\mu'}^+ c_{\mu'}\right)\right\rangle \approx$$

$$\approx \left(\frac{\Omega \rho_g \Delta_g}{2\pi\, r k_g}\right)^2 \left(\frac{l_c}{\pi r}\right) e^{-2r/l_c} \tag{4.6.22}$$

The characteristic correlation length l_c is inversely proportional to the small parameter in the theory, and certainly it is much larger than a lattice constant. The long range correlation is the consequence of the short range Coulomb repulsion, which is expressed in the constraint (4.2.16) for $N=1$.

Let me now discuss the physical implications of the above results. It has been shown in (4.5.11) that the symmetry-breaking regime characterized by spin delocalization is more energetically favorable than the localized regime. The question that arises is how the system is able to go into such a regime. Indeed, the way to understand the spin delocalization is to picture the electrons jumping from site to site, so that the average number of electrons at

each site is close to one and the average spin is zero. A problem that may arise with this picture is as follows. Suppose a localized electron jumps into the conduction band as an intermediate state. At that moment the delocalization length of that electron is equal to the size of the conduction electron cloud with the characteristic dimension l_c (see (4.6.17) and [40]). That means that the electron has approximately equal probability of landing at another site within distance l_c of the site at which it was previously localized. The problem is that in the Kondo regime the occupation number of f-electrons at another f-electron site on which it lands is close to one. Therefore such delocalization would cost us a very large amount of energy because of the strong Coulomb repulsion ($U \rightarrow \infty$), or equivalently would violate (4.2.16). That would result in the suppression of the dispersion term and the electrons will stay localized, which corresponds to the localized regime ($2J+1$ saddle points) discussed above (see (4.4.16,17) and the discussion thereafter).

To produce hopping unsuppressed by Coulomb repulsion, an electron hopping from site one to site two must find that site two has just been vacated by the second electron. A second electron in turn must find that the site three has just been vacated by the third electron, etc. To put this in formal language, one must have the phase coherence of f-c excitations over the delocalization length of the conduction electron. This means that the state of the system is characterized by the collective electron-hole excitations over the correlation length l_c, which is exactly what has been shown in (4.6.22). Therefore the above argument shows that in order to produce the demagnetization by spin delocalization one has to have the long range phase coherence, which *can* be obtained from the symmetry-breaking saddle point.

The problem with the slave boson and other equivalent approaches [20] is that they consider only one or few electron-hole excitation(s) in the intermediate state of pertubation diagrams. It is clear that the above long range coherent behavior cannot follow

from the pertubation theory, and therefore the demagnetization by spin delocalization is not possible in that theory. Also it has been shown [40] that the conduction cloud in the lattice cannot screen the magnetic ions. Therefore there is no adequate mechanism in the slave boson model that would explain the onset of coherence and consequently the demagnetizing effect at low temperature.

The new ground state that I have obtained must have a very small overlap with the noninteracting ground state. Indeed, it has been shown in Sec. 4.4 that the average magnetic moment at each site vanishes due to spin delocalization, which is in contrast with a noninteracting ground state where spins are essentially frozen. This phenomenon has long been understood in the single Kondo impurity problem as the so-called "orthogonality catastrophe" (see [64]). The name refers to the infrared divergencies arising in the pertubation theory from the Goldstone modes, which means that the infinite number of electron-hole pairs are formed in the intermediate state due to the symmetry-breaking of the ground state. The advantage of the method presented above is that it makes possible to obtain the new ground state by using the nonpertubative tools of the functional integral formalism and the decoupling canonical transformation. This allows us to avoid the problems of divergencies present in the pertubation theory.

4.7 Contribution of the Empty State to the Ground State Properties of the System.

So far we have concentrated on the symmetry-breaking solution to the decoupling equation (4.3.9) and the new saddle point associated with it. That solution can only be present in the almost degenerate case. By contrast four other solutions (4.3.11) are similar to the Bogoliubov-type coefficients in (3.2.12) for the nondegenerate case. It is my task now to show that the resultant saddle points are similar to the corresponding saddle points in the nondegenerate case. I will then discuss their relative weight in various regimes.

Substituting (3.2.12) into (4.4.1)-(4.4.3) and following the same derivation as in Sec. 4.4 we obtain the following dispersion relations in this channel:

$$\lambda_0 = \frac{1}{2}\left(E_{0m} + \xi + \varepsilon_k \pm \sqrt{\Delta^2 + 4\bar{a}_{0f}^2(h)} \right) \tag{4.7.1}$$

$$\lambda_m = \left(E_{0m} + \xi \right) + \mu_B\, g\, H\, m \left(1 - \frac{2\Theta_m^2}{|\Theta|^2} \right) +$$

$$+ \frac{1}{2}\frac{\Theta_m^2}{|\Theta|^2}\left(\Delta \mp \sqrt{\Delta^2 + 2\bar{a}_{0f}^2(h)} \right) \tag{4.7.2}$$

where now

$$\bar{a}_{0f}(h) \equiv \sqrt{\bar{a}_{0f}^2 - 2\left(\frac{1-x^2}{x^2}\right)\left(\bar{h}^{(2)} - \bar{h}^2\right)} \approx \bar{a}_{0f}^2$$

since x given by (4.3.11) is not small in the limit of small h. Therefore the main difference in the above dispersion relations compared to (4.4.7) and (4.4.9) is the different value of the effective mixing term.

Let us now calculate the saddle points for the Bogoliubov-type solution. Since the corresponding dispersion relations have the form similar to (4.4.7) and (4.4.9), the saddle point calculations are identical to the calculations in Sec. 4.4 and the corresponding equation is:

$$\frac{\Omega}{2(2\pi)^3}\int d^3k \quad \left\{ \frac{1}{|\Theta|^2}\left[1 \pm \frac{\Delta}{\sqrt{\Delta^2 + 2\bar{a}_{0f}^2}} \right] \times \right.$$

$$\times \sum_m \Theta_m^2 n_m(\beta,k)\Big\} \approx \pm\left[1 - \frac{\Omega}{(2\pi)^3}\Big\{\int d^3k \sum_m n_m(\beta,k)\Big\}\right] \tag{4.7.3}$$

I have already discussed the solution to (4.7.3) in Sec. 4.4 for the minus (lower) channel. In the limit $U \to \infty$, one obtains the identical $2J+1$ solutions which correspond to one of the $2J+1$ quantum levels being occupied and the electrons being completely localized around their atomic sites. Let me now discuss a solution for the plus channel. I will neglect the small crystal-field splitting which is unimportant for the Bogoliubov-type solution. In that case one writes:

$$\frac{\Omega}{2(2\pi)^3 N_d}\int d^3k \quad \left\{\left[1 + \frac{\Delta}{\sqrt{\Delta^2 + 2\tilde{a}_{0f}^{-2}}}\right]\sum_m n_m(\beta,k)\right\} \approx$$

$$\approx 1 - \frac{\Omega}{(2\pi)^3}\Big\{\int d^3k \sum_m n_m(\beta,k)\Big\} \tag{4.7.4}$$

Both sides of the equation are sketched in Fig. 30. The intersection of the two graphs is at the point where the LHS falls sharply while the RHS sharply rises. That happens when $\varepsilon_f \equiv E_0 + \xi \approx 0$, i.e. when the renormalized resonance is at the Fermi level. As in Sec. 3.4 let us define T_K as the temperature at which the magnetic and nonmagnetic saddle points have equal weight, which as in (3.4.23) corresponds to

$$E_0 = \frac{\Omega}{(2\pi)^3}\int_{BZ} d^3k \sum_m \lambda_{mk}(\xi_c)\, n_m(\beta,k) \tag{4.7.5}$$

Using the dispersion relation (4.7.2) one obtains:

$$E_0 - \varepsilon_f = \frac{\rho_0}{2N_d}\int_{-D}^{T_K} d\varepsilon \left[\Delta + \sqrt{\Delta^2 + 2\bar{a}_{0f}^2}\right] \sum_m n_m(\beta,k)$$

where the notation is similar to Sec. 3.4. As in Sec. 3.4 we expand the integrand in powers of the mixing parameter, and neglecting ε_f relative to E_0 we obtain:

$$E_0 = \frac{\rho_0}{2N_d}\int_{-D}^{T_K} d\varepsilon \ \frac{\bar{a}_{0f}^2}{\varepsilon - \varepsilon_f} \sum_m n_m(\beta,k)$$

Evaluating the above integral we finally obtain:

$$k_B T_K = D \exp\left(\frac{2E_0 N_d}{\rho_0 \bar{a}_{0f}^2}\right) \tag{4.7.6}$$

To make a connection to Sec. 3.4 we take $N_d = 2$, and since (see (4.3.7)) $\bar{a}_{0f}^2 = 4V^2$ the result obtained from (4.7.6) is identical to (3.4.25). Therefore (4.7.6) is the generalization of Kondo temperature for the orbitally degenerate case and is similar to the expressions for Kondo temperature obtained elsewhere [52].

Let me now compare (4.7.6) to (4.5.11). Define:

$$T_L = \frac{\left(1 - \frac{1}{2J+1}\right)\Omega}{2(2\pi)^3}\int d^3k \left(\Delta(k) + \sqrt{\Delta(k)^2 + 2\bar{a}_{0f}^2(h)}\right) \tag{4.7.7}$$

From (4.3.9) and (4.3.13) we rewrite and expand (4.7.7) (take $\rho_0 \approx 1/D$):

$$T_L \approx \left(1 - \frac{1}{N_d}\right) \frac{\left(\bar{h}^{(2)} - \bar{h}^{2}\right) D}{\bar{a}_{0f}^{2}} \tag{4.7.8}$$

Several important features now emerge. First of all to the leading order T_L is independent of the degeneracy number, while T_K decreases with increasing N_d. More importantly, however, T_K exponentially goes to zero in the Kondo limit of large negative E_0. To understand this, it is important to realize that the value of T_K critically depends on the contribution of the uncoupled empty state. The degree of that contribution depends on the mixing parameter which in the renormalized form is proportional to $\bar{a}_{0f}\sqrt{1-n_f}$. Clearly, as $n_f \to 1$, the empty state contribution vanishes and $T_K \to 0$.

On the other hand, the symmetry breaking state is not directly coupled to the bare empty state. Constraint (4.2.16) forces the number of electrons to be equal to one in the uncoupled case. The trick is that in the coupled case one generates the renormalized empty state due to intersite hopping. Mathematically this has to do with the fact that the constraint (4.2.16) does not commute with the f-c mixing term. The canonical transformation (4.3.8) therefore does not preserve that constraint and in effect is substituted by the new time-independent condition (4.4.18). The renormalized empty state is characterized by the coherent hole hopping, so that as in the case of electrons the renormalized empty state has a vanishingly small overlap with the uncoupled state. Therefore it cannot be directly generated from the uncoupled state.

Combining all the saddle points, we can write the partition function in the saddle point approximation in the following form

$$Z = (2J+1)\, e^{f_1} + e^{f_0} + e^{f_K} \tag{4.7.9}$$

where subindex 1 refers to $2J+1$ magnetic states, subindex 0 refers to the delocalized saddle point in the symmetry-breaking channel, and the subindex K refers to the Kondo saddle point. For $T_L > T_K$, which requires a sufficiently strong lattice-induced splitting of the uncoupled f-band or E_0 being sufficiently negative, the symmetry-breaking state is dominant at low temperature, and the zero temperature results derived in sections 4.4-4.6 are still valid. However, as the splitting goes to zero and therefore $T_L \to 0$, the Kondo saddle point becomes dominant. In that case the results derived in Sec. 3.4 and generalized here become applicable. At higher temperatures, however, the localized regime always becomes the most dominant one as I have previously discussed.

4.8 Summary of Section 4.

The following important steps have been taken toward understanding the behavior of heavy fermions at low temperature. I have set up the propagator (eqns. (4.2.13)-(4.2.15)) that would allow me to find the possible saddle points that preserve the spin rotational symmetry. Then I performed the canonical transformation that decouples the effective f- and c- bands. The requirement that this transformation decouples the effective f- and c- bands leads to decoupling equations. In the absence of any crystal splitting for the uncoupled f-band the decoupling equation is of the fourth order, and the corresponding four solutions are just Bogoliubov type coefficients, i.e. of SU(2) type. With small crystal field splitting, however, the decoupling equation becomes a sixth order equation. Two additional solutions emerge, which I call the symmetry-breaking solutions.

Next I studied the physical properties of above solutions. It turns out that the first four solutions correspond to the localized (noncorrelated) state of f-electrons or the nonmagnetic Kondo resonance. In the former case the delocalization term is suppressed

by the strong contact-type Coulomb repulsion. Such state is represented by $2J+1$ saddle points, corresponding to one of the $2J+1$ quantum levels being occupied. In the latter case the Kondo solution generalizes the corresponding solution in the nondegenerate case.

In addition to above $2J+2$ saddle points, which have an analogue in the nondegenerate case, I have found yet another saddle point that corresponds to the symmetry-breaking solution of the decoupling equation, which has no analogue in the nondegenerate case. Such a saddle point can only exist in the lattice not only because it requires the presence of small crystal field splitting, but also because it describes the collective excitation of the system with the correlation length much larger than the lattice constant. This is reflected in the form of phase-phase correlation function (eq. (4.6.22)). I have argued that such coherence is necessary to account for the onset of demagnetization at low temperatures, and is in fact one of the important characteristics of all Heavy Fermion Metals [1]. I have also noted that the Kondo saddle point cannot account for the

onset of demagnetization since it cannot properly account for the low temperature coherence leading to spin delocalization.

I have also calculated the partition function and the free energy densities corresponding to each saddle point. In particular, I have addressed a question of stability of the delocalized state. *The stability criterion that I have deduced requires the degeneracy of uncoupled and unsplit f-band to be higher than the degeneracy of the conduction band.* This is clearly the situation in Heavy Fermion Metals. Therefore I feel that making the assumption that the conduction band has the same degeneracy as f-band is not only incorrect in the lattice, but also misses some important physics present in this problem. Finally I have calculated the thermodynamic properties of the delocalized state. Both the specific heat constant and the magnetic susceptibility show large enhancement over their normal values in the delocalization regime. The calculated Wilson ratio is smaller than one ($R \approx 0.4$ for $J=5/2$) which is in agreement with the experimental results [1].

5. The Perturbation Theory and the Dynamical Properties of the Degenerate Lattice Anderson Hamiltonian at Higher Temperatures.

In this section I want to extend the calculations of the physical properties of HFS to higher temperatures ($T < T_L$). There are several contributions at higher temperatures that must be taken into account. One contribution comes from the destruction of long range coherence at higher temperatures. I will consider that contribution first. Other contributions come from other saddle points which may become important at higher temperatures.

5.1 The Perturbation Theory for the Degenerate Lattice Anderson Hamiltonian at Higher Temperatures.

In order to consider the process of the destruction of long range

coherence I will use the self-consistent type pertubation theory described below. Zero-order Hamiltonian in the coherent approximation is given as:

$$H_0 = \sum_k \left[\sum_m \lambda_{mk} a^+_{mk} a_{mk} + \lambda_{0k} a^+_{0k} a_{0k} \right] \tag{5.1.1}$$

where the renormalized f- and c-bands are given by the dispersion relations (4.4.4) and (4.4.9). It is now my task to calculate the contribution of the inelastic terms, which are especially important in calculating the transport properties of HFS. The inelastic terms comes from $Q \neq 0$ ξ-term, which has been neglected in (4.2.14). Let me explain this. What I have done in deriving (4.2.14-15) was to substitute the local constraint

$$\sum_m n_{\mu m}(\beta) = 1 \tag{5.1.2}$$

by the global (in real space) constraint (4.2.16) for $N=1$. This has been done because HFS have a coherent ground state, so that coherent terms have dominant contributions at zero temperature. As the temperature increases, however, the coherent approximation starts to break down. In that case one has to consider the contributions of inelastic terms. Those terms arise from nonzero Fourier components of the local fields ξ which are introduced to enforce (5.1.2), and in terms of bare operators have the following form:

$$H_1 = \frac{1}{\sqrt{N_L}} \sum_{kqm} \xi(q) f^+_{mk} + q f_{mk} \tag{5.1.3}$$

Let me now transform (5.1.3) using the canonical transformation given by (4.3.8) in the symmetry-breaking channel, i.e. for the symmetry-breaking solution (4.3.13) of the decoupling equation (4.3.9). Later on I will consider the contributions from other saddle

points, corresponding to the remaining solutions of the symmetry-breaking equation. Then one can write:

$$H_1 \rightarrow U\ H_1 U^{-1} \tag{5.1.4}$$

where:

$$U = e^{R} \qquad R = i \sum_n \Theta_n T_{0n}^{-}$$

and Θ_n is determined by (A6.41), (A6.46) and (4.3.13). Transforming H_1 we then obtain:

$$H_1 = \frac{1}{\sqrt{N_L}} \sum_{kq\,\mu\nu} \xi(q)\, S_{\mu\nu}\, a^{+}_{\mu k + q}\, a_{\nu k} \tag{5.1.5}$$

where the the coefficient matrix is given by:

$$S_{nm} = -\frac{\Theta_n \Theta_m}{|\Theta|^2}(1 - x^2) \qquad n \neq m \tag{5.1.6}$$

$$S_{0n} = -x\,(1 - x^2)^{1/2}\,\frac{\Theta_n}{|\Theta|}$$

$$S_{nn} = 1 - \frac{\Theta_n^2}{|\Theta|^2}(1 - x)$$

$$S_{00} = 1 - x^2$$

It is my intention now to calculate the contributions of H_1 to the conductivity using the Kubo formalism. To do that I define the

current operator. It is invariant under the canonical transformation and therefore has the following form:

$$j = -\frac{e}{m^*}\sum_k\sum_\mu k\, a^+_{\mu k}\, a_{\mu k} \tag{5.1.7}$$

Here m^* is the effective mass of f-electrons, proportional to the enhanced value of the Sommerfeld specific heat constant (see (4.5.18)). Following the Kubo formalism I define the following current-current correlation function:

$$\pi(i\omega) = -\frac{1}{3N_L}\int_0^\beta d\tau\; e^{i\omega t}\left\langle T_\tau \hat{S}(\beta)\, e^{\tau H_0} j\, e^{-\tau H_0} j\right\rangle \tag{5.1.8}$$

where $\hat{S}$ is the many-body S-matrix. Using (5.1.7) it can be rewritten as:

$$\pi(i\omega) = -\frac{e^2}{3N_L\, m^{*2}}\sum_{k,\,k'} k\cdot k' \int_0^\beta d\tau\; e^{i\omega\tau} \times \tag{5.1.9}$$

$$\times \sum_{\mu\nu}\left\langle T_\tau \hat{S}(\beta)\, a^+_{\mu k}(\tau)\, a_{\mu k}(\tau)\, a^+_{\nu k'}, a_{\nu k'}\right\rangle$$

The corresponding diagrams are shown in Fig. 31. The first diagram represents the self-energy correction to the correlation function which is given by the following equation:

$$\pi^{(0)}(i\omega) = \frac{e^2}{3N_L\, m^{*2}}\sum_{\mu k}\frac{k^2}{\beta}\sum_n \mathcal{G}_\mu(i\omega_n, k)\,\mathcal{G}_\mu(i\omega_n + i\omega, k) \tag{5.1.10}$$

where $G_{\mu}(i\omega_n, k)$ is the Matsubara f-electron Green's function with the total angular momentum quantum number μ. Next series of diagrams represents the leading order vertex corrections which can be summed up in the following closed form:

$$\pi^{(1)}(i\omega) = \frac{e^2}{3N_L^2 m^{*2}} \sum_{\mu k,\, \nu k'} \frac{k \cdot k'}{\beta} \sum_n G_{\mu}(i\omega_n + i\omega, k) \times$$

$$\times G_{\nu}(i\omega_n + i\omega, k') G_{\nu}(i\omega_n, k') G_{\mu}(i\omega_n, k) \times$$

$$\times W^{(1)}_{\mu\nu}(i\omega_n, i\omega; k, k') \qquad (5.1.11)$$

where the first order vertex function $W^{(1)}$ is given in terms of the T-matrices:

$$W^{(1)}_{\mu\nu}(i\omega_n, i\omega; k, k') \equiv T_{\mu\nu}(i\omega_n + i\omega; k, k') \times \qquad (5.1.12)$$

$$\times T_{\nu\mu}(i\omega_n; k, k')$$

and the corresponding T-matrices are defined by the following integral equation:

$$T_{\mu\nu}(\omega; k, k') = \xi(k - k') S_{\mu\nu} + \frac{1}{N_L} \sum_{\kappa,\, k''} \xi(k - k'') S_{\mu\kappa} \times$$

$$\times T_{\kappa\nu}(\omega; k'', k') G^{ret}_{\kappa}(\omega, k'') \qquad (5.1.13)$$

Higher order diagrams can be summed up, as is graphically shown in Fig. 31. That summation, however, does not include the crossing diagrams, such as the one shown at the bottom of Fig. 31. In the single impurity (dilute impurities) case, such diagrams are neglected since they are proportional to the higher power of impurity concentration than noncrossing diagrams (see [66]). Moreover, in the single angular momentum channel all vertex corrections (which have an odd parity as in (5.1.11)) will vanish. In that case only the self-energy corrections ought to be considered. In the lattice case, however, the angular momentum is not well defined, and in general one should take the vertex corrections into account. I will, however, simplify the problem and consider only the cubic lattices with an inversion symmetry. This is in fact true for many HF metals such as UBe_{13}, $CeCu_2Si_2$, and UPt_3. In that case I can restrict the calculation to the self-energy contributions to the correlation function. To do that I must solve (5.1.13) since

$$\Sigma_\mu(\omega, \boldsymbol{k}) = T_{\mu\mu}(\omega; \boldsymbol{k}, \boldsymbol{k}) \tag{5.1.14}$$

It is my task therefore to solve (5.1.13). To do that, I will need to make certain approximations. The first approximation is very straightforward. Since x in (5.1.6) is small, one can write the the matrix in (5.1.6) in the following symmetric form:

$$S_{\mu\nu} \approx \delta_{\mu\nu} - l_\mu l_\nu \tag{5.1.15}$$

where

$$l_\mu = \begin{cases} x & \mu = 0 \\ \dfrac{\Theta_m}{|\Theta|} & \mu = m \end{cases} \tag{5.1.16}$$

The next approximation deals with the form of $\xi(q)$. At zero temperature the components with $q > 1/l_c$ (l_c is given by (4.6.17))

have a negligible contribution. The fact that l_c is much greater than the lattice constant served as justification for the coherent approximation. As the temperature increases, the correlation length starts decreasing so that the range of q with finite contribution to physical quantities increases correspondingly. Therefore I will assume the following form of the scattering potential $\xi(q)$:

$$\xi(q) = \begin{cases} \xi(0) & q < q_c \\ 0 & q > q_c \end{cases} \tag{5.1.17}$$

where

$$q_c(T) = \frac{1}{l_c(T)} \tag{5.1.18}$$

and $l_c(T)$ is the temperature dependent correlation length. With that form I can solve (5.1.13) using the self-consistent type approximation. The details are given in the Appendix 7 and the result is:

$$T_{\mu\nu}(\omega; \boldsymbol{k}, \boldsymbol{k}') = \xi(0)\delta_{\mu\nu} \frac{1}{C_\nu(\omega, \bar{k})} - \frac{l_\mu}{C_\mu(\omega, \bar{k})} \times$$

$$\times \frac{l_\nu}{C_\nu(\omega, \bar{k})} \frac{\xi(0)}{1 + \xi(0) \sum_\kappa l_\kappa^2 \hat{G}_\kappa^{ret}(\omega, \bar{k}) / C_\kappa(\omega, \bar{k})} \tag{5.1.19}$$

where $\hat{G}_\kappa^{ret}(\omega, \bar{\mathbf{k}})$ and $C_\kappa(\omega, \bar{\mathbf{k}})$ are defined in the Appendix 7.

5.2 Self-Energy Calculations in the Self-Consistent Approximation.

I will now use (5.1.19) to calculate the self-energy. It is given by the self-consistent equation:

$$\Sigma_\mu(\omega,\boldsymbol{k}) = T_{\mu\mu}(\omega;\boldsymbol{k},\boldsymbol{k}) \tag{5.2.1}$$

Define the energy parameter corresponding to the resonance width:

$$\Delta_\mu(\omega,\boldsymbol{k}) = -\,\mathrm{Im}\;\Sigma_\mu(\omega,\boldsymbol{k}) \tag{5.2.2}$$

Then taking the imaginary parts of both sides of (5.2.1) we obtain:

$$\Delta_\mu(\omega,\boldsymbol{k}) = \sum_\kappa K_{\mu\kappa}(\omega;\boldsymbol{k},\boldsymbol{k}'')\frac{1}{N_L}\sum_{|\boldsymbol{k}''-\bar{\boldsymbol{k}}|<q_c}\Bigg\{ \tag{5.2.3}$$

$$\frac{\Delta_\kappa(\omega,\boldsymbol{k}'')}{\left(\omega-\lambda_\kappa(\boldsymbol{k}'')-\mathrm{Re}\Sigma_\kappa(\omega;\boldsymbol{k}'')\right)^2+\Delta_\kappa(\omega,\boldsymbol{k}'')^2}\Bigg\}$$

where the kernel K is defined as follows:

$$K_{\mu\kappa}(\omega,\boldsymbol{k},\boldsymbol{k}'') \equiv \left(\frac{\xi(0)}{|C_\mu(\omega,\boldsymbol{k})|}\right)^2\Big\{\left(1-l_\mu^2 A_\mu(\omega,\boldsymbol{k})\right)\delta_{\mu\kappa}+$$

$$+\left(\frac{l_\mu l_\kappa}{|C_\kappa(\omega,\boldsymbol{k}'')|}\right)^2 B_\mu(\omega,\boldsymbol{k})\Big\} \tag{5.2.4}$$

and

$$A_\mu(\omega,k) \equiv \frac{2\left(1-\xi(0)\,\mathrm{Re}\hat{G}_\mu^{\,\mathrm{ret}}(\omega,k)\right)}{\left|C_\mu(\omega,k)\left(1+\xi(0)\sum_\kappa \frac{l_\kappa^{\,2}\hat{G}_\kappa^{\,\mathrm{ret}}(\omega,k)}{C_\kappa(\omega,k)}\right)\right|^2} \times$$

$$\left(1+\xi(0)\sum_\kappa \frac{l_\kappa^{\,2}\left(\mathrm{Re}\hat{G}_\kappa^{\,\mathrm{ret}}(\omega,k)-\xi(0)\left|\hat{G}_\kappa^{\,\mathrm{ret}}(\omega,k)\right|^2\right)}{\left|C_\kappa(\omega,k)\right|^2}\right)^2 \tag{5.2.5}$$

$$B_\mu(\omega,k) \equiv \frac{\left[1-\xi(0)\mathrm{Re}\hat{G}_\kappa^{\,\mathrm{ret}}(\omega,k)\right]^2-\left[\xi(0)\mathrm{Im}\hat{G}_\kappa^{\,\mathrm{ret}}(\omega,k)\right]^2}{\left|C_\mu(\omega,k)\left(1+\xi(0)\sum_\kappa \frac{l_\kappa^{\,2}\hat{G}_\kappa^{\,\mathrm{ret}}(\omega,k)}{C_\kappa(\omega,k)}\right)\right|^2} \tag{5.2.6}$$

Using (5.1.17) we break the k-integration in (5.2.3) into three parts, corresponding to three different regions (see Fig. 32). Each region is characterized by the corresponding value of the energy parameter Δ_μ, which is approximately constant within that region. The zeroth region extends from k_c to $k_c + q_{c0}$, where $k_c(\omega)$ is defined as:

$$\omega = \tilde{\lambda}_\kappa(k_c) \equiv \lambda_\kappa(k_c) - \mathrm{Re}\Sigma_\kappa(\omega; k_c) \tag{5.2.7}$$

and q_{c0} is defined as (see (4.6.17)):

$$q_{c0} \equiv q_c(T=0) = \frac{\Delta_g}{v_F} \tag{5.2.8}$$

Both regions one and two are defined in Fig. 32. The contribution beyond the region two is zero. Let us calculate the energy parameters in each region. We will start with the zeroth region which is most important at low temperatures. In that case we obtain:

$$\Delta_{0\mu}(\omega) = T_c + \sum_{\kappa} K_{\mu\kappa}(\omega, k, k)\, \rho_{\kappa}^{*} \tan^{-1}\left(\frac{\lambda - \omega}{\Delta_{1\kappa}} \right) \Bigg|_{\lambda(k_c+q_{c0})}^{\lambda(k_c+q_c)} \tag{5.2.9}$$

where $\rho^* \equiv \rho^*(k_c)$, and the energy parameters Δ_i (i=0,1,2) denote the value of the energy parameter within the corresponding region. The new temperature scale T_c is defined below.

The energy parameters Δ_i are taken to be approximately constant within the corresponding region. Then we obtain:

$$\Delta_{0\mu}(\omega) \approx T_c + \frac{\rho^* v_F^*}{\Delta_1} \left\{ \sum_{\kappa} K_{\mu\kappa}(\omega, k_c, k_c) \right\} (q_c - q_{c0}) \tag{5.2.10}$$

and similarly for the first regions:

$$\Delta_{1\mu}(\omega) \approx \pi \rho^* \left\{ \sum_{\kappa} K_{\mu\kappa}(\omega, k_c, k_c) \right\} \tag{5.2.11}$$

Substituting (5.2.11) into (5.2.10) we obtain:

$$\Delta_{0\mu}(\omega) \approx T_c + \frac{v_F^*}{\pi} (q_c - q_{c0}) \tag{5.2.12}$$

Here T_c is the new energy scale in the problem, and is defined as:

$$k_B T_c \equiv x^2 \Delta_g \tag{5.2.13}$$

where x^2 is defined defined in (4.3.13). This new temperature scale is much smaller than T_L, which is of the order of Δ_g (see (4.6.17b) and (4.7.4)). It is important now to understand how the inverse correlation length varies with temperature. This will also help us understand the physical importance of the new temperature scale.

To do that let us see how the inverse correlation length varies with temperature. Since the correlation length is defined in the exponent of the correlation function (4.6.3), one must evaluate that function at finite temperature. The problem is that the correlation function depends on the electron's self-energy, which in turn depends on the inverse correlation length. This makes those equations difficult to solve. For our purposes, however, we are interested in obtaining the qualitative solution to (4.6.3).

It has been noted in Sec. 4.6 that the dominant contribution to (4.6.3) comes from the shaded region in Fig. 12. The temperature dependent factor in (4.6.10) is:

$$n_f(k,\beta)(1 - n_c(k',\beta)) + n_c(k,\beta)(1 - n_f(k',\beta)) \tag{5.2.14}$$

Looking at Fig. 33 it is clear that the temperature dependent factor remains constant for temperatures much smaller than the width of the resonance at the Fermi level. To calculate that width we use equation (5.2.12) at zero temperature ($q_c = q_{c0}$). In that case the width is just T_c. This means that for $T < T_c$ we can regard the correlation length as approximately constant, so that $q_c = q_{c0}$. Therefore T_c can be interpreted as the energy scale of the coherent regime. Above T_c the correlation length begins to shrink, and the

rate of decrease is controlled by the temperature dependent factors in (4.6.10). Let us estimate that average rate.

To do that let us calculate the width of the resonance at zero temperature which defines T_c. Let us write the dispersion relation near the Fermi surface as (see Fig. 33):

$$\lambda = \lambda_0 + \frac{k^2}{2 m_e^*} \tag{5.2.15}$$

Therefore the width of the resonance is:

$$\lambda(k_g + q_c) - \lambda(k_g) \approx v_F q_c \tag{5.2.16}$$

At zero temperature $q_c = q_{c0}$, and using (5.2.8) one obtains:

$$\lambda(k_g + q_{c0}) - \lambda(k_g) \approx k_B T_c \tag{5.2.17}$$

At temperatures $T \approx T_L$, the lower temperature scale T_c is lost, and Δ_g is the width of the resonance. Then at $T \approx T_L$ one writes:

$$v_F^* q_c = \Delta_g \tag{5.2.18}$$

and from that one obtains:

$$l_c = \frac{1}{q_c} = \frac{v_F^*}{\Delta_g} \tag{5.2.19}$$

This equation tells us that at $T \approx T_L$ the coherence is lost and the correlation length is of the order of the lattice constant.

To estimate Δ_0 assume that $\partial q_c / \partial T$ is constant for $T_c < T < T_L$. Then one can rewrite (5.2.10) as:

$$\Delta_{0\mu}(\omega) \approx T_c + \alpha (T - T_c) \tag{5.2.20}$$

where

$$\alpha = \frac{\rho^* v_F^*}{\Delta_1} \frac{\partial q_c}{\partial T} \left\{ \sum_{\kappa} K_{\mu\kappa}(\omega, k_c, k_c) \right\} \tag{5.2.21}$$

or using (5.2.11) we obtain:

$$\alpha \equiv \frac{v_F^*}{\pi} \frac{\partial q_c}{\partial T} \Bigg|_{T = T_c} \tag{5.2.22}$$

In view of our assumption that $\partial q_c / \partial T$ is constant, and using (5.2.8) and (5.2.19), write:

$$\frac{\partial q_c}{\partial T} = \frac{\Delta_g / v_F^* - \Delta_g / v_F}{T_L - T_c} \approx \frac{\Delta_g}{v_F^* T_L} \tag{5.2.23}$$

so that

$$\alpha \approx \frac{1}{\pi} \frac{\Delta_g}{T_L} \tag{5.2.24}$$

In other words α is of order one. Finally below T_c we have $q_c = q_{c0}$ so that:

$$\Delta_{0\mu}(\omega) \approx T_c \tag{5.2.25}$$

5.3 Contributions of the Inelastic Terms to the Conductivity.

Let me now apply above formulas to the calculation of the conductivity. As I have discussed above, the leading contribution to the conductivity comes from the self-energy corrections, which from (5.1.10) are equal to:

$$\sigma^{(0)} = \frac{e^2}{6 N_L m^{*2}} \sum_{\mu k} k^2 \int_{-\infty}^{+\infty} \frac{d\varepsilon}{2\pi} \left[- \frac{dn_F(\varepsilon)}{d\varepsilon} \right] A_\mu^2(\varepsilon, k) \tag{5.3.1}$$

where the spectral function is:

$$A_\mu(\varepsilon, k) \equiv \frac{2\Delta_\mu(\varepsilon, k)}{(\varepsilon - \lambda(k))^2 + \Delta_\mu(\varepsilon, k)^2} \tag{5.3.2}$$

Let us now evaluate the integral in (5.3.1). Consider the following integral:

$$\frac{1}{m^{*2}} \int \frac{d^3k}{(2\pi)^3} k^2 \left[\frac{2\Delta_\mu(\varepsilon, k)}{(\varepsilon - \lambda(k))^2 + \Delta_\mu(\varepsilon, k)^2} \right]^2 \tag{5.3.3}$$

The dominant contribution to this integral will come from the zeroth region, which we will first evaluate for $T < T_c$. In that case using (5.2.15) we obtain:

$$\frac{8\rho^* \Delta_\mu(\varepsilon, k)^2}{m^*} \int_{\varepsilon}^{T_c} d\lambda \frac{\lambda - \lambda_0}{\left[(\varepsilon - \lambda)^2 + \Delta_{0\mu}(\varepsilon, k)^2 \right]^2} = \tag{5.3.4}$$

$$= \frac{4\rho^*}{m^*}\left\{(\varepsilon - \lambda_0)\left(\frac{1}{\Delta_0}\tan^{-1}\left(\frac{\lambda-\varepsilon}{\Delta_0}\right) + \frac{\lambda-\varepsilon}{(\lambda-\varepsilon)^2+\Delta_0^2}\right) - \right.$$

$$\left. - \frac{\Delta_0^2}{(\lambda-\varepsilon)^2+\Delta_0^2}\right\}\Bigg|_{\varepsilon}^{T_c}$$

From Fig. 33 we can see that the bottom of the resonance is at $\Delta_g - T_c$, so we may take $|\lambda_0| \approx \Delta_g$. In that case:

$$\sigma^{(0)} \approx \frac{e^2\rho^*}{3\pi m^*}(2J+1)\left(\ln 2\left(1+\frac{\pi}{4}\right)\frac{\Delta_g}{\Delta_0} - 0.2\pi^2\left(\frac{T}{\Delta_0}\right)^2\right)$$

$$\rho^{(0)} \approx \frac{3\pi m^*}{e^2\rho^*}(2J+1)\left(0.8\frac{\Delta_0}{\Delta_g} + 1.3\left(\frac{T}{\Delta_g}\right)^2\right) \qquad (5.3.5)$$

For $T < T_c$ one has $\Delta_0 \approx T_c$, then

$$\rho^{(0)} \approx \frac{3\pi m^*}{(2J+1)e^2\rho^*}\left(0.8\frac{T_c}{\Delta_g} + 1.3\left(\frac{T}{\Delta_g}\right)^2\right) \qquad (5.3.6)$$

This formula has several important features. First of all, it shows that zero temperature resistivity is decreased by a factor T_c/Δ_g, which is the ratio of the coherence scale to the spin delocalization scale. Since the relatively small coherence scale is related to a long correlation length, the above formula gives an explicit connection between the long-range coherence and small resistivity at zero temperature. The second important feature is the fact that the

contribution from the second term is Fermi-liquid like, with the coefficient of T^2 scaling as $1/\Delta_g^2$.

Let us extend these calculations to higher temperatures. Although we have done our expansion for $T < T_c$, eq. (5.3.6) shows that the range of validity of the expansion may be for $T < T_L$. Substituting (5.2.20) into (5.3.5) one obtains for $T \geq T_c$:

$$\rho^{(0)} \approx \frac{3\pi m^*}{(2J+1)e^2\rho^*}\left(0.8\frac{(1-\alpha)T_c + \alpha T}{\Delta_g} + 1.3\left(\frac{T}{\Delta_g}\right)^2\right) \tag{5.3.7}$$

The new feature now is the appearance of a non-Fermi correction in the resistivity. This linear term is explicitly related to the decreasing correlation length, as the coherent FL regime is gradually destroyed. For temperatures just above coherence temperatures the linear term becomes dominant. In fact it has been reported [1] that the range of Fermi-liquid behavior, where $\rho \propto T^2$ is quite limited. At some critical temperature of order of 0.3K and higher, there are deviations from the quadratic dependence. One can interpret that critical temperature as approximately equal to the coherence temperature T_c. In fact, taking the typical values-T_L equal to 30K, the mass enhancement factor equal to 600, and the total angular momentum J=5/2, one obtains T_c is approximately 0.3K which is right in the neighborhood of the observed values.

5.4 The Conductivity at Finite Magnetic Field.

Let me extend above calculations to finite magnetic field. Write:

$$\rho^{(0)}(H) = \rho^{(0)} + \delta\rho^{(0)} \tag{5.4.1}$$

Assuming $\delta \rho^{(0)}$ is sufficiently small (linear approximation) and using (5.3.5), we can write:

$$\delta \rho^{(0)} = \frac{-3\pi m^*}{(2J+1)e^2\rho^*}\left(\frac{\delta \Delta_g}{\Delta_g}\left[0.8\frac{\Delta_0}{\Delta_g} + 2.6\left(\frac{T}{\Delta_g}\right)^2\right] - 0.8(1-\alpha)\frac{\delta T_c}{\Delta_g}\right) \tag{5.4.2}$$

Then dividing (5.4.2) by (5.3.5) we obtain:

$$-\frac{\delta \rho^{(0)}}{\rho^{(0)}} = \frac{\delta \Delta_g}{\Delta_g}\left[1 + \frac{1.3\left(T/\Delta_g\right)^2}{0.8\Delta_0/\Delta_g + 1.3\left(T/\Delta_g\right)^2}\right] - \frac{0.8(1-\alpha)\left(T_c/\Delta_g\right)}{0.8\Delta_0/\Delta_g + 1.3\left(T/\Delta_g\right)^2}\cdot\frac{\delta T_c}{T_c} \tag{5.4.3}$$

Let us first of all discuss the source of the dependence of $\rho^{(0)}$ on the magnetic field. As it is apparent from the above formula there are two such sources, corresponding to the field dependence of spin delocalization and coherence order parameters. First of all let me discuss the field and temperature dependence of the delocalization order parameter. From (4.6.17b), (4.3.9) and (4.3.13) one obtains:

$$\Delta_g \approx \frac{2\delta(T)\sqrt{2\left(\bar{h}^{(2)} - \bar{h}^2\right)}}{\bar{a}_{0f}} \tag{5.4.4}$$

where

$$h(m) \equiv \delta |m| + \mu_B g H m$$

$$\bar{h}^{(n)} \equiv \frac{\sum_m h(m)^n \Theta_m^2}{|\Theta|^2}$$

$$\bar{h} \equiv \bar{h}^{(1)}$$

Expanding (5.4.4) in powers of H we obtain:

$$\delta \Delta_g \approx \frac{\kappa H^2}{\bar{a}_{0f}} \tag{5.4.5}$$

where κ is the coefficient, proportional to the degeneracy of the system. Therefore the leading contribution of the delocalization order parameter to the magnetoresistance is negative and proportional to the square of the magnetic field. This is the consequence of the delocalization regime becoming more stable.

The dependence of T_c on the magnetic field is more complex. As I have discussed before T_c is inversely proportional to the correlation length. This correlation length refers to the phase coherence of f-c excitations, which in turn leads to the spin delocalization regime. It is clear that such coherence is very sensitive to the magnetic field, which would decrease such coherence, thereby decreasing the correlation length. Therefore T_c must also be very sensitive to the magnetic field, and must in fact increase. Such rate of increase must then be proportional to the degree of phase disorder, which is proportional to the field. Therefore within the framework of the linear approximation, I can neglect the first term in (5.4.2), and therefore I will rewrite (5.4.2) as:

$$-\frac{\delta \rho^{(0)}}{\rho^{(0)}} \approx -(1-\alpha)\frac{\delta T_c}{\Delta_0} \tag{5.4.6}$$

The sign of magnetoresistance then depends on whether or not α is greater than one. This on turn depends on the ratio of Δ_g to T_L (see (5.2.24)). For relatively small values of T_L, which roughly corresponds to the resistivity peak (see discussion below) as is the case for UBe_{13} (~2K) and $CeCu_2Si_2$ (~6K) (see [1]), $\alpha > 1$ and the magnetoresistance is negative. For $CeAl_{13}$ T_L is much higher (~35K) and the magnetoresistance is either small negative or positive. Finally UPt_{13} is the special case because the resistivity has no peak. The interpretation is that T_L is too high for any peak to be observed. This is confirmed by the observation of magnetoresistance which is large positive.

Eq. (5.4.2) can then be understood as the competition between two different things. Spin delocalization produces a coherent current with temperature- and field-dependent correlation length. Increasing the magnetic field would stabilize the current (since the order parameter is proportional to the splitting, it becomes more energetically favorable for electrons to become delocalized) which decreases the resistivity, while decreasing its correlation length which increases the resistivity. Whatever is the net effect, it is clear that above behavior is peculiar only to the low temperature regime. At temperatures of order T_L, where the coherence and the current are completely destroyed, one expects the magnetoresistance to be small. This correlation between the magnetoresistance as a function of temperature and coherence is explicitly exhibited in (5.4.6), where as we know Δ_0 is proportional to the inverse correlation length.

This mechanism for the temperature-dependent magnetoresistance is similar to the temperature dependence of the specific heat constant, as I will now show. The expression for the specific heat constant is:

$$\gamma = -\beta^3 \Omega \frac{\partial}{\partial \beta} \int_{-\infty}^{\infty} \frac{d\omega}{2\pi} \int \frac{d^3k}{(2\pi)^3} \omega \sum_m A_m(\omega, k) n_m(\omega, \beta) \tag{5.4.7}$$

Using the spectral density formula and restricting the k-integration to the zeroth region, one obtains:

$$\gamma = 2(2J+1)\beta^3 \rho^* \int_{-\infty}^{\infty} \frac{d\omega}{2\pi} \tan^{-1}\left(\frac{T_c - \omega}{\Delta_0}\right) \frac{\omega^2 e^{\omega\beta}}{\left(1 + e^{\omega\beta}\right)^2} \tag{5.4.8}$$

At zero temperature take $\Delta_0 \to 0$. Then one obtains:

$$\gamma = \frac{(2J+1)\rho^* \pi^2}{3} \tag{5.4.9}$$

which is identical to (4.5.18). At $T > T_c$ Δ_0 begins to increase and up to a linear term one obtains:

$$\gamma = \frac{(2J+1)\rho^* \pi^2}{3} \cdot \frac{T_c}{\pi \Delta_0} \tag{5.4.10}$$

Therefore both the specific heat constant and the fractional magnetoresistance are inversely proportional to the temperature dependent coherence scale Δ_0. This fact has been observed by Stewart and others (see [1]).

Let me finally discuss the question of how the resistivity behaves at or above T_L. The above expansion certainly breaks down at or above that temperature. Let me now discuss what happens in that regime. First important observation is that by hypothesis $\delta(T)$

vanishes at that temperature (see (4.2.1)). Therefore in that regime the spin delocalization saddle point becomes unstable. In that case, the contribution to the resistivity comes from the Kondo saddle point. As it is well known, the Kondo resistivity has a peak at T_K. Since, however, the contribution from the Kondo resistivity is beginning to be felt at the higher temperature T_L, one obtains a peak at T_L, followed by the decreasing resistivity coming from the tail of the Kondo peak. As I have noted above, one exception is UPt_{13}. In that case T_L is sufficiently high, so that no Kondo tail is observed and the resistivity above T_L is governed by a different mechanism, nature of which is beyond the scope of this theory.

5.5 Summary of Section 5.

In this Section I have developed a self-consistent type pertubation theory, that allows me to consider the behavior of the system at all the temperature ranges up to T_L, where T_L is the characteristic temperature scale of the spin delocalization regime and is given in Eq. (4.7.7). I have used the Kubo formalism, along with the pertubation theory to calculate the conductivity of the system in different temperature regimes. I have shown that a new characteristic temperature scale T_c emerges. This new scale characterizes a system with the maximum (zero temperature) correlation length, and in the Fermi-liquid regime. In particular, the conductivity has a quadratic temperature dependence, characteristic of the Fermi-liquid regime. Above that temperature the coherence is gradually destroyed, and the new term proportional to the temperature derivative of the inverse correlation length appears in the conductivity. That term produces a marked deviation from the Fermi-liquid behavior above T_c, which is essentialy the experimental situation.

Finally I have calculated the magnetoresistance in the linear approximation. I have discussed how the sign of magnetoresistance is related to T_L, which roughly corresponds to the experimental situation. In addition I have derived the correlation between the temperature dependence of fractional magnetoresistance and the specific heat constant, first noted by Stewart [1].

6. Extensions of the Work.

There are several basic avenues of research that I am currently pursuing. First of all I want to extend the dynamical calculation in Sec. 5 to calculate other interesting quantities. One such quantity is the dynamical susceptibility, which should provide characteristic time scales of the magnetic moments as they hop from site to site. In particular, I want to calculate the characteristic time scale during which the magnetic moment stays localized. In addition to that I want to study other transport functions such as thermal conductivity, thermopower, etc.

A second avenue of research is to study the most interesting problem of HFS - the question of superconductivity. There are several major points that have to be addressed and I list them below:

a). The mechanism for superconductivity. It seems pretty clear that the origin of the interaction is of nonphonon type

b). Symmetry of the superconducting ground state, and in particular the question of parity. It is still unclear whether the interaction is of the singlet type (even parity) or of the triplet type (odd parity).

c). Developing a new type of perturbation theory (different from the Gorkov-Eliashberg theory) applicable to the small Fermi energy scale.

d). Unusual behavior (non-BCS) of the nuclear relaxation and the ultrasonic attenuation rates below the superconducting temperature.

A third avenue of research is to apply above calculations to the study of each particular system. It seems that the band structure

calculations may be important in understanding the important differences in the behavior of various Heavy-Fermion metals, which were discussed in Sec. 1.1. The most important goal here, however, is to explain why some HFS become superconducting at low temperature, while others become magnetic, and still others neither. This would be the most important goal worth pursuing.

Figure Captions and Figures

Fig. 1 Low-temperature specific heats of three different compounds: ●, $NpBe_{13}$; ○, $Np_{0.68}U_{0.32}Be_{13}$; Δ, UBe_{13}. The lines are guides to the eye.

Fig. 2 Inverse magnetic susceptibility for UBe_{13}, with straight line showing Curie-Weiss behavior at higher temperatures.

Fig. 3 Resistivity vs. temperature: ▲, $CeCu_2Si_2$; ■, UBe_{13}; ●, UPt_3. The relative magnitudes of the three sets of data are arbitrary.

Fig. 4 Resistivity for UBe_{13} as a function of applied field (0, 3, 5, 7, 9, 11 T). Above 5 K, only 0- and 11-T data are shown; at each temperature, the higher the field, the lower the resistivity.

Fig. 5 The potential around the impurity consists of the deep hole in the center and the centrifugal barrier outside. The position of the resonance is shown.

Fig. 6a The double-peaked density of f-states is predicted by HF-approximation is shown by thin lines. The bold curve shows the density of states as predicted by the Friedel's sum rule.

Fig. 6b Typical behavior of the resistivity in the Kondo regime.

Fig. 7 Two time-ordered diagrams in the second order of the pertubation theory. The full lines represent conduction electrons and the dashed line represents the exchange interaction.

Fig. 8 Empty state self-energy at O(1), $\Sigma_0^{(1)}$. Dashed line denotes the f-electron propagator, while the solid line denotes the conduction electron propagator.

Fig. 9 Empty state self-energy at O(1/*N*), $\Sigma_0^{(1/N)}$. Wavy line denotes the bare empty state propagator, while the bold wavy line denotes the dressed empty state propagator.

Fig. 10 Pictorial representation of the summation of the diagrams with noncrossing conduction lines, which lead to the NCA coupled integral equations. Σ_0 and Σ_m represent the empty- and occupied-state self-energies. Bold lines denote the self-consistently dressed propagators.

Fig. 11 Second order contributions to the radial gauge expansion. Bold lines denote f-electrons, while thin lines denote conduction electrons. Wavy lines denote the Fourier transform of $r - r_0$, while the dashed lines denote the Fourier transform of $i\lambda$. Finally small crosses denote the vertices r_0.

Fig. 12 The dispersion relations for the Kondo lattice in the slave boson mean-field approximation. It also serves as the schematic representation of the upper and lower branches of the dispersion relations given by (4.4.7) and (4.4.9). The minimum gap between two branches.is represented by Δ_g The shaded area represents the region of k-integration that gives the dominant contribution to the correlation function (4.6.3).

Fig. 13 The interaction vertices represented by H_{int} (see (1.2.35)). Bold lines denote f-electrons, while thin lines denote conduction electrons. Wavy lines denote the zero frequency and momentum A-propagator, while the dashed lines denote zero frequency and momentum λ-propagator.

Fig. 14 The first order tadpole diagrams arising from the terms in H_A (represented by little dark circles) and H_{int} (represented by fermion loops). Requiring that those contributions vanish determines the mean-field parameters ε_f and z (see (1.2.39)).

Fig. 15 Higher order tadpole diagrams arising from the terms in H_A and H_{int}. Little crosses mean that higher order values of ε_f and z should be substituted into the expression.

Fig. 16 Diagrams for the free energy. The dashed lines denote the bare boson propagators. The diagrams involving λ-propagators do not contribute to the imaginary part of the self-energy but merely produce an energy shift approximately constant around the Fermi level. Those diagrams can therefore be ignored.

Fig. 17 General path becomes discontinuous in the limit $\Delta\tau \to 0$.

Fig. 18 Weight factor has a sharp peak around the saddle point X_S. Peak's width is denoted by Δ_1.

Fig. 19 The path 1 gives a finite contribution to the partition function, while the path 2 gives a vanishing contribution.

Fig. 20 Low temperature magnetic susceptibility in the units of $\frac{10^{-3} emu}{mol\ G}$ is plotted vs. temperature for three different regimes **a**, **b** and **c** (see table 1). The small crosses, triangles and stars correspond to the numerically calculated points. The deviation from the Curie power law increases as one increases the value of the uncoupled f-electron energy level. This is also accompanied by the increase in the characteristic temperature T_{max}, which corresponds to an approximate location of the renormalized f-level (ε_f)

Fig. 21 Low temperature specific heat is in the units of $\frac{mJ}{mol\ K}$ vs. temperature. Note that the peaks in the specific heat are slightly ahead of the corresponding peaks in the magnetic susceptibility (graphs **b** and **c**).

Fig. 22 High temperature inverse magnetic susceptibility in the units of $\frac{10^{3} mol\ G}{emu}$ vs. temperature. This graph shows that the high temperature magnetic susceptibility follows the Curie power law for all three regimes.

Fig. 23 Low temperature thermal energy is plotted in arbitrary units vs. temperature. Graph **a** shows no phase transition. The drop in the thermal energy increases, however, as one goes away from the magnetic regime (graphs **b** and **c**). Note that the region of the falloff broadens as well.

Fig. 24 Electron occupation numbers are plotted vs. temperature for three different regimes (corresponding to the letters on each figure). The fourth branch (p=1, spin up) lies well above the Fermi surface and is not plotted here. These pictures clearly show the onset of demagnetization for graphs **b** and **c**, but not for graph **a**.

Fig. 25 Relative weight factors $W(x)$ are plotted vs. x for three different regimes (corresponding to the letters on each figure) and three different temperatures (plotted in the offset fashion). The nonmagnetic peak is always centered around 0, while the magnetic peak is around 2.8. Note gradual disappearance of the magnetic peak for regimes **b** and **c**. Also note the extreme narrowness of both peaks which validates the double saddle point approximation.

Fig. 26 Three possible solutions of eq. (3.4.2) for $y \geq 0$ are represented as the intersection of two graphs (small circles), corresponding to both sides of eq. (3.4.2). Two solutions ($y \approx 0, \sqrt{U/2\pi}$) give two maxima of free energy density, while a middle point represents its minimum.

Fig. 27 The symmetric solution z_c (for $y = 0$) to the eq. (3.4.21) is represented as the intersection of two graphs corresponding to both sides of eq. (3.4.21).

Fig. 28 The antisymmetric solution $z \approx \sqrt{U/4\pi}$ (for $y \approx \sqrt{U/4\pi}$) to the eq. (3.4.21) is represented as the intersection of two graphs corresponding to both sides of eq. (3.4.21).

Fig. 29 Self-energy diagram for the eq. (3.4.26). Solid line indicates the conduction band propagator G_c, while the vertices correspond to factors V.

Fig. 30 The symmetric solution to the eq. (4.7.1) is represented as the intersection of two graphs corresponding to both sides of eq. (4.7.1). This solution corresponds to the Kondo resonance generalized for the orbitally degenerate case.

Fig. 31 The Feynman diagrams for the correlation function defined in (5.1.9). Bold lines represent the full f-electron Green's functions, while thin lines represent zero order f-electron Green's functions. the dashed lines represent the vertices $\xi(k'-k)S_{\mu\nu}$. First row represents the self-energy plus vertex corrections. The renormalized Green's function is defined in the second row. Third and fourth row represent the summation of all noncrossing contributions to the renormalized vertex function. The typical crossing diagram is represented in the last row.

Fig. 32 Three regions of k-integration in (5.2.3). Wave vector k_c is defined in (5.2.7) and q_{c0} is defined in (5.2.8).

Fig. 33 The simplified representation of Fig. 12. T_c represents the localized portion of the upper branch (see (5.2.12-13), the slope of which has been exaggerated to show the details. The shaded area represents the region of k-integration that gives the dominant contribution to the correlation function (4.6.3). The integrand of (4.6.10) over that region is temperature independent for $T < T_c$, which leads to the temperature independent correlation length below T_c.

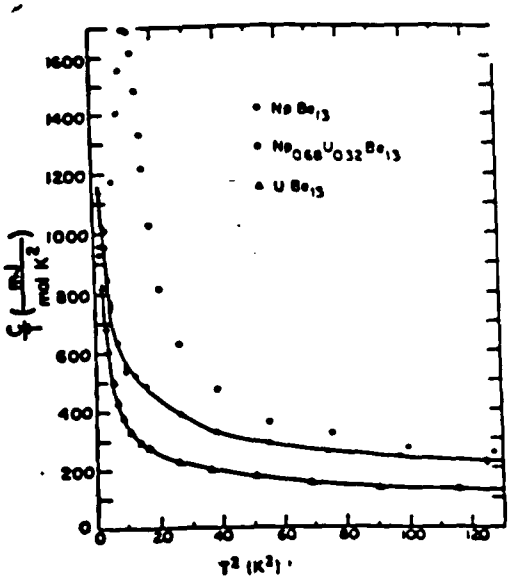

Fig. 1

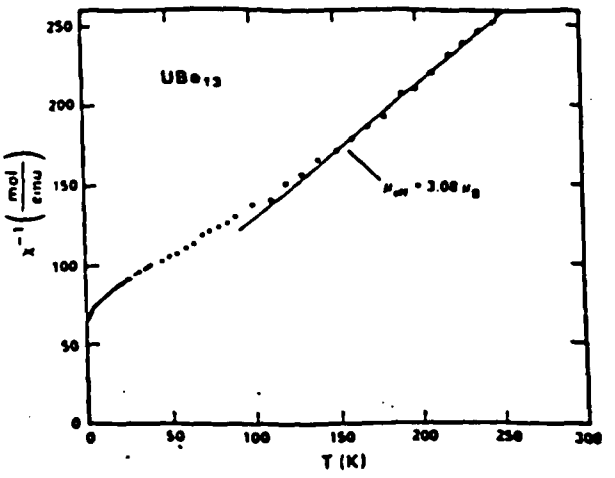

Fig. 2

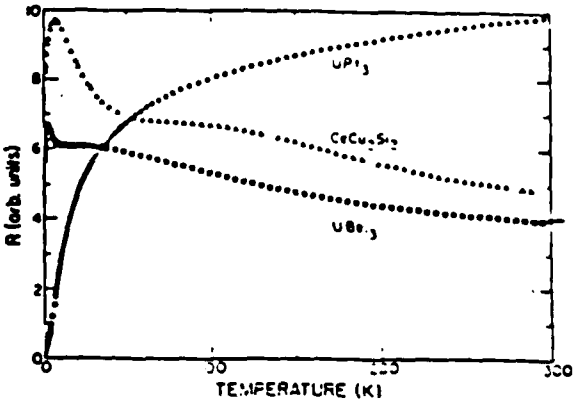

Fig. 3

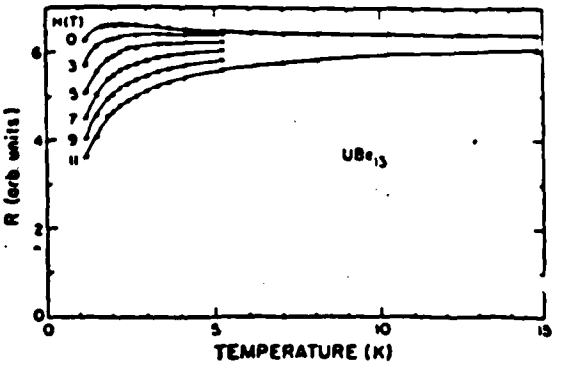

Fig. 4

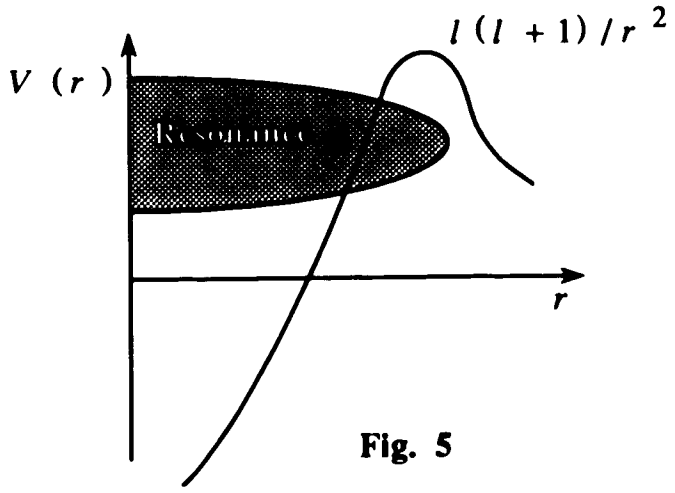

Fig. 5

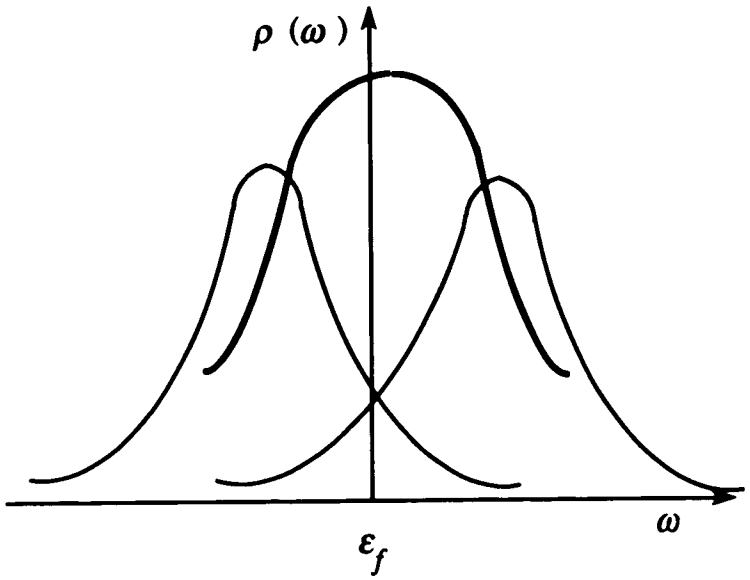

Fig. 6a

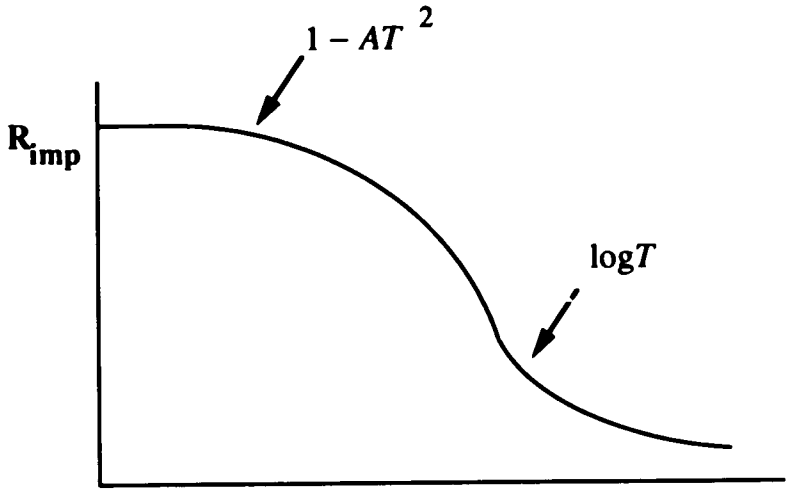

Fig. 6b

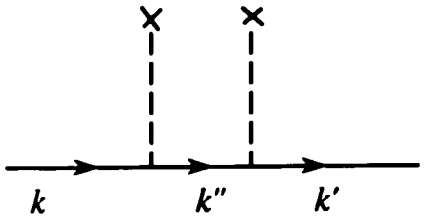

Fig. 7a

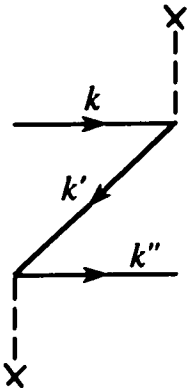

Fig. 7b

Fig. 8

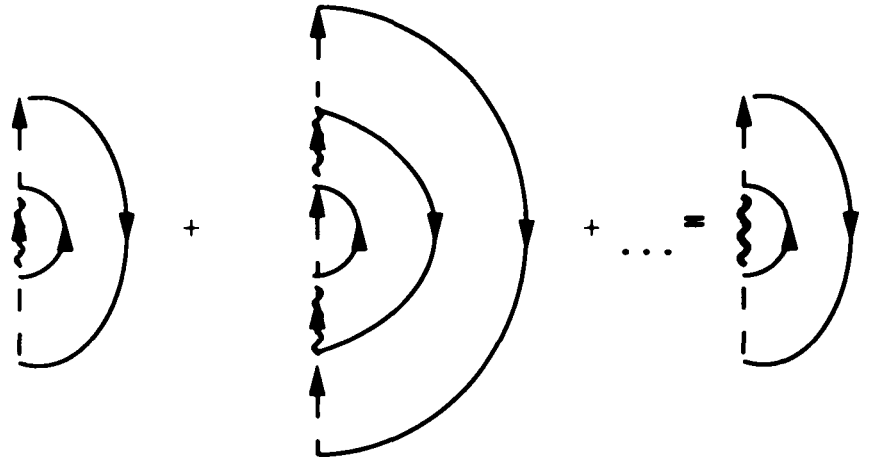

Fig. 9

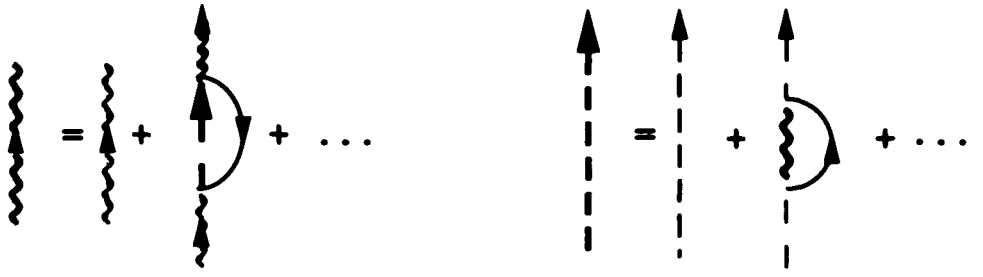

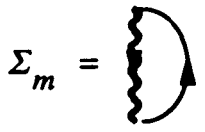

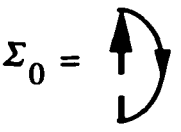

Fig. 10

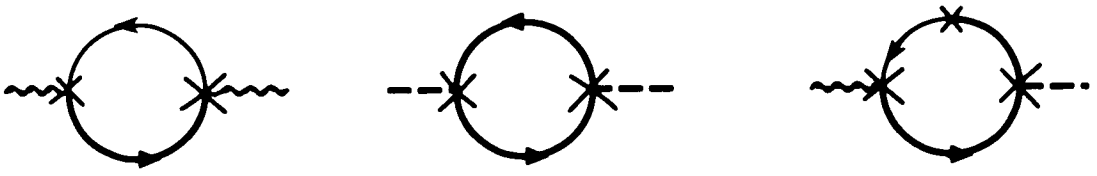

Fig. 11

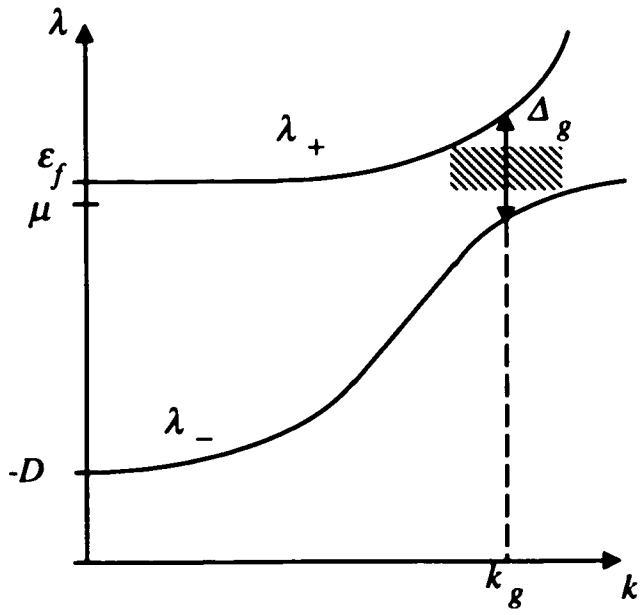

Fig. 12

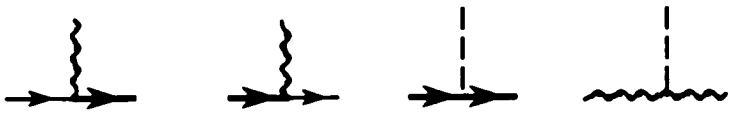

Fig. 13

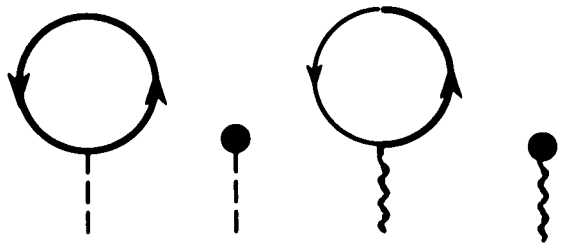

Fig. 14

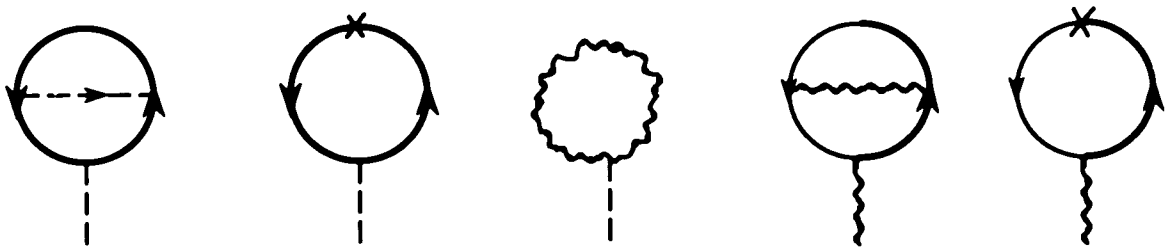

Fig. 15

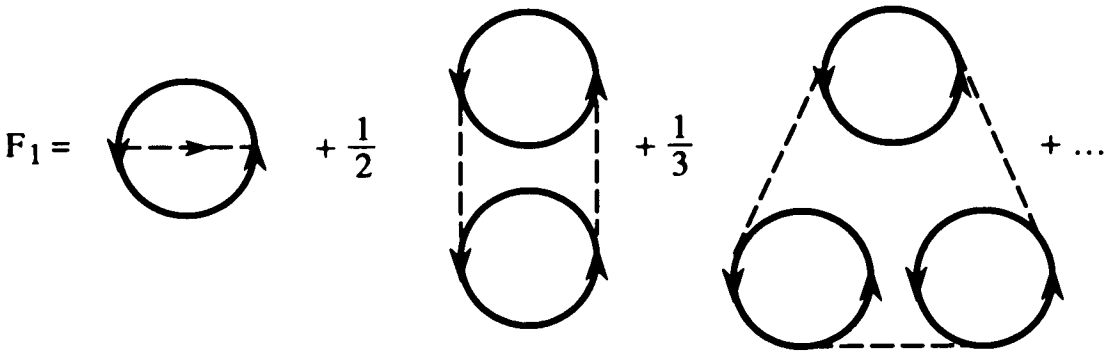

Fig. 16

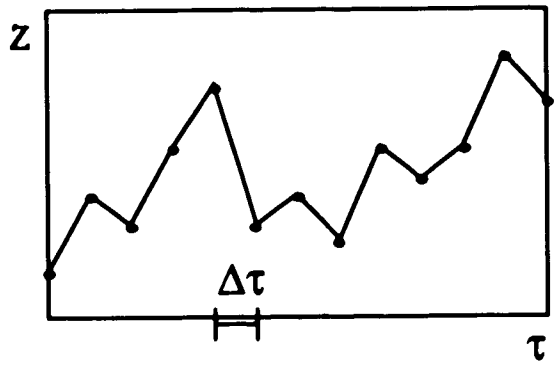

Fig. 17

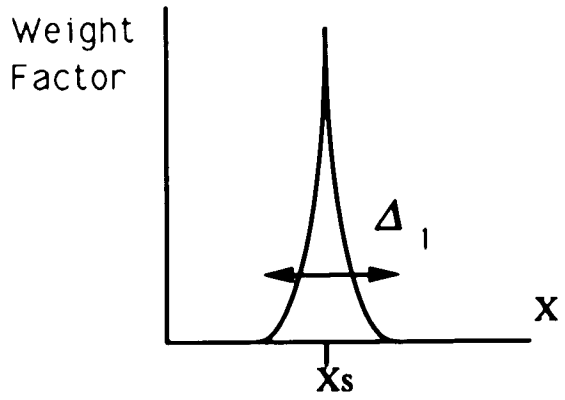

Fig. 18

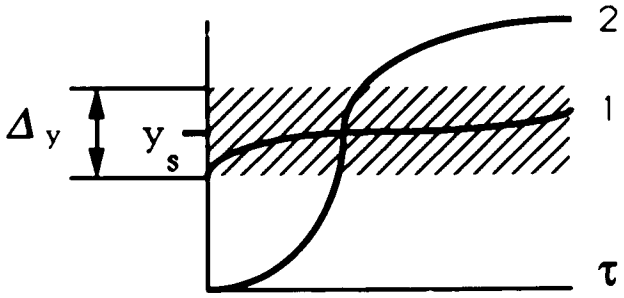

Fig. 19

DATA FOR FIG. 20-25				
graph / qtty	a	b	c	units
V	10	10	10	10^{-20} J
U	50	50	50	10^{-20} J
E_f	-22.347	-22.343	-22.339	10^{-20} J
Ω	100	100	100	$\mathring{A}^3$
W [a]	-50	-50	-50	10^{-20} J

[a] indicates the position of the bottom of the conduction band relative to the Fermi level

Table 1

LOW TEMPERATURE MAGNETIC SUSCEPTIBILITY
AND SPECIFIC HEAT

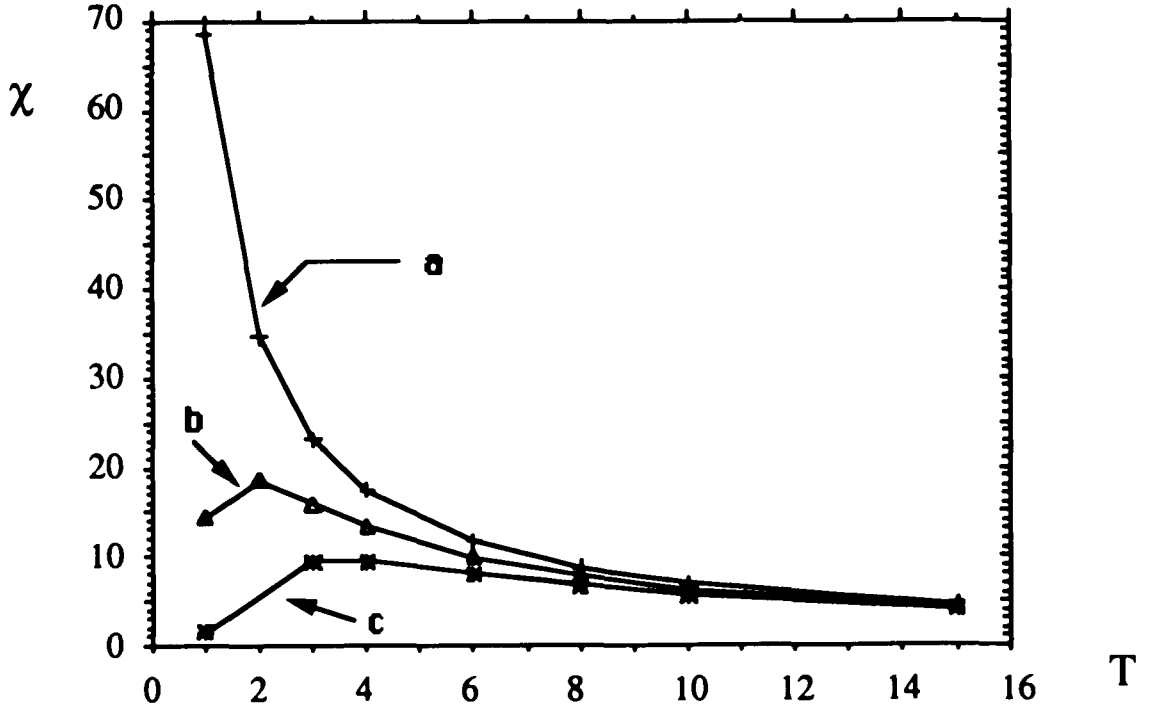

Fig. 20

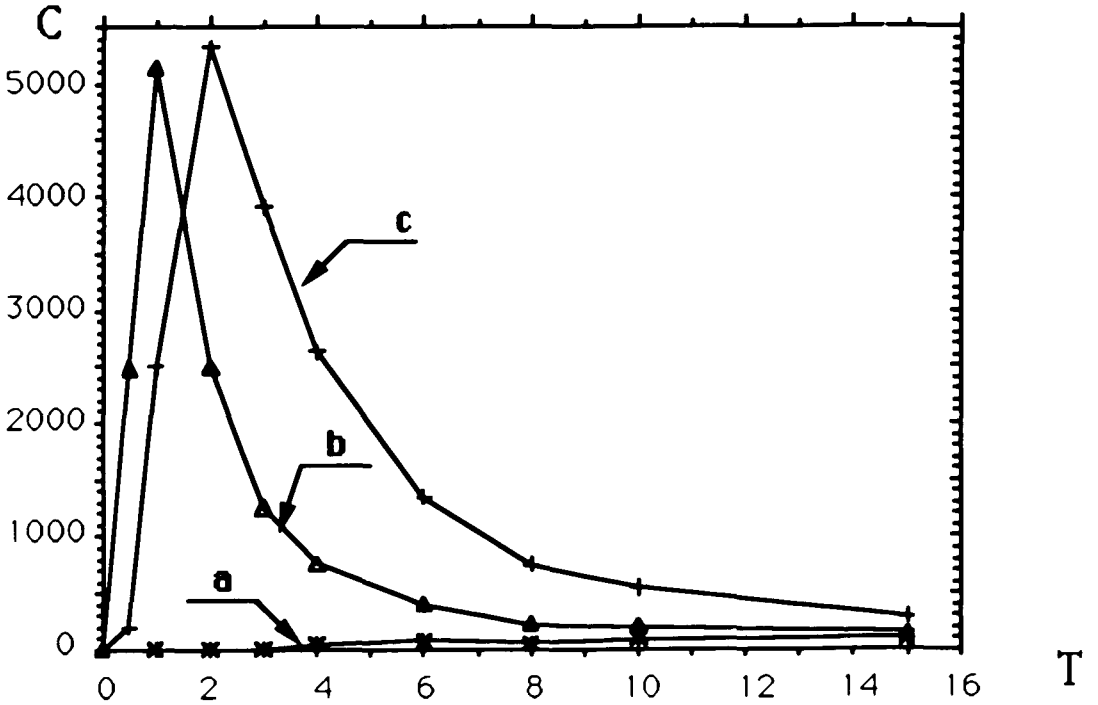

Fig. 21

HIGH TEMPERATURE INVERSE MAGNETIC SUSCEPTIBILITY

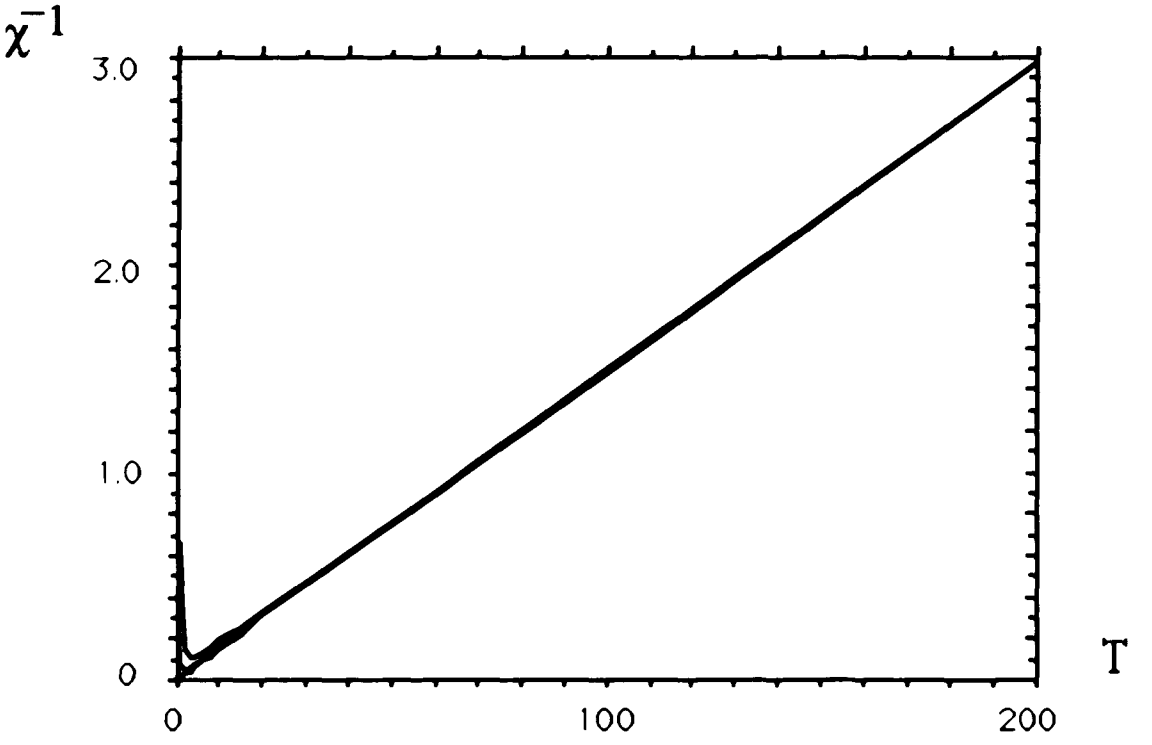

Fig. 22

THERMAL ENERGY

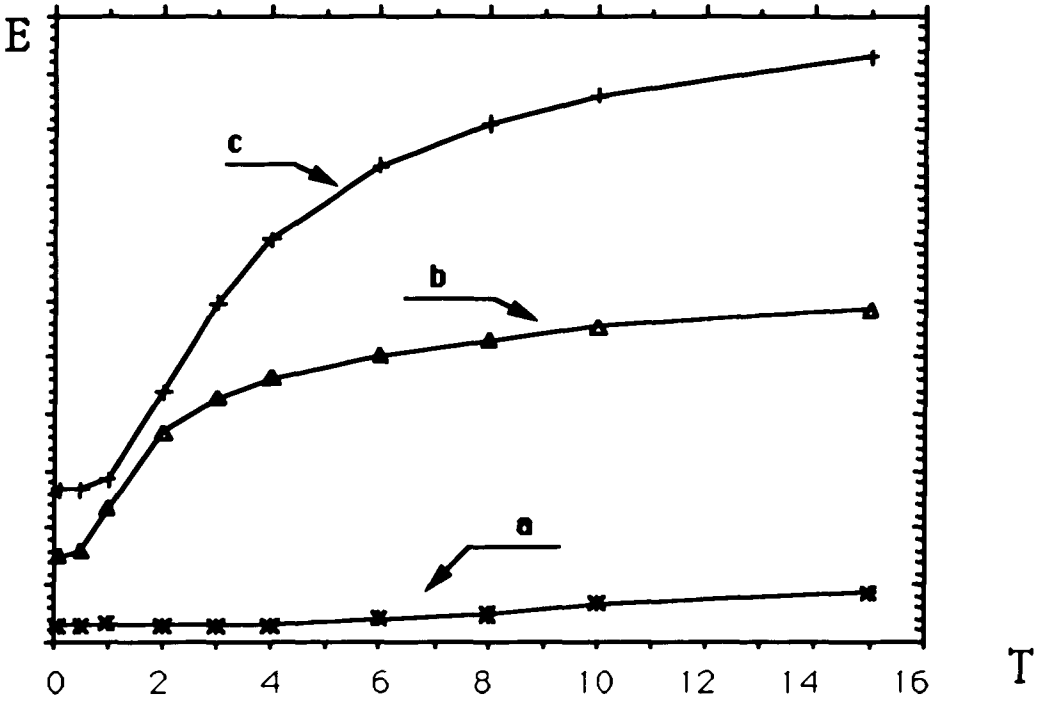

Fig. 23

ELECTRON OCCUPATION NUMBERS

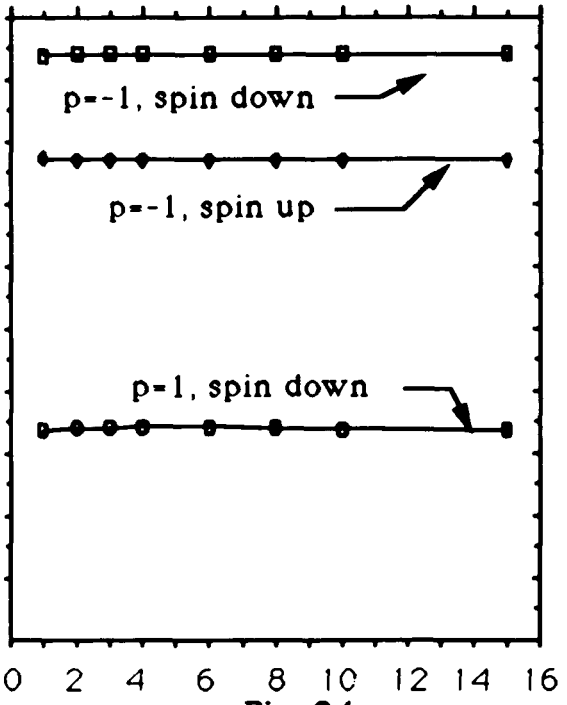

Fig. 24a

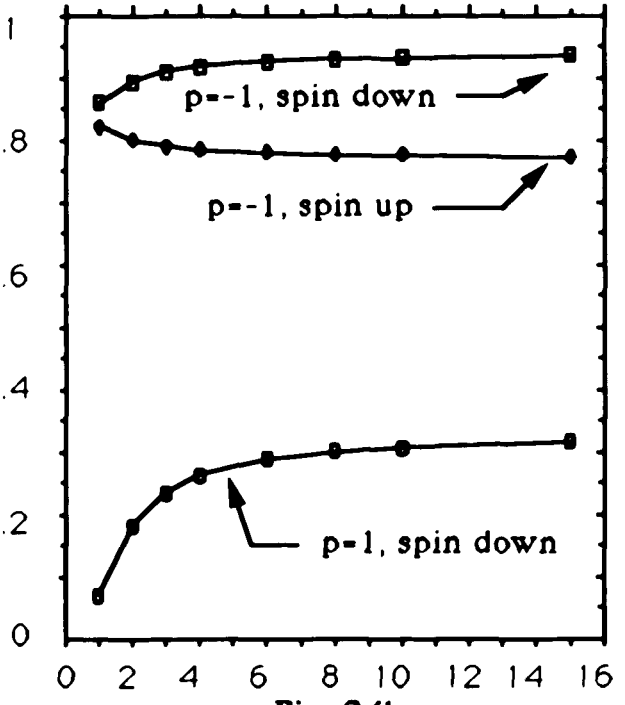

Fig. 24b

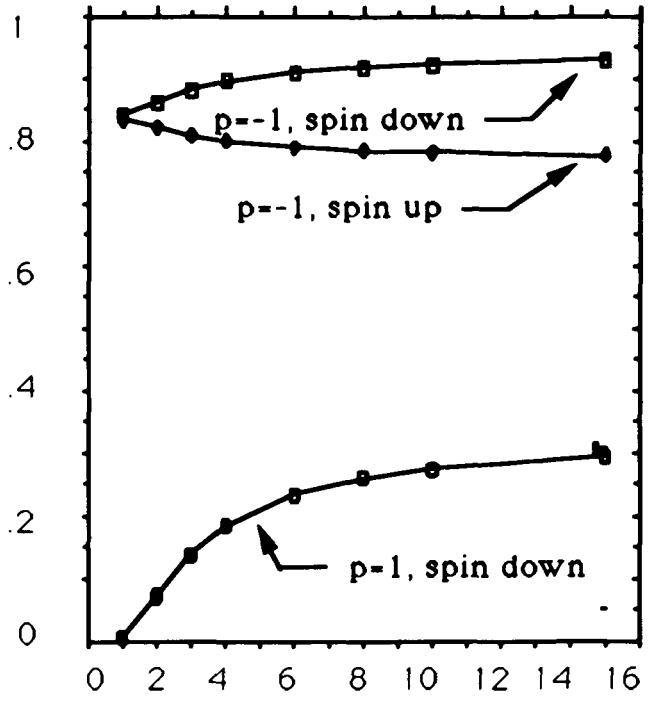

Fig. 24c

RELATIVE WEIGHT FACTORS FOR VARIOUS REGIMES

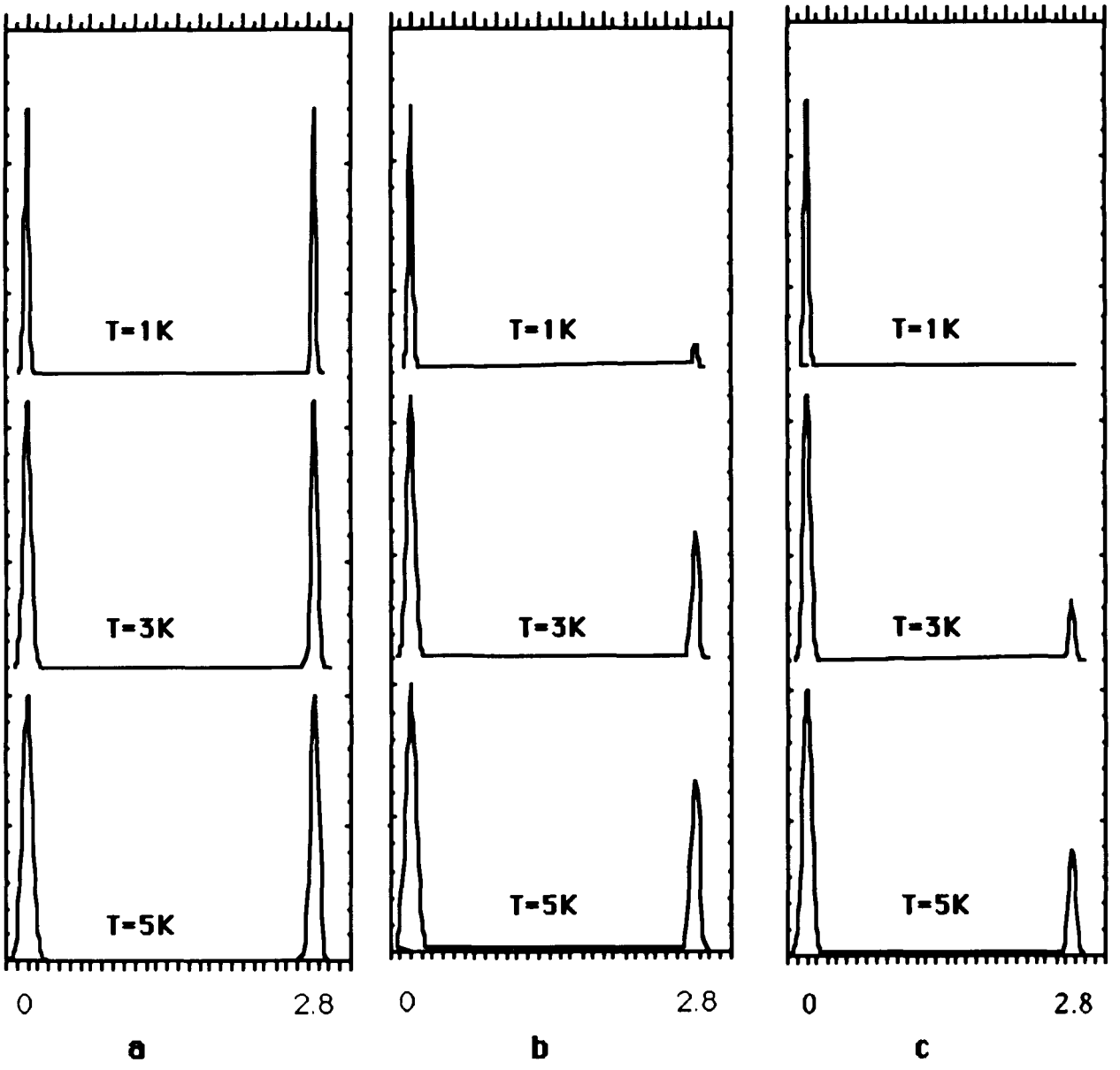

Fig. 25

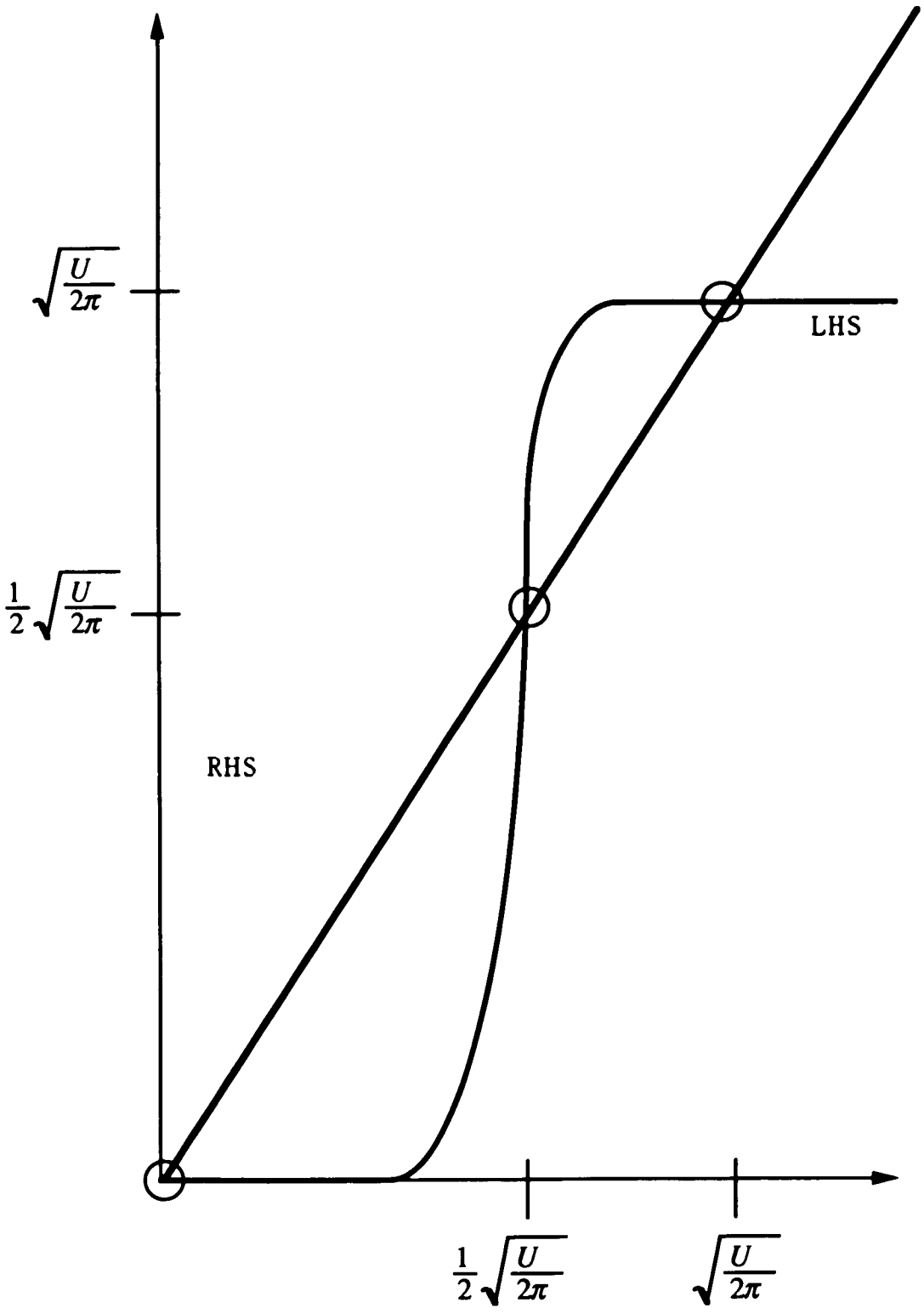
$\sqrt{\frac{U}{2\pi}}$
$\frac{1}{2}\sqrt{\frac{U}{2\pi}}$
LHS
RHS
$\frac{1}{2}\sqrt{\frac{U}{2\pi}}$
$\sqrt{\frac{U}{2\pi}}$

Fig. 26

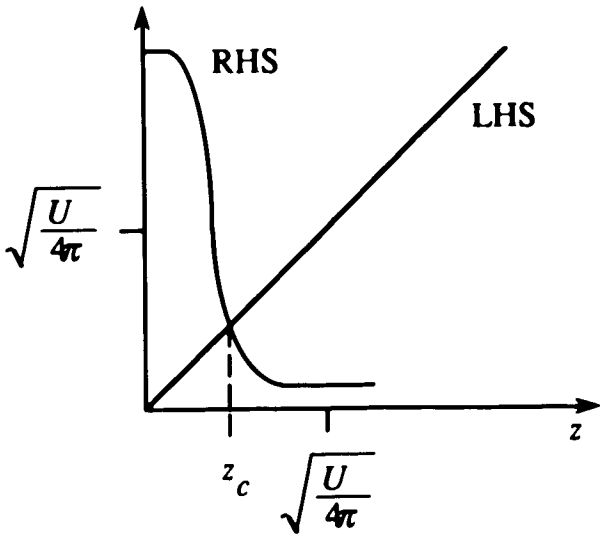
RHS
LHS
$\sqrt{\frac{U}{4\pi}}$
z
z_c
$\sqrt{\frac{U}{4\pi}}$

Fig. 27

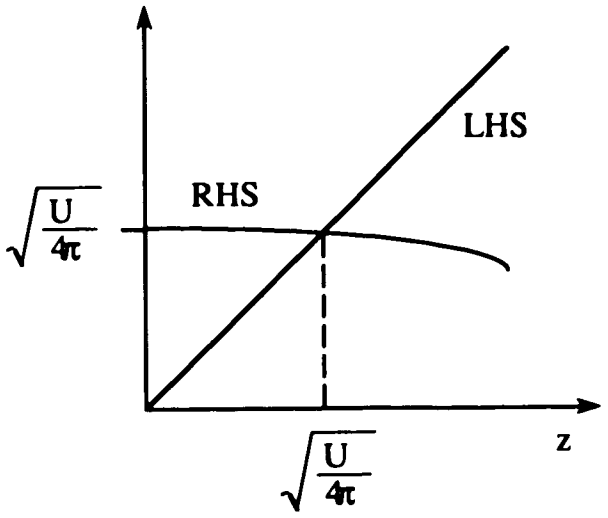
LHS
RHS
$\sqrt{\frac{U}{4\pi}}$
z
$\sqrt{\frac{U}{4\pi}}$

Fig. 28

Fig. 29

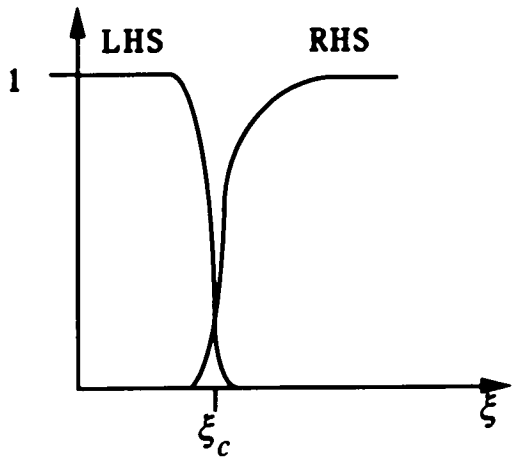

Fig. 30

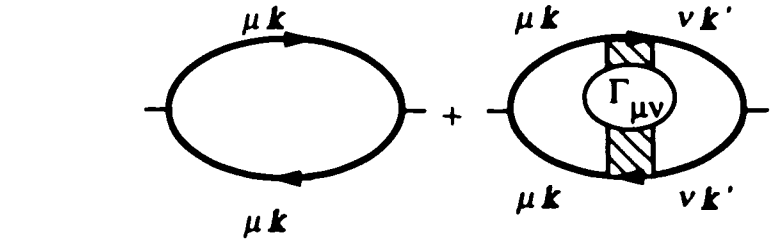
μ k
μ k
+
μ k
ν k'
Γ μν
μ k
ν k'

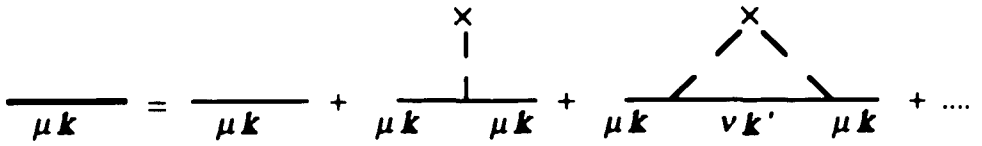
μ k
=
μ k
+
μ k
μ k
+
μ k
ν k'
μ k
+ ....

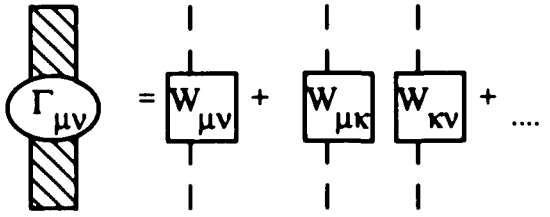
Γ μν
= W μν
+
W μκ
W κν
+ ....

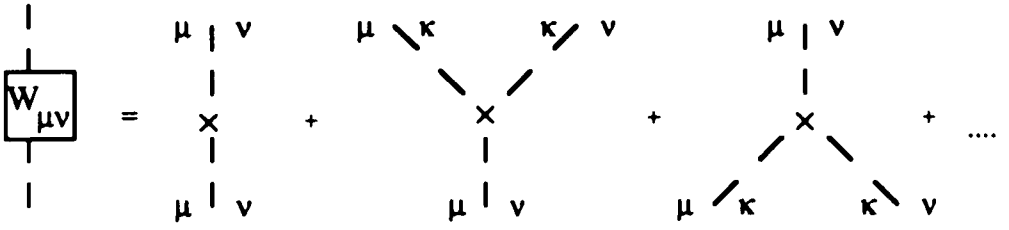
W μν
=
μ
ν
μ
ν
+
μ
κ
κ
ν
μ
ν
+
μ
ν
μ
κ
κ
ν
+ ....

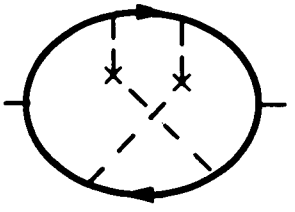

Fig. 31

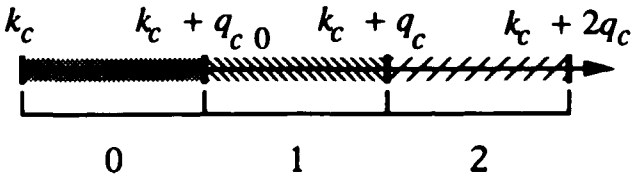
k_c
$k_c + q_{c\,0}$
$k_c + q_c$
$k_c + 2q_c$
0
1
2

Fig. 32

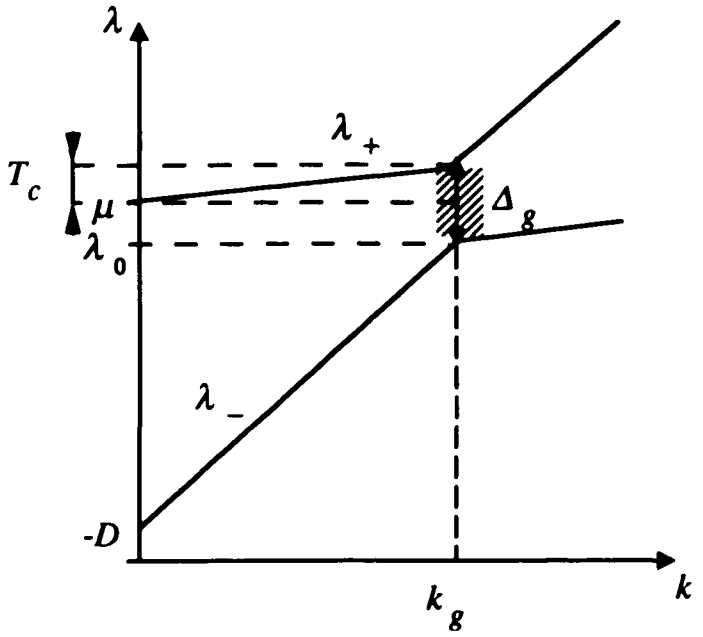
λ
λ_+
T_c
μ
Δ_g
λ_0
λ_-
$-D$
k
k_g

Fig. 33

Appendix 1. Diagrammatic Rules for Evaluating the Self-Energies in the Infinite-U Anderson Model

Listed below are the diagrammatic rules for evaluating the configurational self-energies in the infinite-U Anderson model. To compute a general contribution to the empty or occupied state self-energies at $O(V^{2n})$, $n \geq 1$:

(a) Set down $2n$ vertices in a vertical line. Beginning at the bottom with a dashed (wavy) line, connect the vertices with alternate dashed and wavy lines (all descending). A total of $2n$-1 lines now appear.

(b) Always working to the right of the vertical line, connect the vertices with full lines in all possible ways that maintain the direction of the dashed lines at each vertex. Disregard diagrams that may be disconnected by cutting a single local configuration line-they do not contribute to the irreducible self-energy.

(c) Assign quantum numbers km (m) to full (dashed) lines, conserving angular momentum at each vertex.

(d) Assign to ascending lines a Fermi factor $\langle c_{km} c_{km}^{+} \rangle = 1 - n_{km}$ and to descending conduction lines a Fermi factor $\langle c_{km}^{+} c_{km} \rangle = n_{km}$. Draw a perpendicular to each local configuration line, and assign to it an energy denominator $(z - E_{\alpha})^{-1}$, where E_{α} is found by adding the energies of ascending lines intersected by the perpendicular and subtracting energies of descending lines intersected.

(e) Multiply the product by energy denominators and Fermi factors by $(gV)^{2n}(-)^{c}$, where c is the number of conduction line crossings. Sum on all internal variables.

Appendix 2 Proof that Conditions (2.2.1) and (2.2.2) determine $L(t)$ uniquely

I want to prove now that the two conditions (2.2.1) and (2.2.2) determine $L(t)$ uniquely. Indeed, finding $L(t)$, such that (2.2.1) and (2.2.2) are satisfied is equivalent to solving the problem. To prove that, assume (2.2.1) and (2.2.2) are valid. Then get:

$$H^{2} = \left(\frac{d}{dt}\frac{d}{dt'}L(t)\,L(t')\right)_{t,\,t'=0} = \frac{d}{dt}\frac{d}{dt'}L(t+t')_{t,\,t'=0}$$

$$= \frac{d^{2}}{dt^{2}}L(t)|_{t=0}$$

The last step follows by making the substitution $t + t' \to t$. In fact, since

$$\frac{d^{n}}{dt^{n}}\cdot\frac{d}{dt'} = \frac{d^{n+1}}{d(t+t')^{n+1}} + O\left(\frac{d}{d(t-t')}\right)$$

then assuming

$$H^{n} = (-1)^{n}\frac{d^{n}}{dt^{n}}L(t)_{t=0} \qquad \text{(A2.1)}$$

it follows for n+1-st power:

$$H^{n+1} = (-1)^n \frac{d^n}{dt^n} L(t)(-1)\ \frac{d}{dt} L(t')\Big|_{t,\ t'=0}$$
$$= (-1)^{n+1} \frac{d^{n+1}}{dt^{n+1}} L(t)\Big|_{t=0}$$

so (A2.1) is true in general. Then from (A2.1) it follows that

$$e^{-Ht} = \sum_{n=0}^{\infty} \frac{d^n}{dt^n} L(t)_{t=0} \cdot \frac{t^n}{n!} \qquad \text{(A2.2)}$$

Assuming that $L(t) \in C_\infty$(which means that the matrix elements of $L(t)$ evaluated over some complete set of states are infinitely differentiable), then the RHS of (A2.2) is simply $L(t)$, and therefore one obtains:

$$e^{-Ht} = L(t) \qquad \text{(A2.3)}$$

which shows that $L(t)$ is indeed the correct propagator. Going the other way one one has to show that (A2.3) implies (2.2.1) and (2.2.2), which is trivial.

Appendix 3 Canonical Transformations Defined in Terms of Local Operators.

The basic idea of the canonical transformation approach is to define the transformation as a sum of local transformations. That would enable us to independently rotate all the local operators with different localization indices. This is a much more powerful approach than the standard canonical transformation approach. The difference can be understood intuitively if we consider a large puzzle which we want to get (transform) into a certain form. Local transformation approach allows me to rotate each piece of puzzle independently, while the standard approach would rotate all pieces

simultaneously by the same amount (because it does not depend on a field variable)

Let us now turn to the formal theory, and let U be some rotation. Then $U = \int D x\, U_x$. One chooses U in such a way that each U diagonalizes the corresponding H_{mx}: $U_x H_{mx} U_x^{-1} \equiv H_{mdx}$. One then writes:

$$U\, e^{-Ht} U^{-1} = \int Dy\, Dx\, U_x\, \tilde{A}_x(y, t) U_x^{-1} \equiv \tag{A3.1}$$

$$\equiv \int Dy\, Dx\, \tilde{A}_{dx}(y, t)$$

One can now calculate the trace of (A3.1). Let $|\psi_m>$ be some complete basis in which H operates. Then

$$\sum_m \langle \psi^m | e^{-Ht} | \psi^m \rangle = \tag{A3.2}$$

$$= \sum_m \int Dy\, Dx \langle \psi^m | \tilde{A}_{dx}(y, t) | \psi^m \rangle$$

Now define

$$\tilde{A}_d(y, t) \equiv \int Dx\, \tilde{A}_{dx}(y, t)$$

Then

$$\sum_m \int Dy \langle \psi^m | \tilde{A}_{dx}(y, t) | \psi^n \rangle = \tag{A3.3}$$

$$= \int Dy \langle \psi^m | P_x \tilde{A}_d(y, t) | \psi^n \rangle$$

Now, combining (A3.2), (A3.3) and bringing $\int Dx$ inside the trace, get:

$$Tr\ e^{-Ht} = \sum_m \int Dy \left\langle \psi^m \middle| \tilde{A}_d(y,t) \int Dx\ P_x \middle| \psi^m \right\rangle$$

$$= \int Dy\ Tr\ \tilde{A}_d(y,t) \qquad \text{(A3.4)}$$

(A3.3) and (A3.4) show how one can go back from local to global operators. One must however be aware that automatically substituting local operators by global operators may lead to erroneous results if localization projection operators are not taken into account. Such error may occur if there are cross-terms with different values of the localization label. Eq. (A3.4) solves our problem in principle.

Appendix 4 Proof of Eq. (2.4.4)

To prove (2.4.4) let me consider a discrete sequence of points in time:

$$t_N > t_{N-1} > .... > t_2 > t_1 \qquad \text{(A4.1)}$$

Also define:

$$S_n(t_n, t_{n-1}, ..., t_1) \equiv \sum_{i=1}^{n} \left\{ a_-(t_i) b^+ + a_+(t_i) b \right\} \qquad \text{(A4.2)}$$

I now want to prove that:

$$\prod_{i=N}^{1} e^{S_1(t_i)} = e^{S_N(t_i)} \exp\left(\frac{1}{2} \left(\sum_{i=1}^{N} a_+(t_i) \sum_{j=1}^{i-1} a_-(t_j) \right) \right)$$

$$\times \exp\left(-\frac{1}{2}\left(\sum_{i=1}^{N} a_{+}(t_i) \sum_{j=i+1}^{N} a_{-}(t_j)\right)\right) \qquad \text{(A4.3)}$$

Going to the continuum limit, it is obvious that (A4.3) can be rewritten as (2.4.4). I will prove (A4.3) by induction. First of all, it is obvious that (A4.3) is true for N =2. Indeed, using the Baker-Hausdorff formula, one can write:

$$\prod_{i=2}^{1} e^{S_1(t_i)} = e^{S_2(t_i)} \exp\left(\frac{1}{2}\left(a_{+}(t_2)a_{-}(t_1)\right)\right) \qquad \text{(A4.4)}$$
$$\times \exp\left(-\frac{1}{2}\left(a_{+}(t_1)a_{-}(t_2)\right)\right)$$

Now assume that (A4.3) holds for N =n. I will prove that the same then holds for N =n +1. To prove that, write:

$$e^{S_1(t_{n+1})} \prod_{i=n}^{1} e^{S_1(t_i)} = e^{S_1(t_{n+1})} e^{S_n(t_i)} = \qquad \text{(A4.5)}$$

$$\exp\left(\frac{1}{2}\left(\sum_{i=1}^{n} a_{+}(t_i) \sum_{j=1}^{i-1} a_{-}(t_j)\right)\right)\times$$

$$\times \exp\left(\frac{1}{2}\left(\sum_{i=1}^{n} a_{+}(t_i) \sum_{j=i+1}^{n} a_{-}(t_j)\right)\right)$$

Again, using the Baker-Hausdorff formula, write:

$$e^{S_{n+1}(t_i)} \exp\left(\frac{1}{2}\left(\sum_{i=1}^{n} a_+(t_i) \sum_{j=1}^{i-1} a_-(t_j)\right)\right)\times \qquad \text{(A4.6)}$$
$$\times \exp\left(\frac{1}{2}\left(a_+(t_{n+1}) \sum_{j=1}^{n} a_-(t_j)\right)\right)\times$$
$$\times \exp\left(\frac{1}{2}\left(\sum_{i=1}^{n} a_+(t_i) \sum_{j=i+1}^{n} a_-(t_j)\right)\right)\times$$
$$\times \exp\left(\frac{1}{2}\left(a_-(t_{n+1}) \sum_{i=1}^{n} a_+(t_j)\right)\right)$$

Combining the first and the second exponents, as well as the third and the fourth, one can write:

$$\prod_{i=n+1}^{1} e^{S_1(t_i)} = e^{S_{n+1}(t_i)} \exp\left(\frac{1}{2}\left(\sum_{i=1}^{n+1} a_+(t_i) \sum_{j=1}^{i-1} a_-(t_j)\right)\right)$$
$$\times \exp\left(-\frac{1}{2}\left(\sum_{i=1}^{n+1} a_+(t_i) \sum_{j=i+1}^{n+1} a_-(t_j)\right)\right) \qquad \text{(A4.7)}$$

which is identical to (A4.3).

Appendix 5 Transformation to the Modified KQ-Representation.

As it has been pointed out [52], HFS is characterized by the apparent duality of its behavior: there are equally convincing arguments pointing toward localization, as well as itinerancy. It is obvious that wave vector plays a very important role in a coherent behavior of the system. Also, since f-electrons seem to be almost localized, a location index should also be important. The Heisenberg uncertainty principle, however, prevents the existence of a representation with both wave vector and location labels. One must realize however, that the information we seek is more than

sufficient. One does not need to know the cell label, since the system possesses translational invariance (within space group). Therefore the relevant labels are: i - site index within the cell, and k - wave vector within first Brillouin zone. This representation is an analogue of kq-representation [55], and below I will show how it can be derived from kq-representation (to differentiate it from the standard kq-representation I will refer to it as ik-representation).

Let K_δ and R_μ be inverse and direct lattice vectors. Also, let n_s represent the number of HF atoms within a cell, and N be a number of cells. Then a localized expansion has labels i, μ; Bloch expansion - k, μ ; i,k-expansion - i, k.

Let $u(r- R_\mu)$ be a localized Wannier orbital. Also define

$$\Psi(k, r) = \frac{1}{\sqrt{N}} \sum_{\mu} u(r - R_\mu) e^{i k R_\mu} \tag{A5.1}$$

Then the localized expansion has the following form:

$$\Phi(r) = \frac{1}{\sqrt{N n_s}} \sum_{\mu i} a_{\mu i} u(r - r_i - R_\mu) \tag{A5.2}$$

For a Bloch expansion:

$$\Phi(r) = \frac{1}{\sqrt{N n_s}} \sum_{k} c_k \Psi(k, r) \tag{A5.3}$$

And for ik-expansion (k is restricted to the first Brillouin zone):

$$\Phi(r) = \frac{1}{\sqrt{N n_s}} \sum_{ik} b_{ik} \Psi(k, r - r_i) \tag{A5.4}$$

Now, the original Zak kq-expansion has the following basis:

$$\Psi^{Z}(k,\ r-q)=\frac{1}{\sqrt{N}}\sum_{\mu}e^{i\,k\,R_{\mu}}\delta\left(r-q-R_{\mu}\right) \tag{A5.5}$$

where k and q are quasimomentum and quasicoordinate respectively. Connection to ik representation can now be established. Combining (A5.1), (A5.4), and (A5.5), obtain (see (A5.4)):

$$\Psi\ \left(k\ ,\ r\ -r_{i}\right)=\frac{1}{\sqrt{n_{s}}}\int dq\,u\,(q\ -r_{i}\ )\Psi^{\ Z}\ (k\ ,\ r\ -q\ )$$

which means that we summed over localized delta-functions to form a wave-packet, which serves as a building block for ik-representation.

Let us now find the relations between the coefficients of all three representations. This will enable us to represent the Hamiltonian (see next section) in kq-representation. From (A5.1), (A5.2), and (A5.4) get:

$$a_{\mu i}=\frac{1}{\sqrt{N}}\sum_{k}b_{ik}\,e^{i\,k\,R_{\mu}} \tag{A5.6a}$$

Similarly, comparing (A5.1), (A5.3), and (A5.4) get:

$$c_{k\,+\,K_{\delta}}=\frac{1}{\sqrt{n_{s}}}\sum_{i}b_{ik}\,e^{-\,i\left(k\,+\,K_{\delta}\right)r_{i}} \tag{A5.6b}$$

where k is restricted to the first Brillouin zone. If we quantize the Bloch states in the usual manner, then from (A5.6a) and (A5.6b) it follows that kq operators obey the following anticommutation rules:

$$\left\{b_{ik}^{\ +},\ b_{jp}\right\}_{+}=\delta_{ij}\ \delta_{kp}$$

Let me close this section by writing down some transformation formulas to be used in the next section.

$$\sum_{\mu} a_{\mu i}^{+} a_{\mu i} = \sum_{k} b_{ik}^{+} b_{ik} \tag{A5.7a}$$

$$\sum_{k} \varepsilon_k c_k^{+} c_k = \frac{1}{n_s} \sum_{ik} \varepsilon_k b_{ik}^{+} b_{ik} \tag{A5.7b}$$

$$\frac{1}{\sqrt{N n_s}} \sum_{ik} V_k a_{\mu i}^{+} c_k e^{-ikR_{\mu}} = \tag{A5.7c}$$

$$\frac{1}{n_s} \sum_{ijk} V_k b_{ik}^{+} b_{jk} e^{-ik(r_i - r_j)} \tag{A5.7d}$$

In (A5.7b), the use was made of the fact that ε_k forms a periodic band. In the next section I will simplify the above representation by considering only one atomic site per unit cell, which in the lattice Anderson Hamiltonian is represented by a magnetic impurity. The above representation, however, may be a useful tool for considering a more general problem of two impurities per unit cell, as in the case of UBe_{13}.

Appendix 6 Canonical Transformation Decoupling the Effective f- and c- Bands.

In this Appendix I will perform the explicit calculations that will decouple the effective f- and c- bands, and in particular I will derive the important decoupling equation (4.3.9).

The following commutation rules for the generators of SU(2J+2) algebra defined in (4.3.2)-(4.3.4) will prove to be useful and are catalogued here:

$$\left[T_{0k}^{-}, T_{\nu} \right] = i \left[\delta_{k\nu} T_{0\nu}^{+} - \delta_{0\nu} T_{0k}^{+} \right] \tag{A6.1}$$

$$\left[T_{0k}^{-}, T_{mn}^{+}\right]=\begin{cases} i\left[T_0 - T_m\right] & k = m \\ -\frac{i}{\sqrt{2}} T_{mk}^{+} & k \neq m \end{cases} \tag{A6.2}$$

Now write:

$$U\hat{h}U^{-1} = \hat{h} + \left[R, \hat{h}\right] + \frac{1}{2}\left[R, \left[R, \hat{h}\right]\right] + \ldots +$$

$$+ \frac{1}{p!}\underbrace{\left[R, \ldots \left[R, \hat{h}\right]\right]}_{p\ -\ \text{times}} + \ldots \tag{A6.3}$$

In the first order we obtain:

$$\left[R, \hat{h}\right] = \sum_m a_m^{(1)} T_m + a_0^{(1)} T_0 + \sum_m a_{0m}^{(1)} T_{0m}^{+} + \sum_{m>n} a_{mn}^{(1)} T_{mn}^{+} \tag{A6.4}$$

where

$$a_{0m}^{(1)} = \left(a_0^{(0)} - a_m^{(0)}\right)\Theta_m - \frac{1}{\sqrt{2}} \sum_n{}' \Theta_n\, a_{mn}^{(0)} \tag{A6.5}$$

$$a_m^{(1)} = a_{0m}^{(0)} \Theta_m \tag{A6.6}$$

$$a_0^{(1)} = -\sum_m a_{0m}^{(0)} \Theta_m \tag{A6.7}$$

$$a_{mn}^{(1)} = \frac{1}{\sqrt{2}}\left(a_{0m}^{(0)} \Theta_n + a_{0n}^{(0)} \Theta_m\right) \tag{A6.8}$$

Here Σ' indicates that the value n=m is to be excluded from the summation. More generally, for p+1 -st order bracket we have the following closed set of recurrence relations:

$$a_{0m}^{(p+1)} = \left(a_0^{(p)} - a_m^{(p)}\right)\Theta_m - \frac{1}{\sqrt{2}}\sum_n{}' \Theta_n a_{mn}^{(p)} \tag{A6.9}$$

$$a_m^{(p+1)} = a_{0m}^{(p)}\Theta_m \tag{A6.10}$$

$$a_0^{(p+1)} = -\sum_m a_{0m}^{(p)}\Theta_m \tag{A6.11}$$

$$a_{mn}^{(p+1)} = \frac{1}{\sqrt{2}}\left(a_{0m}^{(p)}\Theta_n + a_{0n}^{(p)}\Theta_m\right) \tag{A6.12}$$

It is an important property of any closed Lie algebra that we get a finite number of recurrence relations of the above form, which can then in principle be solved. It is my intention to solve the above recurrence relations at this time. Using those relations write:

$$a_{0m}^{(p)} = -\frac{3}{2}\sum_n \Theta_m \Theta_n a_{0n}^{(p-2)} - \frac{1}{2}\sum_n \Theta_n{}^2 a_{0m}^{(p-2)} \tag{A6.13}$$

Define:

$$C^{(p)} \equiv \sum_m a_{0m}^{(p)}\Theta_m \qquad |\Theta|^2 \equiv \sum_n \Theta_n{}^2 \tag{A6.14}$$

Then multiplying both sides of (A6.13) by Θ_m and summing over m, we obtain:

$$C^{(p)} = -2|\Theta|^2 C^{(p-2)} \tag{A6.15}$$

so that

$$C^{(p)} = \begin{cases} \left(-2|\Theta|^2\right)^{\frac{p}{2}} C^{(0)} & p \text{ even} \\ \left(-2|\Theta|^2\right)^{\frac{p-1}{2}} C^{(1)} & p \text{ odd} \end{cases} \tag{A6.16}$$

Take p even. Then combining (A6.13) and (A6.16) obtain:

$$a_{0m}^{(p)} = -\frac{3}{2}\Theta_m \left(-2|\Theta|^2\right)^{\frac{p-2}{2}} C^{(0)} - \frac{1}{2}|\Theta|^2 a_{0m}^{(p-2)} \tag{A6.17}$$

To solve (A6.17) assume the following p-dependence:

$$a_{0m}^{(p)} = l_A A^p + l_B B^p \tag{A6.18}$$

Then (A6.17) takes the following form:

$$l_A A^p + l_B B^p = \frac{3}{4}\frac{\Theta_m}{|\Theta|^2}\left(-2|\Theta|^2\right)^{\frac{p}{2}} C^{(0)} -$$

$$-\frac{1}{2}|\Theta|^2\left(l_A A^{p-2} + l_B B^{p-2}\right) \tag{A6.19}$$

Now take

$$l_A A^p = \frac{3}{4}\frac{\Theta_m}{|\Theta|^2}\left(-2|\Theta|^2\right)^{\frac{p}{2}} C^{(0)} + \frac{1}{4}\left(-2|\Theta|^2\right) l_A A^{p-2} \tag{A6.20}$$

$$l_B B^p = -\frac{1}{2}|\Theta|^2 l_B B^{p-2} \tag{A6.21}$$

From (A6.20) it follows that:

$$A = \sqrt{\left(-2|\Theta|^2\right)} \tag{A6.22}$$

and

$$l_A = \frac{\Theta_m}{|\Theta|^2} C^{(0)} \tag{A6.23}$$

Similarly from (A6.21) we obtain:

$$B = \sqrt{\left(-\frac{1}{2}|\Theta|^2\right)} \tag{A6.24}$$

l_B can be determined from the initial condition. Combining (A6.18) and (A6.22)-(A6.24) write:

$$a_{0m}^{(p)} = \frac{\Theta_m}{|\Theta|^2}\left(-2|\Theta|^2\right)^{p/2} C^{(0)} + l_B\left(-\frac{1}{2}|\Theta|^2\right)^{p/2} \tag{A6.25}$$

For p=0 then get:

$$a_{0m}^{(0)} = \frac{\Theta_m}{|\Theta|^2} C^{(0)} + l_B \tag{A6.26}$$

or

$$l_B = a_{0m}^{(0)} - \frac{\Theta_m}{|\Theta|^2} C^{(0)} \tag{A6.27}$$

where $a_{0m}^{(0)}$ is given by (4.3.7). So finally:

$$a_{0m}^{(p)} = \frac{\Theta_m}{|\Theta|^2}\left(-2|\Theta|^2\right)^{p/2} C^{(0)} + \qquad \text{(A6.27)}$$
$$+\left(a_{0m}^{(0)} - \frac{\Theta_m}{|\Theta|^2} C^{(0)}\right)\left(-\frac{1}{2}|\Theta|^2\right)^{p/2}$$

and (see (4.3.11)):

$$A_{0m}^{\text{even}} \equiv \sum_{p\ even} \frac{1}{p!} a_{0m}^{(p)} = \frac{\Theta_m}{|\Theta|^2} C^{(0)} \cos\left(\sqrt{2|\Theta|^2}\right) +$$
$$+\left(a_{0m}^{(0)} - \frac{\Theta_m}{|\Theta|^2} C^{(0)}\right) \cos\left(\sqrt{\frac{1}{2}|\Theta|^2}\right) \qquad \text{(A6.29)}$$

Now consider p odd. Following the same procedure obtain:

$$a_{0m}^{(p)} = \frac{-2\Theta_m}{\left(-2|\Theta|^2\right)^{3/2}}\left(-2|\Theta|^2\right)^{p/2} C^{(1)} + \qquad \text{(A6.30)}$$
$$+\frac{1}{\left(-\frac{1}{2}|\Theta|^2\right)^{1/2}}\left(a_{0m}^{(1)} - \frac{\Theta_m}{|\Theta|^2} C^{(1)}\right)\left(-\frac{1}{2}|\Theta|^2\right)^{p/2}$$

and

$$A_{0m}^{\text{odd}} \equiv \sum_{p\ odd} \frac{1}{p!} a_{0m}^{(p)} = \frac{2\Theta_m}{\left(2|\Theta|^2\right)^{3/2}} C^{(1)} \sin\left(\sqrt{2|\Theta|^2}\right) +$$

$$+\sqrt{\frac{2}{|\Theta|^2}}\left(a_{0m}^{(1)}-\frac{\Theta_m}{|\Theta|^2}C^{(1)}\right)\sin\left(\sqrt{\frac{1}{2}|\Theta|^2}\right) \qquad \text{(A6.31)}$$

Adding even and odd contributions together obtain:

$$A_{0m}=A_{0m}^{\text{even}}+A_{0m}^{\text{odd}}=\frac{\Theta_m}{\left(2|\Theta|^2\right)^{3/2}}\times$$

$$\times\left[C^{(0)}\cos\left(\sqrt{2|\Theta|^2}\right)+-\frac{C^{(1)}}{\sqrt{\left(2|\Theta|^2\right)}}\sin\left(\sqrt{2|\Theta|^2}\right)\right]+$$

$$+\left[\left(a_{0m}^{(0)}-\frac{\Theta_m}{|\Theta|^2}C^{(0)}\right)\cos\left(\sqrt{\frac{1}{2}|\Theta|^2}\right)+\right.$$

$$\left.+\sqrt{\frac{2}{|\Theta|^2}}\left(a_{0m}^{(1)}-\frac{\Theta_m}{|\Theta|^2}C^{(1)}\right)\sin\left(\sqrt{\frac{1}{2}|\Theta|^2}\right)\right] \qquad \text{(A6.32)}$$

We now seek the solution of the equation (I will call it the decoupling equation):

$$A_{0m}=0 \qquad \text{(A6.33)}$$

This would decouple the effective f- and c-bands, which would create new quasiparticles. It would be interesting to explore the physics of those quasiparticles, which would require us to find all the possible solutions of the decoupling equation.

Using (A6.5) and (A6.32) one can rewrite (A6.33) as:

$$\frac{\Theta_m}{|\Theta|^2}\left\{C^{(0)}(1+x-2x^2)+\sqrt{\frac{2}{|\Theta|^2}}\,C^{(1)}\sqrt{1-x^2}\times\right.$$

$$\left.\times\left[(1-x)-\sqrt{(2|\Theta|^2)}\,\left(a_0^{(0)}-a_m^{(0)}\right)\right]\right\}=a_{0m}^{(0)}x \tag{A6.34}$$

where

$$x\equiv\cos\left(\sqrt{\frac{1}{2}|\Theta|^2}\right) \tag{A6.35}$$

Multiplying both sides of (A6.34) by Θ_m and summing over m, one obtains:

$$C^{(1)}=-\sqrt{\frac{|\Theta|^2}{2}}\,\frac{2x^2-1}{x\sqrt{1-x^2}}\,C^{(0)} \tag{A6.36}$$

and from (A6.34) and (A6.36) one can write:

$$\Theta_m=\frac{x}{\sqrt{1-x^2}}\times$$

$$\times\frac{a_{0m}^{(0)}|\Theta|^2}{C^{(0)}\dfrac{\sqrt{1-x^2}}{x}-\sqrt{(2|\Theta|^2)}\,\left(a_0^{(0)}-a_m^{(0)}\right)} \tag{A6.37}$$

From (4.2.1) and (4.3.7) write:

$$a_0^{(0)}-a_m^{(0)}=\Delta-h(m) \tag{A6.38}$$

where

$$\Delta=\varepsilon_k-E_0-\xi \tag{A6.39}$$

$$h(m) = \delta |m| + \mu_B g H m \tag{A6.40}$$

so that one can rewrite (A6.37) as:

$$\Theta_m = \frac{x}{\sqrt{1-x^2}} \times \times \frac{a_{0m}^{(0)} |\Theta|^2}{C^{(0)} \frac{\sqrt{1-x^2}}{x} - \sqrt{(2|\Theta|^2)}\ (\Delta - h(m))} \tag{A6.41}$$

Define:

$$\bar{a}_{0f}^{\,2} \equiv \sum_m a_{0m}^{(0)^2} \tag{A6.42}$$

$$\bar{h}^{(n)} \equiv \frac{\sum_m h(m)^n \Theta_m^{\,2}}{|\Theta|^2} \tag{A6.43}$$

Then combining (A6.5), (A6.14), and (A6.38) one can write:

$$C^{(1)} = \sum_m (\Delta - h(m)) \Theta_m^{\,2} = |\Theta|^2 (\Delta - \bar{h}) \tag{A6.44}$$

where

$$\bar{h} \equiv \bar{h}^{(1)} \tag{A6.45}$$

Then using (A6.44) and (A6.36) write:

$$C^{(0)} = \sqrt{(2|\Theta|^2)}\ \frac{x\sqrt{1-x^2}}{1-2x^2} (\Delta - \bar{h}) \tag{A6.46}$$

Now, rewrite (A6.41) as:

$$\Theta_m a_{0m}^{(0)}\left(C^{(0)} \frac{\sqrt{1-x^2}}{x} - \sqrt{\left(2|\Theta|^2\right)}\ (\Delta - h(m))\right) =$$

$$= \frac{x}{\sqrt{1-x^2}}\, a_{0m}^{(0)^2} |\Theta|^2 \qquad \text{(A6.47)}$$

and summing over m obtain:

$$C^{(0)^2} \frac{\sqrt{1-x^2}}{x} - \sqrt{\left(2|\Theta|^2\right)}\ \left(C^{(0)}\Delta - \right.$$

$$\left. - \sum_m \Theta_m a_{0m}^{(0)} h(m)\right) = \frac{x}{\sqrt{1-x^2}}\, \bar{a}_{0f}^2 |\Theta|^2 \qquad \text{(A6.48)}$$

Using (A6.41) one can write:

$$\sum_m \Theta_m a_{0m}^{(0)} h(m) = \frac{\sqrt{1-x^2}}{x}\left\{ \frac{\sqrt{1-x^2}}{x} C^{(0)} \bar{h} - \right. \qquad \text{(A6.49)}$$

$$\left. - \sqrt{\left(2|\Theta|^2\right)}\left(\Delta \bar{h} - \bar{h}^{(2)}\right)\right\}$$

and putting this formula into (A6.48), write:

$$C^{(0)^2} = |\Theta|^2 \bar{a}_{0f}^2(h) \qquad \text{(A6.50)}$$

where

$$\bar{a}_{0f}^2(h) \equiv \left[\bar{a}_{0f}^2 - 2\left(\frac{1-x^2}{x^2}\right)\left(\bar{h}^{(2)} - \bar{h}^2\right)\right]$$

Now using (A6.46) we finally obtain:

$$2\frac{x^2(1-x^2)}{(1-2x^2)^2} = \frac{\bar{a}_{0f}^2 - 2\left(\frac{1-x^2}{x^2}\right)\left(\bar{h}^{(2)} - \bar{h}^2\right)}{(\Delta - \bar{h})^2} \qquad \text{(A6.51)}$$

We can perform the calculations of other coefficients of the transformed Hamiltonian in the manner similar to the one described above in this Appendix. In that case one obtains:

$$A_{mn} \equiv \sum_{p=1}^{\infty} \frac{a_{mn}^{(p)}}{p!} = \frac{\Theta_m \Theta_n}{|\Theta|^2}\left[\mp \bar{a}_{0f}(h)\frac{\sqrt{1-x^2}}{x} - \right.$$

$$\left. - \sqrt{2}\frac{1-x}{x}(2\bar{h} - h(m) - h(n)) \right] \qquad \text{(A6.52)}$$

$$A_m \equiv \sum_{p=1}^{\infty} \frac{a_m^{(p)}}{p!} = \frac{1}{\sqrt{2}}\frac{\Theta_m^2}{|\Theta|^2}\left[\mp \bar{a}_{0f}(h)\frac{\sqrt{1-x^2}}{x} - \right.$$

$$\left. - 2\frac{1-x}{x}(\bar{h} - h(m)) \right] \qquad \text{(A6.53)}$$

$$A_0 \equiv \sum_{p=1}^{\infty} \frac{a_0^{(p)}}{p!} = \pm \frac{1}{\sqrt{2}}\bar{a}_{0f}(h)\frac{\sqrt{1-x^2}}{x} \qquad \text{(A6.54)}$$

and the transformed Hamiltonian has the following form:

$$H_D = \sum_k \hat{h}_k \qquad \text{(A6.55)}$$

where (drop the common subscript k):

$$\hat{h} = \sum_m A_m T_m + A_0 T_0 + \sum_m A_{0m} T_{0m}^{+} + \sum_{m>n} A_{mn} T_{mn}^{+} \qquad \text{(A6.56)}$$

and the corresponding coefficients are given by Eqs. (A6.32), (A6.33), and (A6.52)-(A6.54).

Formulas (4.4.1)-(4.4.3) can be derived in the straightforward fashion by combining (A6.10)-(A6.12), (A6.28), (A6.30) and then substituting the expressions derived in (A6.44), (A6.46), as well as (4.3.10) and (4.3.11).

Appendix 7 Solution of the Self-Consistent *T*-matrix Equation (5.1.13).

Let me rewrite (5.1.13) as:

$$T_{\mu\nu}(\omega; \boldsymbol{k}, \boldsymbol{k}') = \xi(0)\left(S_{\mu\nu} + \sum_\kappa S_{\mu\kappa} V_{\kappa\nu}(\omega; \boldsymbol{k}, \boldsymbol{k}') \right) \qquad \text{(A7.1)}$$

where

$$V_{\kappa\nu}(\omega; \boldsymbol{k}, \boldsymbol{k}') \equiv \frac{1}{N_L} \sum_{|\boldsymbol{k}'' - \boldsymbol{k}| < q_c} T_{\kappa\nu}(\omega; \boldsymbol{k}'', \boldsymbol{k}') G_\kappa^{\text{ret}}(\omega, \boldsymbol{k}'') \qquad \text{(A7.2)}$$

Let us now define:

$$L_{\mu\nu}(\omega; \boldsymbol{k}'', \boldsymbol{k}') \equiv \xi(0)\left(S_{\mu\nu} + \sum_\kappa S_{\mu\kappa} V_{\kappa\nu}(\omega; \boldsymbol{k}'', \boldsymbol{k}') \right) \qquad \text{(A7.3)}$$

Then one can rewrite (A7.1) as:

$$V_{\mu\nu}(\omega; \boldsymbol{k}, \boldsymbol{k}') = \frac{1}{N_L} \sum_{|\boldsymbol{k}'' - \boldsymbol{k}| < q_c} L_{\mu\nu}(\omega; \boldsymbol{k}'', \boldsymbol{k}') G_\mu^{\text{ret}}(\omega, \boldsymbol{k}'') \qquad \text{(A7.4)}$$

Let us define the average wave vector $\bar{k}$, so that the following equality holds (at least approximately):

$$\sum_{|k''-k|<q_c} L_{\mu\nu}(\omega;k'',k')G_{\mu}^{ret}(\omega,k'') \approx L_{\mu\nu}(\omega;k,k') \times$$

$$\times \sum_{|k''-\bar{k}|<q_c} G_{\mu}^{ret}(\omega,k'') \qquad \text{(A7.5)}$$

Such $\bar{k}$ will always be found provided the range of the LHS of (A7.5) (as the function of k) is the subset of the range of the LHS of (A7.5) (as the function of $\bar{k}$). In that case (A7.5) is exact and defines $\bar{k}$ as the implicit function of k and k'). Otherwise (A7.5) can be considered as an approximation with $\bar{k}$ defined as the value giving the best possible fit. The approximation can then be considered as the self-consistent type approximation.

Let us further define:

$$\hat{G}_{\mu}^{ret}(\omega,\bar{k}) \equiv \frac{1}{N_L} \sum_{|k''-\bar{k}|<q_c} G_{\mu}^{ret}(\omega,k'') \qquad \text{(A7.6)}$$

$$C_{\mu}(\omega,\bar{k}) \equiv 1 - \xi(0)\hat{G}_{\mu}^{ret}(\omega,\bar{k}) \qquad \text{(A7.7)}$$

Using (A7.5)-(A7.7) we then obtain:

$$V_{\mu\nu}(\omega;k,k')C_{\mu}(\omega,\bar{k}) \equiv \xi(0)S_{\mu\nu}\hat{G}_{\mu}^{ret}(\omega,\bar{k}) - \qquad \text{(A7.8)}$$

$$-\xi(0)l_{\mu}\sum_{\kappa} l_{\kappa}V_{\kappa\nu}(\omega;k,k')\hat{G}_{\mu}^{ret}(\omega,\bar{k})$$

Defining:

$$B_\nu(\omega;k,k') \equiv \sum_\kappa l_\kappa V_{\kappa\nu}(\omega;k,k') \tag{A7.9}$$

Eq. (A7.8) then takes the following form:

$$B_\nu(\omega;k,k') = \xi(0)\sum_\mu \frac{l_\mu S_{\mu\nu}\hat{G}_\mu^{ret}(\omega,\bar{k})}{C_\mu(\omega,\bar{k})} - \tag{A7.10}$$

$$- \xi(0)B_\nu(\omega;k,k')\sum_\mu \frac{l_\mu^2\hat{G}_\mu^{ret}(\omega,\bar{k})}{C_\mu(\omega,\bar{k})}$$

Solving (A7.10) we obtain:

$$B_\nu(\omega;k,k') = \frac{\xi(0)l_\nu}{1+\xi(0)\sum_\kappa l_\kappa^2\hat{G}_\kappa^{ret}(\omega,\bar{k})/C_\kappa(\omega,\bar{k})} \times$$

$$\times\left(\hat{G}_\nu^{ret}(\omega,\bar{k})/C_\nu(\omega,\bar{k}) - \sum_\kappa l_\kappa^2\hat{G}_\kappa^{ret}(\omega,\bar{k})/C_\kappa(\omega,\bar{k})\right) \tag{A7.11}$$

Substituting this result into (A7.9) obtain:

$$V_{\mu\nu}(\omega;k,k') = \xi(0)\delta_{\mu\nu}\frac{\hat{G}_\nu^{ret}(\omega,\bar{k})}{C_\nu(\omega,\bar{k})} - \frac{1}{C_\mu(\omega,\bar{k})} \times \tag{A7.12}$$

$$\times \frac{1}{C_\nu(\omega,\bar{k})}\frac{\xi(0)l_\mu l_\nu\hat{G}_\mu^{ret}(\omega,\bar{k})}{1+\xi(0)\sum_\kappa l_\kappa^2\hat{G}_\kappa^{ret}(\omega,\bar{k})/C_\kappa(\omega,\bar{k})}$$

and finally substituting (A7.12) into (A7.1) we finally obtain:

$$T_{\mu\nu}(\omega; k, k') = \xi(0)\delta_{\mu\nu}\frac{1}{C_\nu(\omega,\bar{k})} - \frac{l_\mu}{C_\mu(\omega,\bar{k})} \times \quad \text{(A7.13)}$$

$$\times \frac{l_\nu}{C_\nu(\omega,\bar{k})} \frac{\xi(0)}{1+\xi(0)\sum_\kappa l_\kappa^2 \hat{G}_\kappa^{ret}(\omega,\bar{k}) / C_\kappa(\omega,\bar{k})}$$

which solves (5.1.13). This solution allows us to calculate the self-energy corrections, which is the task in Sec. 5.2.

REFERENCES

1. Stewart G.R., Rev. Mod. Phys., **56**, 755 (1984)
2. Coffey L., Phys. Rev. B, **35**, 8440 (1987)
3. Volovik G.E., Gorkov L.P., preprint
4. Blount E.I., Phys. Rev. B, **32**, 2935 (1985)
5. Rice T.M., Ueda K., Phys. Rev. B, **31**, 7114 (1985)
6. Kitaoka Y. et al, Sol. St. Comm., **51**, 461 (1984)
7. Friedel J., Nuovo Cim. (Suppl.), **7**, 287 (1958)
8. Anderson P.W., Phys. Rev., **124**, 41 (1961)
9. Kondo J., Prog. Theor. Phys., **32**, 37 (1964)

9a. Schrieffer J. R., Wolff P. A., Phys. Rev. **149**, 491 (1966)

10. Kasuya T, Prog. Theor. Phys., **16**, 45 (1956)
11. Yosida K., Phys. Rev., **106**, 893 (1957)
12. Abrikosov A. A., Physics, **2**, 5 (1965)
13. Suhl H., Physics, **2**, 39 (1965)
    Phys. Rev., **141**, 483 (1966)
14. Nozieres P., J. Low Temp. Phys. **17**, 31 (1974) and J. Phys. (Paris) **39**, 1117 (1978)
    Nozieres P., Blandin A., J. Phys. (Paris) **41**, 193 (1980)
15. Anderson P.W., Comm. Solid St. Phys., **5**, 73 (1973)
16. Wilson K. G., Collective Properties in Physical Systems, Nobel Symposium 24, Academic Press, 1974
17. Newns D. M. and Hewson A. C., J. Phys. F, **10**, 2429 (1980)
18. Abe R., Prog. Theor. Phys., **48**, 1414 (1972)
    Ma S., Phys. Rev. A, **7**, 2172 (1973)
19. Anderson P.W., in Valence Fluctuations in Solids, edited by L.M. Falicov, W. Hanke, and M.B. Maple, North-Holland, Amsterdam, 1981
20. Bickers N. E., Review of Mod. Phys., **59**, 845 (1987)
21. Hubbard J., Proc. Royal Soc. London, Ser. A, **277**, 237 (1964)
22. Keiter H. and Kimball J. C., Int. J. Magn., **1**, 233 (1971)
23. Yamada K., Prog. Theor. Phys., **53**, 970 (1975)
24. Yosida K., Yamada K., Prog. Theor. Phys., **53**, 1286 (1975)
25. Yoshimori A., Prog. Theor. Phys., **55**, 67 (1976)
26. Bickers N. E., unpublished (1987)

27. Rasul J. W. and Hewson A. C., J. Phys. C, **17**, 2555 (1984)
J. Phys. C, **17**, 3332 (1984)
28. Kuramoto Y., Z. Phys. B, **53**, 37 (1983)
29. Maekawa S., Kashiba S., Takahashi S., Tachiki M., in Valence Fluctuations in Solids, p. 90, edited by Kasuya and Saso, Springer, New York, (1985)
30. Bickers N. E., Cox D. L., Wilkins J. W., Phys. Rev. B, **36**, 2036 (1987)
31. Kuramoto Y. and Kojima H., Z. Phys. B, **57**, 95 (1984)
32. Coleman P., Phys. Rev. B, **29**, 3035 (1984)
33. Read N., Newns D. M., J. Phys. C, **16**, 3273 (1983)
34. Read N., Newns D. M., J. Phys. C, **16**, L1055 (1983)
35. Vollhardt D., Rev. Mod. Phys. **56**, 99 (1984)
36. Valls O.T., Tesanovic Z., Phys. Rev. Lett. **53**, 1497 (1984)
37. Rice T.M., Ueda K., Phys. Rev. B **34**, 6420 (1986)
38. Kotliar G., Ruckenstein A.E., Phys. Rev. Lett. **57**, 1362 (1986)
39. de Chatel P.F., Solid St. Comm., **41**, 853 (1982)
40. Millis A.J. and Lee P.A., Phys. Rev. B, **35**, 3394 (1987)
41. Auerbach A. and Levin K., Phys. Rev. Lett., **57**, 877 (1986)
42. Read N., J. Phys. C, **18**, 2651 (1985)
43. Abrikosov A.A., Gorkov L.P., Dzyaloshinski I.E., "Methods of Quantum Field Theory in Statistical Physics", edited by R.A. Silverman, Dover Publications, New York, 1975
44. Mühlshlegel B., in "Path Integrals and their Applications in Quantum, Statistical, and Solid State Physics", NATO Advanced Study Institute, Series B: Physics, edited by G.J. Papudopoulos and J.T. Devreese, vol. 34, p. 383, Plenum, New York, 1978
L.S. Shulman, in "Path Summation: Achievements and Goals", edited by S.O. Lundquist, A. Ranfagni, V. Sa-yakanit and L.S. Schulman, World Scientific, Singapore (in press)
45. Stratanovich R.L., Soviet Physics - Doklady, **2**, 416 (1958)
46. Keiter H., Phys. Rev. B, **2** (1970), 3777
47. Feynman R. P., Phys. Rev. **84**, 108 (1951)
48. Blaizot J.P. and Orland H., Phys. Rev. C, **24** (1981), 1740
49. Riesz F. and Sz.-Nagy B., "Functional Analysis", Ungar, New York, 1955

50. For reviews, see Jefferson J.M. and Stevens K.W., J. Phys. **11**, 319 (1978), and various articles in *Proceedings of the International Conference on Valence Fluctuations in Solids*, edited by L.M. Falicov, W. Hanke, and M.B. Maple, North-Holland, Amsterdam, 1981, as well as the more recent *Theory of Heavy Fermions and Valence Fluctuations*, edited by T. Kasuya and T. Saso, Springer, New York, 1985

51. Robinson J.M., Phys. Rep. **51**, 1 (1979)

52. Lee P.A., Rice T.M., Serene J.W., Sham L.J. and Wilkins J.W., in Comments on Condensed Matter Physics **128**, 99 (1986)

53. Anderson P.W., Phys. Rev. **124**, 41 (1961)

54. Blandin A., in *Magnetism*, edited by H. Suhl, vol. V, p. 58, Academic Press, New York, 1973

55. Zak J., in Solid State Physics, Advances in Research and Applications, edited by H.Ehrenreich, F. Seitz, D. Turnbull, Vol. 27, page 1 (1972)

56. At finite temperature the fluctuations are of order exp (-w/T), where w is the peak's width.

57. Xianxi D. and C.-S. Ting, Phys Rev B **28**, 5243 (1983)

58. Krishna-Murthy H.R., Wilkins J.W., and Wilson K.G., Phys. Rev. B **21**, 1003 (1980); 1044 (1980)

59. Brandt U., Keiter H., and Liu F.-S., Z. Phys. B **58**, 267 (1985)

60. Treating the constraint field in the saddle point approximation is discussed in the review article [20] , where it has been shown that the error introduced is highly temperature dependent and is exponentially small at low temperatures

61. $f_1 = f_1(H=0)$ denotes the common value of the free energy density for the corresponding $2J+1$ saddle points in the

absence of the magnetic field. Any lattice-induced splitting vanishes due to spin delocalization.

62. Here and below I will neglect the contributions from the conduction band to the various derivatives of the free energy density, which are very small compared to the contribution from the localized band.

63. See Sec. 3 for a more extensive discussion of the question of phase transitions as well as the importance of the Gaussian fluctuations of the derivatives of the free energy density in the above situation.

64. Anderson P.W., Phys. Rev. Lett., **18**, 1049 (1967)

65. The same trick does not however apply to the symmetry-breaking state, which does not explicitly include the contributions of the uncoupled empty f-electron state (see the discussion later on in this section).

66. Mahan G. D., "Many-Particle Physics", Plenum Press, New York and London, 1981